THE STRUCTURE AND FUNCTION OF EIMER'S ORGAN IN THE MOLE

By

Paul D. Marasco

Dissertation

Submitted to the faculty of the

Graduate School of Vanderbilt University

in partial fulfillment of the requirements

for the degree of

DOCTOR OF PHILOSOPHY

in

Neuroscience

December, 2006

Nashville, Tennessee

Approved:

Professor Kenneth C. Catania

Professor Jon H. Kaas

Professor David E. McCauley

Professor Terry L. Page

I dedicate this dissertation to my wife Sue Marasco

who has made considerable sacrifices to help me complete

this project and move to the next step

ACKNOWLEDGEMENTS

I thank Kenneth Catania for his mentorship through this entire process. I look to Ken as the model for how to be an intelligent, productive and, above all, creative scientist. During my tenure in his laboratory he has always provided me with the freedom and autonomy to design and tailor my research projects to my interests while simultaneously steering me towards the successful conclusion of my work.

I also thank Terry Page for his mentorship and advice as I pursued my research. His help with the electrophysiological portion of my project was especially invaluable. He was always available to answer my questions and to serve as a sounding board, and always did so with good humor and a dry wit. I am grateful to the other members of my committee as well. Jon Kaas has always been very supportive of me and has provided help and sage advice on many occasions (particularly when I was searching for a post-doctoral position). David McCauley's willingness to serve on my committee as my non-neuroscience member has been very helpful.

It is important to recognize the contribution that the Neuroscience program has made to my education. Elaine Sanders-Bush and the staff of the Vanderbilt Brain Institute have provided a supportive academic environment that is unparalleled by any other institution that I have ever experienced. It is unusual to find a program so deeply committed to the success of their students and I appreciate it greatly.

I am deeply indebted to Pamela Tsuruda, Diana Bautista and David Julius at the University of California, San Francisco for all that they have done for me. Major portions of my research would not have been possible without their help. They have become good

friends and true colleagues and I look forward to working with them again in the future. I am also thankful to Bruce Appel for giving me my start in science. He took me into his laboratory, when I had no research experience, and then ultimately helped me to enter the Interdisciplinary Graduate Program at Vanderbilt University. Bruce is a true gentleman scientist. Hae-Chul Park was instrumental in teaching me the skills that I use everyday to conduct my work.

I am thankful to the past and present members of the Catania lab for their help. Most notably, Fiona Remple, Erin Clark-Henry, Christine Dengler-Crish, and Sam Crish. In addition, I thank Denny Kearns of the Electron Microscopy core for help processing material and Mary Dietrich of the Vanderbilt University Advanced Computing Center for Research and Education for her statistical contribution to my work. I also thank Tim Sheehan and Kevin Campbell for providing me with coast moles. This research was supported financially by a Fundamental Neuroscience Training Grant through the Neuroscience Graduate Program, a National Science Foundation Career Award 00238364 to Kenneth Catania and National Science Foundation Grant 0518819.

TABLE OF CONTENTS

Page

DEDICATION ii

ACKNOWLEGEMENTS iii

LIST OF TABLES vii

LIST OF FIGURES viii

Chapter

I. INTRODUCTION 1

References 8

II. NEUROANATOMICAL EVIDENCE FOR SEGREGATION OF NERVE FIBERS CONVEYING LIGHT TOUCH AND PAIN SENSATION IN EIMER'S ORGAN OF THE MOLE 9

Introduction 9
Materials and Methods 13
Experimental Animals 13
AM1-43 Labeling 13
Immunocytochemistry 14
DiI Labeling 15
Imaging 15
Scanning Electron Microscopy 16
Results 16
Labeling patterns of AM1-43 within Eimer's organ 16
Coast Mole Intraepidermal Free Nerve Endings 19
Star-Nosed Mole Intraepidermal Free Nerve Endings 19
Merkel Cell-Neurite Complexes and Lamellated Corpuscles 22
Neurofilament 200 Immunocytochemistry 23
Neurofilament 200 and Substance P Double Labeling 26
DiI Tracing 29
Discussion 32
Anatomy and Function of Eimer's Organ 32
AM1-43 and Immunocytochemistry 34
DiI and Eimer's Organ Innervation 36

References....38

III. THE FINE STRUCTURE OF EIMER'S ORGAN IN THE COAST MOLE....41

Introduction....41
Materials and Methods....45
Results....46
Intraepidermal Free Nerve Endings and Associated Epithelium....46
Merkel Cell-Neurite Complexes....57
Lamellated Corpuscles....62
Discussion....65
Tonofibrils and the Central Column....66
The Condition of the Central Column Free Nerve Endings Within the Stratum Corneum....67
The Structure of the Peripheral Free Nerve Endings and the Nature of Their Cellular Sheath....69
The Structure of the Merkel Cell-Neurite Complexes....71
The Structure of the Lamellated Corpuscles....72
References....74

IV. RESPONSE PROPERTIES OF PRIMARY AFFERENTS SUPPLYING EIMER'S ORGAN....78

Introduction....78
Materials and Methods....82
Results....92
Receptor Classes....96
Peak Activation Frequency....99
Quantitative Receptive Fields....105
Indentation Velocity....105
Depression Thresholds....109
Directional Sensitivity....114
Temporal Patterning....119
Manipulation of Individual Eimer's Organs....127
Discussion....128
Receptive Fields....128
Receptor Classes....130
Mole Behavior and Eimer's Organ Stimulation....133
Temporal Precision....134
Directional Sensitivity and the Function of Eimer's Organ....135
References....140

V. CONCLUSIONS....147

References....153

LIST OF TABLES

Table Page

1. Summary of Directional Measures 116

LIST OF FIGURES

Figure Page

1. DiI Treated Eimer's Organs....4

2. The Coast Mole and the Star-Nosed Mole....11

3. Three AM1-43 Treated Eimer's Organs....18

4. Components of Eimer's Organ Labeled with AM1-43....21

5. Main Components of Eimer's Organ Labeled for NF 200....25

6. Eimer's Organ Labeled with NF 200 and sP....28

7. Free Nerve Ending Terminals Differentially Labeled with DiI....31

8. Eimer's Organ of the Coast Mole....43

9. Horizontal Section of Central Column....48

10. Central Column Free Nerve Endings....51

11. Condition of Central Column Free Nerve Endings....54

12. Peripheral Free Nerve Endings....56

13. The Cellular Sheath of the Peripheral Free Nerve Endings....59

14. Merkel Cell Neurite Complexes....61

15. Lamellated Corpuscles....64

16. Eimer's Organ Schematic....80

17. Directional Stimulation....87

18. Qualitative Receptive Fields in the Coast Mole....91

19. Response Profiles in the Coast Mole....95

20. Response Profiles in the Star-Nosed Mole 98

21. Frequency of Maximum Sensitivity.....101

22. Quantitative Receptive Fields in the Coast Mole 104

23. Indentation Velocity.....107

24. Static Displacement Thresholds.....111

25. Qualitative Directional Responses in the Coast Mole 113

26. Directional Sensitivity 118

27. Directional Comparison.....121

28. Phase Locking.....123

29. Receptive Fields and Single Eimer's Organs.....126

30. Eimer's Organ Function Model 138

CHAPTER I

INTRODUCTION

Eimer's organ is a complex mechanosensory structure that is found on the nose of most species of talpid moles. Because the moles live underground their eyes are of limited use for navigating through their tunnel systems. The moles instead rely on their sense of touch. As they move about and forage for food they repeatedly tap their noses to the ground and to objects of interest to essentially "feel" their way around their environment. The moles are adept at navigating and making rapid discriminations using touch and it appears that the Eimer's organs play a key role in providing the moles with a high level of tactile acuity.

The external surface of the mole's glabrous rhinarium is covered in a multitude of small epidermal bumps or papillae. Depending on species, these epidermal papillae range from 40-70 μm in diameter and in all species they are tightly packed into a hexagonally arranged array. Every epidermal papilla at the surface represents the top-most portion of a single Eimer's organ below and each individual Eimer's organ is composed of a stereotypical arrangement of epidermal cells and four different kinds of sensory receptor terminals. The center of each organ is defined by a central column of epidermal cells that extends from the dermis up to the surface. This column is generally formed from layers of 1-3 circularly arranged keratinocytes stacked one on top of the other. This central column structure is invested with a number of large diameter mechanosensory intraepidermal free nerve ending terminals that stem from myelinated afferents in the

dermis. These receptor terminals course up from the bottom of the organ directly to the surface of the skin. The majority of the central column associated free nerve endings are enclosed within a cleft of the plasma membranes of the keratinocytes and arrayed around the outer margin of the column. One to two free nerve ending terminals track directly through the center of the column and reside in the margin between keratinocytes. A set of smaller diameter nociceptive intraepidermal free nerve endings is arrayed in a palisade around the central column. These terminals reside 1-2 cell diameters removed from the outside edge of the central column and they are found in the spaces between keratinocytes. In similar fashion to the mechanosensory free nerve endings these smaller terminals extend from the base of the epidermis up to the surface of the skin. However, they follow a more convoluted path to the surface and they stem from unmyelinated afferents. In the stratum germinativum at the base of Eimer's organ there are from 1-15 Merkel cell-neurite complexes grouped in a flat circular arrangement. Just below the epidermis, in the dermal compartment, there are 1-2 lamellated corpuscles positioned with their long axis parallel to the skin surface. Every Eimer's organ across the surface of the nose has this collection of sensory receptors and specialized epithelial cells in a similar configuration.

One of my first experiences with Eimer's organ was when I was shown a red confocal fluorescent micrograph of a sheet of DiI labeled Eimer's organs (Fig. 1). In that picture it was easy to see the hexagonally arrayed Eimer's organs, each with a circular arrangement of free nerve ending terminals at the top. I was absolutely struck by the beauty and symmetry of this system. After this first

Fig. 1. Fluorescent confocal micrograph of the surface of a nasal appendage from the star-nosed mole. This tissue was treated with DiI. The stereotypic arrangement of the free nerve terminals can be seen at the center of each organ. The organs are packed tightly into a hexagonal array.

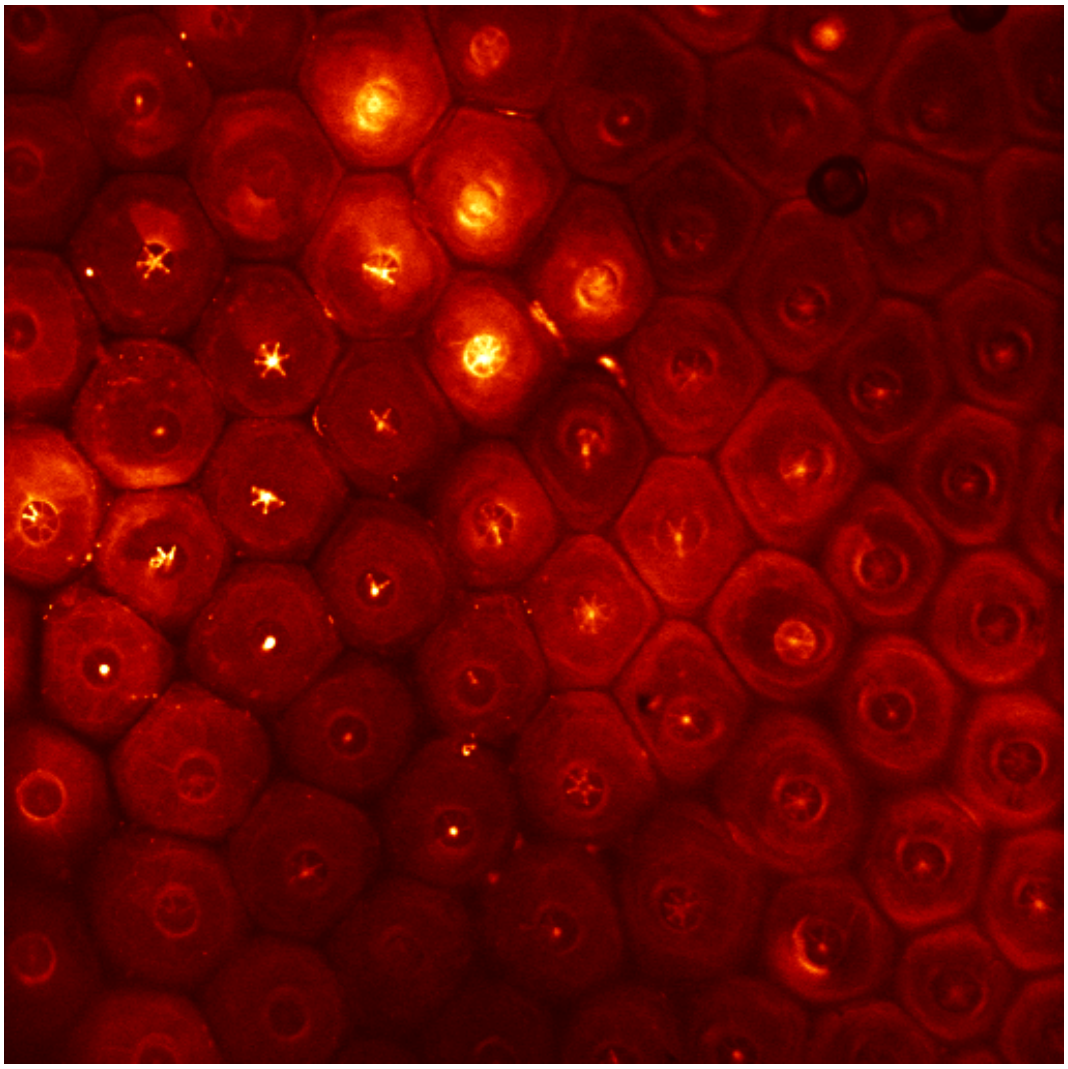

introduction to these organs I became very interested in trying to figure out how they might work to transduce tactile information.

Eimer's organs were first described in the 19th century and since then the question of how they might function has been only a matter of speculation. One of the first issues that I felt needed to be addressed was: What are the conspicuously arranged intraepidermal free nerve endings doing? Particularly, are these receptors mechanoreceptive and is there the possibility that they are able to encode the displacement of the organ in different directions? Previous recordings in cortex provided evidence that the Eimer's organ array of the star-nosed mole was sensitive to mechanosensory stimulation (Catania and Kaas, 1995; Sachdev and Catania, 2002 a,b). However, positive assignment of mechanoreceptor function directly to Eimer's organ had not been accomplished. With this in mind I set about to investigate the possible function of Eimer's organ paying particular attention to the intraepidermal free nerve endings.

I had the occasion to examine an excellent paper by Meyers et al. (2003). This paper described the novel use of the styryl pyridinium dye FM1-43 to label sensory cells. Most striking, in this paper, was the beautiful fluorescent micrographs of AM1-43 labeling in multiple sensory structures in juvenile mice. Of particular interest was the clear labeling of mechanosensory structures as was the bright labeling of the Merkel cell-neurite complexes in the vibrissae. I supposed that nose of the mole might be a prime place to utilize this dye, as Meyers et al. provided evidence that the dye entered the ion channels of mechanosensory cells. I simply reasoned that if the dye showed so clearly in Merkel cells it might also label lamellated corpuscles, and in addition to that, if the intraepidermal free nerve endings in Eimer's organ were mechanoreceptive it might label

them as well. This line of reasoning was the basis for Chapter II. During the course of this study I began what has become a fruitful collaboration with Dr. Diana Bautista and Dr. Pamela Tsuruda in the lab of Dr. David Julius at the University of California San Francisco. Together we coupled the examination of Eimer's organ with AM1-43 to immunocytochemical analysis to begin to distinguish functional characteristics of Eimer's organ. Through the course of this work many new aspects of Eimer's organ were revealed.

The findings stemming from this first study lead me to begin to examine the fine structure of Eimer's organ in the coast mole. This was the basis for Chapter III. I was specifically interested in examining the structural aspects of the newly characterized nociceptive intraepidermal free nerve endings. One topic of interest was the state of the cellular sheath surrounding these afferents in the dermis. This subject was a source of much discussion between us and our collaborators in San Francisco because the confocal imagery from the first study was not conclusive as to whether or not these nociceptive fibers were myelinated. In addition, the AM1-43 data was suggestive that the functional terminals of the mechanosensitive intraepidermal free nerve endings might span into the stratum corneum of the epidermis. These questions were examined as were many others concerning the morphological attributes of Eimer's organ in the coast mole.

During the course of these previously mentioned studies I was also pursuing an electrophysiological approach to learning about the function of Eimer's organ. I felt that the best way to assess the activity of the sensory receptors of the nose, as they functioned to transduce mechanosensory signals, was to record single units directly from the primary afferent neurons in the trigeminal ganglion. Using this approach, there was the possibility

that mechanoreceptive function could be directly assigned to Eimer's organ. It had been proposed that the distinct circular arrangements of receptor terminals might impart Eimer's organ with the capacity to code directional input (Quilliam, 1966; Catania, 1996, 2000) and I was very excited about the prospects of determining if this was actually the case. When I started to examine this issue I began to conceptualize the Eimer's organs as almost mechanical entities and in this mindset I set out to design experiments that would interface with this hypothetical mechanical nature. I designed a stimulator that could apply controlled directional stimulus to the sheet of Eimer's organs to test if the receptors could code this type of input. In addition, I also employed a number of different stimulus paradigms to explore other functional aspects of the organs, to differentiate between receptor types and also to derive information from this system that could be compared to other systems in the literature. This approach formed the basis for Chapter IV.

I felt that the best way to learn more about the function of Eimer's organ was to utilize many different approaches using novel methodology. This work has helped to provide clues as to how this unique skin surface transduces mechanosensory stimuli.

References

Catania KC. 1996. Ultrastructure of the Eimer's organ of the star-nosed mole. J Comp Neurol 365:343-354.

Catania KC. 2000. Epidermal sensory organs of moles, shrew moles, and desmans: a study of the family talpidae with comments on the function and evolution of Eimer's organ. Brain Behav Evol 56:146-174.

Catania KC, Kaas JH. 1995. Organization of the somatosensory cortex of the star-nosed mole. J Comp Neurol 351:549-567.

Meyers JR, MacDonald RB, Duggan A, Lenzi D, Standaert DG, Corwin JT, Corey DP. 2003. Lighting up the senses: FM1-43 loading of sensory cells through nonselective ion channels. J Neurosci 23:4054-4065.

Quilliam TA. 1966a. The mole’s sensory apparatus. J Zool 149:76-88.

Sachdev RN, Catania KC. 2002a. Effects of stimulus duration on neuronal response properties in the somatosensory cortex of the star-nosed mole. Somatosens Mot Res 19:272-278.

Sachdev RN, Catania KC. 2002b. Receptive fields and response properties of neurons in the star-nosed mole's somatosensory fovea. J Neurophysiol 87:2602-2611.

CHAPTER II

NEUROANATOMICAL EVIDENCE FOR SEGREGATION OF NERVE FIBERS CONVEYING LIGHT TOUCH AND PAIN SENSATION IN EIMER'S ORGAN OF THE MOLE

Introduction

Moles are fossorial insectivores in the family Talpidae that exhibit a number of adaptations to their underground lifestyle. The most obvious specializations are powerful shoulders and large clawed forelimbs used for digging tunnels (Fig. 2*C*). However, the less apparent sensory specializations for touch are perhaps the most important innovations underlying the survival and success of these species. Unlike most small mammals that depend heavily on their large vibrissae for mechanosensation, moles primarily make use of the tip of their nose to investigate objects through touch.

At first glance, the noses of most moles appear nondescript, although the flourish of nasal appendages on the star-nosed mole is an obvious exception (Fig. 2). Closer examination of a mole's nose under the scanning electron microscope reveals a honeycomb pattern of tiny epidermal swellings covering the skin surface in nearly every species (Catania, 2000). These small swellings are called Eimer's organs (Eimer, 1871) and are complex, well-organized, and densely innervated structures, used to make rapid sensory discriminations of small objects (Catania and Kaas, 1997; Catania and Remple, 2005). Each Eimer's organ contains an array of sensory receptors associated with a

Fig. 2. The coast mole (*Scapanus orarius*) and the star-nosed mole (*Condylura cristata*) showing adaptations to a fossorial lifestyle. (**A)** The coast mole has large claws, tiny eyes, and lacks an external pinna. (**B)** A scanning electron micrograph of the coast mole's snout covered with Eimer's organs. Arrow marks organs worn by soil abrasion - see discussion. **Inset:** An Eimer's organ showing the circular disk at the top of the central cell column (**arrowhead**). (**C**) The star-nosed mole showing the rhinarium composed of 22 appendages. (**D)** A scanning electron micrograph of appendages covered with Eimer's organs from the right lower quadrant of the star. (**E)** Schematic representation of Eimer's organ in the coast mole. The epidermis contains a central epithelial cell column associated with intraepidermal free nerve endings (**CC-FNE**) that course to the stratum corneum (**SC**). A ring of smaller peripheral free nerve endings surrounds the central column free nerve endings (**P-FNE**). Merkel cell-neurite complexes (**MC**) and lamellated corpuscles (**LC**) reside at the base of each organ. (**F**) Schematic representation of the smaller Eimer's organ in the star-nosed mole with only one Merkel-cell and a smaller central column.

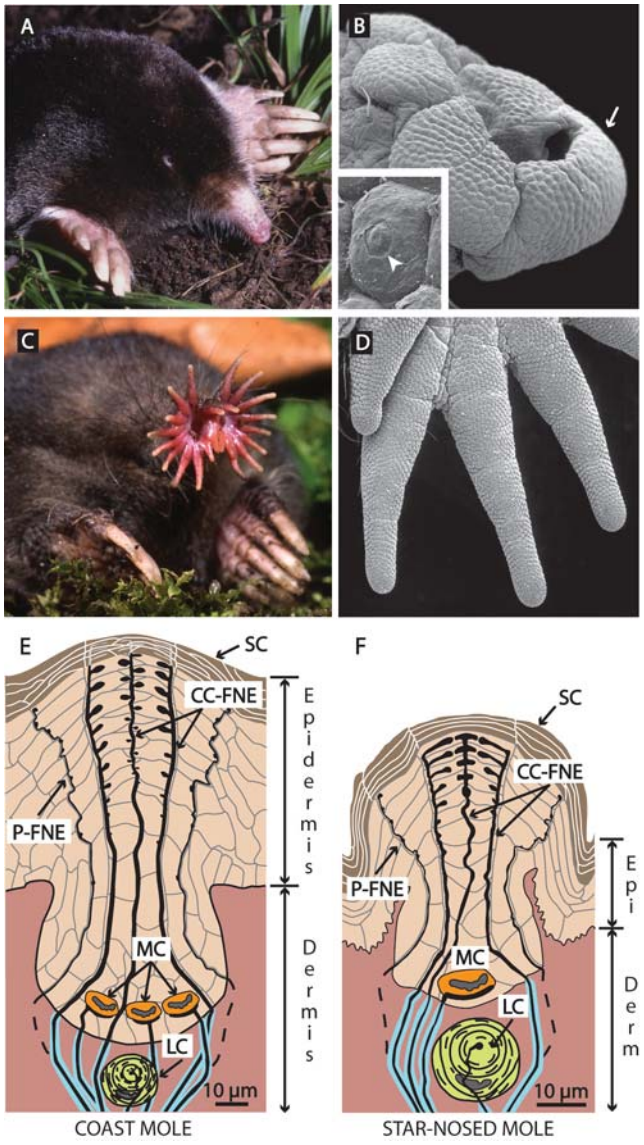
A
B
C
D
E
SC
CC-FNE
P-FNE
MC
LC
Epidermis
Dermis
10 µm
COAST MOLE
F
SC
CC-FNE
P-FNE
MC
LC
Epi
Derm
10 µm
STAR-NOSED MOLE

column of epidermal cells running through the center of each swelling. A circular disk that makes up the tip of the cell column is visible on the outer skin surface (arrowhead, Fig. 2*B*).

The central cell column is associated with a number of intraepidermal free nerve endings that originate from myelinated afferents in the underlying dermis. Figure 2 shows schematics of the complex innervation of the Eimer's organ in the coast mole and the star-nosed mole. The free nerve endings traverse the cell column in a circular arrangement, with one to two free nerve endings in the center of the column (CC-FNE) and a ring of satellite free nerve endings at the margins of the column. A few previous reports (Eimer, 1871; Ranvier, 1880; Halata, 1972) described a second ring of smaller free nerve endings around the periphery of each Eimer's organ of some species (P-FNE). One or more Merkel cell-neurite complexes (MC) are located at the bottom of each Eimer's organ in the basal layer of the epidermis (stratum germinativum). Finally, there are 1-2 lamellated corpuscles (LC) in the dermis just below the epidermal cell column.

Although electrophysiological investigations indicate Eimer's organs are sensitive to mechanosensory stimuli (Catania and Kaas, 1995; Sachdev and Catania, 2002a,b), how the different components of Eimer's organs function remains largely unexplored. The goal of this study was to characterize the individual neural components of Eimer's organ to better understand how this structure transduces tactile information. We used the styryl pyridinium dye AM1-43 to examine the distribution of mechanoreceptive elements while simultaneously appraising the utility of AM1-43 as an anatomical marker for primary sensory afferents. In addition, we explored the primary afferent terminals through

immunocytochemical analysis and revealed innervation patterns of the receptors with the carbocyanine dye DiI.

Materials and Methods

Experimental Animals: Five coast and seven star-nosed moles were examined. Coast moles were provided by Dr Kevin L. Campbell of the University of Manitoba. Star-nosed moles were collected in Potter County under permit COL00087. All procedures followed guidelines for the care and use of laboratory animals from the NIH and were approved by the Vanderbilt University Institutional Animal Care and Use Committee.

AM1-43 Labeling: AM1-43 experiments in coast moles were performed in conjunction with terminal electrophysiology experiments. Each mole was injected intraperitoneally (IP) with a 3mg/kg dose of AM1-43 (Biotium, Hayward, CA) mixed in sterile saline. The animals were allowed to forage and tunnel overnight and then anesthetized with an IP dose of 1.0 g/kg urethane supplemented with 20 mg/kg ketamine hydrochloride and 0.5 mg/kg xylazine respectively as needed. After recordings animals were euthanized with a 250 mg/kg IP injection of sodium pentobarbital and perfused with 1x phosphate buffered saline pH 7.3 (PBS) followed by 4% paraformaldehyde (PFA) in PBS. The dye remained in the system of these animals for an average of 30 hours (ranging from 25-33.5 hrs) before sacrifice. Star-nosed moles were injected with 3mg/kg of AM1-43 in sterile saline; one half IP and the other half sub-cutaneously. One star-nosed mole was injected, returned to its cage for one hour, and then sacrificed and

perfused as described above. The remaining 5 star-nosed moles were first anesthetized with a 1.0 g/kg IP injection of urethane (15% weight/volume) followed by administration of 20 mg/kg ketamine as needed. The left surface of the nose was then brushed back and forth with a piezo-electric driven probe for 5 minutes before it was sacrificed and perfused as outlined above.

The star was post-fixed in 4% PFA in PBS at 4^{o}C overnight and then cryoprotected in 30% sucrose in PBS. The noses of the coast moles and star-nosed moles were sectioned at 15 and 10µm respectively on a Leica SM 2000R microtome. Sections were stored in 4% PFA in PBS for 48 hours to reduced background staining. The sections were mounted on a subbed cover slip and covered with 3 drops of glycerin as a mounting medium. Cyanoacrylate adhesive was placed along each edge of the cover slip, with spaces at the 4 corners and a second cover slip was laid over the samples to allow viewing from either side.

Immunocytochemistry: Coast moles were sacrificed and perfused as described above. The rhinarium was post-fixed in 4% PFA in PBS for 3 hours at 4^{o}C then cryoprotected in 30% sucrose at 4^{o}C. For neurofilament 200 and substance P labeling tissue was first equilibrated and embedded in Tissue-Tek Optimal Cutting Temperature Compound (VWR Scientific, Westchester, PA) and cut on a Jung CM3000 cryostat at 10µm (similar results were obtained cutting on the sledge microtome and mounting in glycerin). Sections were mounted on Superfrost plus slides (VWR Scientific, Westchester, PA) and after staining were cover-slipped with Fluoromount-G (Southern Biotech, Birmingham, AL). Sections were surrounded by a hydrophobic wall with an

Aqua-Hold pap pen (SDL Inc. Des Plains, IL), blocked with PBS (pH 7.4) containing 0.1% Triton X-100 and 10% normal goat serum (NGS) for 1 hour at room temperature. Sections were incubated overnight at 4°C with guinea pig anti-substance P antiserum diluted 1:20,000 (kindly provided by Dr. John Maggio) and mouse anti-neurofilament 200 (Sigma-Aldrich, St Louis, MO) diluted 1:800 in PBS containing 1% NGS and 0.1% Triton X-100. Following 4 washes with 0.1% Triton X-100 in PBS sections were incubated at room temperature for 1-2 hours with AlexaFluor 594-coupled goat anti-guinea pig and AlexaFluor 488-coupled goat anti-mouse secondary antibodies diluted 1:1000 (Molecular Probes/Invitrogen, Carlsbad, CA) in PBS containing 1% NGS and 0.1% Triton X-100. After 4 washes sections were cover-slipped as described above.

DiI Labeling: After perfusion an appendage was removed from the star and a wooden probe was used to diffusely apply DiI crystals (1,1'-dioctadecyl-3,3,3',3'-tetramethylindocarbocyanine perchlorate; Molecular Probes/Invitrogen, Carlsbad, CA) to the exposed nerve. The appendage was embedded in 2% agarose in PBS, immersed in 4% PFA, and stored in darkness for 3 weeks.

Imaging: Images of the AM1-43, NF 200 single-label and DiI treated tissue sections were collected using a Zeiss Upright LSM510 confocal microscope. Measurements were made using the Zeiss LSM Image Browser version 3,2,0,115. NF 200/subtance P co-labeled tissue was imaged with a Zeiss Axioskop and captured with a MetaMorph Imaging system (Molecular Devices, Downingtown, PA). Images were

processed for levels, brightness and contrast with Photoshop CS2 9.0 (Adobe Systems Inc., San Jose, CA).

Scanning Electron Microscopy: Tissue was washed in tap water, dehydrated in ethanol, and then critical point dried, mounted on an aluminum stud and sputter coated with gold. The specimens were imaged on a Cambridge 360 Stereoscan scanning electron microscope and processed as above.

Results

Labeling patterns of AM1-43 within Eimer's Organ

Styryl pyridinium dyes have been shown to label mechanosensory cells (Nurse and Farraway, 1989; Balak et al., 1990; Collazo et al., 1994; Gale et al., 2001; Fukuda et al., 2003; Meyers et al., 2003; Cheatham et al., 2004; Nunzi et al., 2004; Alagramam et al., 2005). In this study we used AM1-43, the fixable analog of the styryl pyridinium dye FM1-43 (Renger et al., 2001), to identify and examine the presumptive mechanosensory receptors in the rhinarium of the mole. We were particularly interested in the intraepidermal free nerve endings supplied by myelinated fibers (Catania, 1996), as they may play a part in the transduction of high resolution tactile signals. Here we show robust labeling of each sensory receptor component of Eimer's organ by AM1-43.

Fig. 3. Confocal image of Eimer's organ in an AM1-43 treated coast mole. This view shows the position and arrangement of the different sensory receptor units. The central column free nerve endings (**FNE**) rise up through the epidermis and terminate at the stratum corneum. The Merkel cell-neurite complexes (**MC**) reside within the stratum germinativum. A lamellated corpuscle (**LC**) (paciniform corpuscle) is situated in the dermis. Scale bar = 20 μm.

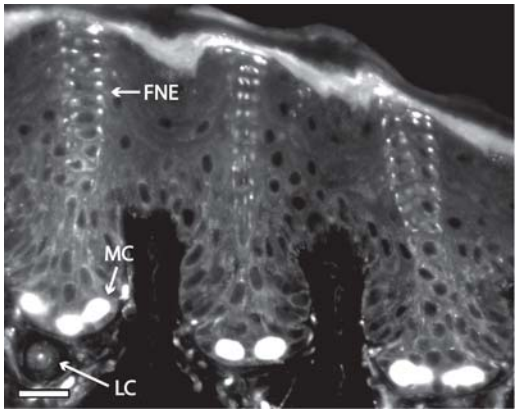
FNE
MC
LC

Coast Mole Intraepidermal free nerve endings: In the coast mole, the structure of the intraepidermal free nerve endings associated with the central cell column was clearly visible 25 to 33 hours after systemic injection of AM1-43 (Figs. 3-4). The column of epidermal cells with its accompanying nerve fibers formed the central core of each Eimer's organ. The nerve terminals associated with the column extended from basal layers of the epidermis to the outer skin surface in a circular arrangement, with one to three fibers in the center and a series of 8 to 24 satellite fibers around the perimeter of the column (Fig. 4*A*).

Along their course through the central column, each neurite exhibited a series of brightly labeled swellings that increased in size close to the outer skin surface. The swellings were connected in bead-on-a-string fashion by a thin neurite (Fig. 4*B*). Interestingly, AM1-43 labeling was also observed in terminal swellings within the stratum corneum.

A second ring of smaller free nerve endings was variably apparent peripheral to the central cell column (Fig. 4*C*). These smaller fibers also had a bead-on-a-string morphology. The path of the peripheral fibers was convoluted and appeared to follow the borders between the epithelial cells at a distance of 1 to 2 cell diameters from the central column.

Star-Nosed Mole Intraepidermal free nerve endings: In the star-nosed mole the structure of the free nerve endings was revealed by AM1-43 five minutes after systemic

Fig. 4. Confocal images showing AM1-43 labeling in Eimer's organ of the coast mole and star-nosed mole (**A-F**) and star-nosed mole (**G-L**). (**A)** A horizontal section near the middle of the cell column showing a ring of 22 satellite nerve endings surrounding the central nerve fibers in the coast mole. (**B**) Brightly labeled varicosities (**arrowheads**) connected by thin neurites (**arrow**) give the free nerve ending terminals a bead-on-a-string appearance. (**C)** Vertical section in the coast mole showing short lengths of peripheral fibers on both sides of the central cell column fibers (**arrows**). The terminals are smaller than their central column counterparts but have a similar bead-on-a-string morphology (**arrowheads**). (**D**) Clustering of Merkel cell-neurite complexes at the base of the coast mole organ. (**E**) Magnified view of a Merkel cell-neurite complex (**MC**) with its characteristic lobulated nucleus (**NUC**) and terminal neurite disk (**ND**). The division is visible between the terminal neurite disk and the Merkel cell (**arrowhead**). (**F**) A vertical section through a lamellated corpuscle. The terminal neurite (**TN**) is aligned within the capsule (**CAP**) parallel to the skin surface. The whole complex sits directly below the epidermis (**EP**). (**G**) Horizontal section from a star-nosed mole approximately 15 µm below the apex of the Eimer's organ showing 7 satellite fibers surrounding a single central fiber. The second ring of smaller diameter peripheral fibers is evident (**PF**) surrounding the center and satellite fibers. (**H**) Horizontal view of the most superficial free nerve ending terminals of an Eimer's organ. The swellings of the satellite free nerve endings extend inward in close apposition to the central swelling. (**I**) Horizontal section showing star-nosed mole Eimer's organs in a hexagonal array. The central free nerve endings (**arrowhead**) are surrounded by the peripheral ring of smaller, less organized, nerve terminals (**arrow**). (**J**) Horizontal view showing the AM1-43 labeled neurite disk (**arrow**) and afferent neuron (**arrowhead**) of a single Merkel cell-neurite complex. (**K**) Vertical view of a Merkel cell-neurite complex. Note the higher level of staining of the neurite disk (**ND**) compared to the Merkel cell (**MC**). (**L**) Horizontal section showing a lamellated corpuscle. The terminal neurite (**arrow**) runs through the center of the capsule (**arrowhead**). Scale bars = 10 µm in A, B, E, F, H, J, K and L. Scale bars = 20 µm in C, D, G, and I.

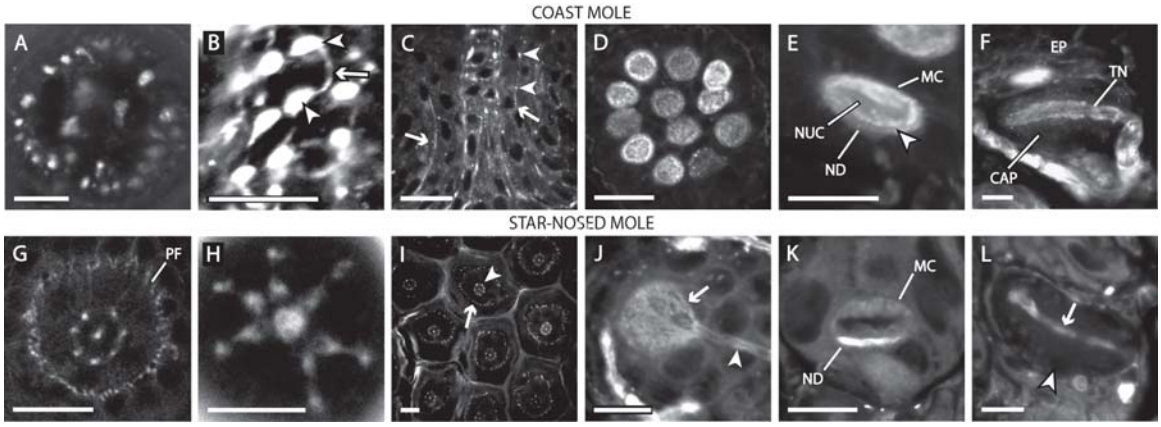
COAST MOLE
A
B
C
D
E
MC
NUC
ND
F
EP
TN
CAP
STAR-NOSED MOLE
G
PF
H
I
J
K
MC
ND
L

injection accompanied by mechanosensory stimulation (Fig 4). Star-nosed moles have Eimer's organs that are smaller than those of other mole species. As a result, several features of the star-nosed mole Eimer's organ are unique. For example, the central cell column in star-nosed moles is only one cell in diameter, forming a single stack of keratinocytes (Catania, 1996). This leaves less room for free nerve endings associated with the column, and as might be expected, there are fewer satellite fibers in star-nosed mole Eimer's organs. Typically, one central fiber was surrounded by five to ten satellite fibers.

At the top of the cell column, the terminal swellings of the neurites in the star-nosed mole form a concise geometric pattern with a single swelling in the center surrounded by a ring of closely opposed terminal swellings from the satellite fibers (Fig. 4*H*). This remarkable configuration of nerve terminals is the predictable result of reducing the size of the Eimer's organ in the coast mole (the likely ancestral condition for moles) to that observed in the star-nosed mole (see scales Fig. 2*E, F*).

Finally, AM1-43 consistently revealed the second ring of less organized and thinner free nerve endings surrounding the central cell column (Fig. 5*G*, *I*). These smaller peripheral free nerve endings were located at a distance of one epithelial cell diameter from the central cell column.

Merkel cell-neurite complexes and lamellated corpuscles: The Merkel cell-neurite complexes in the coast mole were brightly labeled after systemic injection of AM1-43. The coast moles had an average of eleven Merkel cell-neurite complexes at the base of the Eimer's organ in the stratum germinativum. These receptor end organs were tightly

packed in a relatively flat circular arrangement (Fig. 4*D*) with the Merkel cells themselves characteristically situated above their respective neurite disks. Both the Merkel cell and the neurite were well-labeled by AM1-43 (Fig. 4*E*). The lobular nucleus of the Merkel cell was visible as well as the division between the Merkel cell and the terminal neurite.

One hour after systemic injection of star-nosed moles AM1-43 also labeled Merkel cells. The terminal neurite disk appeared to be more robustly labeled with AM1-43 than the Merkel cell after this shorter time course of labeling (Fig. 4*K*). Figure 4*J* shows the labeled neurite disk just below the Merkel cell terminating in an expanded filamentous ending. Similar results were seen in the NF 200 immunolabeling in coast moles (see Fig. 5*B*).

AM1-43 also labeled the terminal neurite and primary afferent neuron of the lamellated corpuscles in both species (Fig. 4*F, L*). The lamellated corpuscles were located directly beneath the epidermis, with the long axis of the receptor aligned parallel to the skin surface. The terminal neurites were brightly labeled but the capsule was devoid of label. The most obvious difference between the two species was the occurrence of 1-2 corpuscles in coast moles and only one in star-nosed moles.

Neurofilament 200 Immunocytochemistry

The stereotypical neural structure of Eimer's organ allows convenient comparisons to be made between AM1-43 labeling and immunofluorescence that may reflect the functional characteristics of the receptor terminals. Neurons that are immunoreactive for the heavy chain (200 kDa) neurofilament 200 (NF 200) have been

Fig. 5. Confocal images showing the main neural components of Eimer's organ in the coast mole immunolabeled for neurofilament 200 **(A)** Horizontal section showing the free nerve endings near the middle in the stratum spinosum where the center and satellite arrangement of the nerve fibers is clearly visible. **(B)** Horizontal section showing NF 200 labeling in the base of a Merkel cell-neurite complex. The label appears to be concentrated in a ring around the perimeter of the disk. **(C)** The terminal neurite of the lamellated corpuscle is brightly labeled for NF 200 (**arrow**) while the capsule of the corpuscle is devoid of label (**arrowhead**). Scale bars = 10 µm.

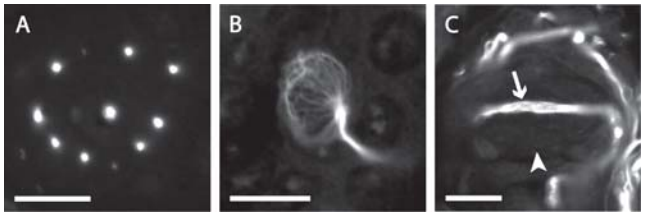
A
B
C

shown to be primarily large diameter myelinated peripheral mechanoreceptors (Lawson et al., 1997; Sann et al., 1995). Here we show that the majority of AM1-43 positive components in the Eimer's organ complex also label for NF 200 (Fig. 5). NF 200 staining was observed throughout the free nerve endings in the central column, but the fibers appeared to become thinner and decreased in luminescence as they approached the stratum corneum where no label was evident.

When viewed from above, the circular configuration of the free nerve endings associated with the central column was clearly evident (Fig. 5*A*). The nerve terminal disk of the Merkel cell-neurite complexes was immunoreactive for NF 200 with the majority of the neurofilaments concentrated in a ring around the periphery (Fig. 5*B*). This pattern was similar to the expanded region of the neurite seen in AM1-43 (Fig. 4*J*) but with a lower intensity of label in the center of the disk. The terminal neurites of the lamellated corpuscles also labeled strongly with NF 200 (Fig. 5*C*).

Neurofilament 200 and Substance P Double Labeling

The two rings of free nerve endings described above (satellite fibers associated with the cell column and the smaller, peripheral fibers that form an outer ring) were of particular interest. Based on location and morphology, it seemed possible they serve different functions. The outer peripheral ring is seldom identified or discussed in accounts of Eimer's organ. In reports from the 19th century there are descriptions of these "peripheral" free nerve endings (Eimer, 1871; Ranvier, 1880) but in later examinations there is only cursory mention of them (Halata, 1972) and in two other reports the

Fig. 6. Fluorescent micrographs of Eimer's organ in the coast mole double labeled for NF 200 (green) and substance P (red). (**A)** The central and satellite free nerve endings label specifically with NF 200 (**arrows**). **(B)** The peripheral free nerve endings are immunoreactive exclusively for substance P (**arrowheads**). **(C)** The overlay shows the lack of co-localization between the two different markers. The convoluted course that the peripheral fibers take to the surface can be seen in contrast to the more direct route taken by the central and satellite fibers. Scale bars = 20 μm.

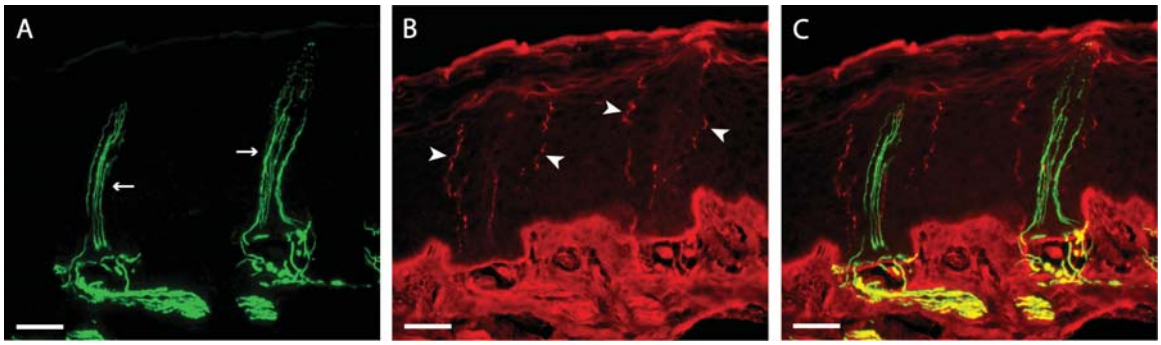
A
B
C

peripheral ring is evident in micrographs but not discussed (Giacometti and Machida, 1965; Quilliam, 1966).

To further explore these different neural components, we used double labeling immunofluorescence for both NF 200 and substance P. Our results provide compelling evidence that these systems play different roles in sensory transduction. Specifically, the fibers associated with the central cell column were labeled exclusively with NF 200 (Fig. 5*A* and 6*A*). However the peripheral ring of finer neurites was labeled for substance P (Fig. 6*B*) a marker for nociceptive primary afferent neurons (Kuraishi et al., 1985; Lawson et al., 1997). A role in nociception is consistent with the location of these peripheral fibers, which encircle the entire organ such that damaging stimuli might be readily detected (see discussion).

DiI Tracing

DiI can be used to trace neuronal pathways in fixed tissues when the cell membrane has been directly exposed to dye crystals. We randomly labeled only a few fibers within a peripheral nerve to explore the patterns of innervation for different components of Eimer's organ in star-nosed moles (Fig. 7). Figure 7*A* illustrates the nerve terminals at the apex of the star-nosed moles' central cell column when all of the afferents are labeled. By sparsely labeling fewer fibers, we found evidence that different fibers supplying the cell column originate from different afferents. For example, we selectively labeled: the satellite fibers of the rings (Fig. 7*B*), the central fiber (Fig. 7*C*), and more often a small portion of the satellite ring (Fig. 7*D*). Importantly, we always

Fig. 7. Confocal images in the horizontal plane of DiI treated free nerve ending terminals within individual star-nosed mole Eimer's organs. (**A**) The central fiber and satellite fibers all labeled with a broad application of DiI crystals. (**B**) Labeling of the satellite fibers only. (**C**) Only the central fiber in this Eimer's organ is labeled. (**D**) DiI label in only three satellite fibers. (**E**) A single Eimer's organ showing the outer ring of peripheral fibers labeled with DiI. There is no label visible in the central and satellite fibers that are denoted by the dashed circle. Scale bars = 5 μm.

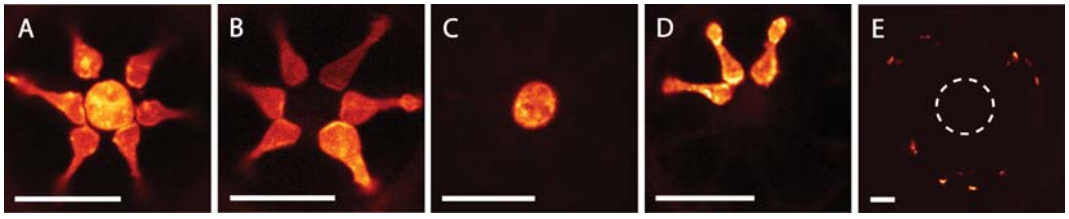
A
B
C
D
E

observed labeling of multiple terminal swellings, suggesting that one afferent branches to supply a number of satellite fibers, consistent with previous observations in star-nosed moles (Catania, 1995).

Finally, the peripheral ring of substance P positive fibers was occasionally labeled (Fig. 7*E*). As would be expected from their unique immunohistochemistry, these were typically labeled independently of other neuronal elements. In each case where the peripheral ring was labeled, a single afferent in the underlying dermis supplied all of the free nerve endings for an organ. We were unable to determine whether it was myelinated, however it was clear that afferents supplying the central cell column fibers were myelinated.

Discussion

In this study we were able to label the different sensory components of Eimer's organ using the fluorescent styryl pyridinium dye AM1-43, immunolabeling for substance P and NF 200, and by using the lipophilic neuronal tracer DiI. The results provide new insights into the structure and possible functions of different components of this sensory organ. They also provide further evidence that AM1-43 is a useful anatomical marker for examining the neural components of mammalian skin.

Anatomy and Function of Eimer's Organ

Eimer's organ was first described by Eimer in the European mole (Eimer, 1871) and has since been found in a number of additional species. This structure is restricted to

moles (family Talpidae, order Insectivora), where it has been identified in most of the 17 genera (Catania, 2000). As illustrated in Figure 2, Eimer's organ is a small but complexly organized receptor organ that includes free nerve endings, merkel-cell neurite complexes, and lamellated corpuscles. The function of this organ has been a matter of speculation since the 1800's, and most investigators conclude it plays a critical role in mechanosensation. This seems obvious from mole exploratory behavior, during which the tip of the nose is repeatedly touched to the ground. However, direct evidence for mechanosensory responses from Eimer's organs was only recently obtained during recordings from the neocortex (Catania and Kaas, 1995; Sachdev and Catania, 2002a,b). Neuronal recordings indicate these organs respond to very slight depressions of the skin surface and responses include both rapidly and slowly adapting classes (Sachdev and Catania, 2002a). This is consistent with the proposed role of Eimer's organ based on anatomical and behavioral studies that indicate moles can make rapid discriminations of objects based on brief contact with the skin of the snout (Catania and Remple, 2005).

Despite these findings, a number of questions remain regarding the function of Eimer's organ. For example, although Merkel cell-neurite complexes and lamellated corpuscles in mammalian skin have been well characterized as slowly and rapidly adapting mechanoreceptors, respectively, the function of the conspicuous free endings associated with Eimer's organ has not been clearly established. These are of special interest, because the central cell column is the defining feature of Eimer's organ, and the associated free nerve endings have a geometric arrangement and structure unparalleled by receptor arrays of most other mammals. Thus one of the goals of the present study was to learn more about the general anatomy, immunohistochemistry, and innervation of Eimer's

organ and to provide additional clues to the possible functions of the different components.

AM1-43 and Immunocytochemistry

One of the most interesting and obvious results of our systemic injection with AM1-43 in moles is the ability to visualize sensory receptors in adult mammalian skin. Although this has been shown in previous investigations of juvenile rodents, we show that AM1-43 is clearly useful for additional mammalian species at various stages of development. The hypothesized mechanism for dye entry, through the associated transduction channels, raises the possibility that AM1-43 could be used for *in vivo* studies of receptor responses in adult mammalian skin. In the present study, we were unable to make enough systematic observations to determine whether stimulation of mechanoreceptors resulted in differential labeling patterns for Eimer's organs.

Each of the components of Eimer's organ was labeled following systemic dye injection in moles. Our current results with AM1-43 are consistent with the mechanosensory hypothesis for Eimer's organ generally and for the free nerve endings within the column specifically. However this is not a definitive test for mechanosensation, as this dye is known to label non-mechanosensitive cells, such as taste buds (Meyers et al., 2003).

By combining the data from AM1-43 with the results of substance P and NF200 immunolabeling, we are able to obtain addition functional clues. Perhaps the most compelling results come from the double-labeling experiments with substance P and NF

200 (Fig. 6). The outermost peripheral ring of free nerve endings was uniquely positive for substance P, whereas the central fibers of the column were positive for NF 200. This strongly suggests the outer ring is composed of high-threshold, peptidergic nociceptors. The outer ring of fibers has been inconsistently reported in previous studies and is seldom included in descriptions of Eimer's organ. This may be due to the smaller size of the fibers (resulting in less consistent appearance in classical silver stains). However the position of these fibers - surrounding the central cell column and associated sensory elements - is ideal for detecting the earliest stages of damage to the organ.

It seems worth pointing out in this regard the critical role nociception probably plays in the maintenance of these receptor arrays. Skin has two important functions - protection of underlying tissues and acting as a sensory surface. These two roles are at odds with one another in Eimer's organ. The skin associated with Eimer's organ is quite thin and vascular (e.g. note the thin stratum corneum covering the organs - Figs. 2, 3) yet these sensory arrays are constantly touched to the soil. As a result, the delicate Eimer's organs of wild-caught specimens invariably show signs of abrasion at the distal end of the snout where most frequent contact occurs (e.g. arrow Fig. 2*B*). It seems there is a delicate balance maintained between the two functions of skin in these species, and nociception probably plays a critical role in this balance. As a testament to the effects of the environment of these sensory arrays, the eastern American mole (*S. aquaticus*) that lives in the driest, most abrasive soil, has an uncharacteristically thick stratum corneum on its rhinarium with degenerate Eimer's organs (Catania, 2000).

In contrast to the peripheral ring of free nerve endings, the fibers associated with the central cell column were not positive for substance P. However, as was the case for

the mechanoreceptor neurites associated with Merkel cells and lamellated corpuscles, the central cell column fibers were positive for NF 200. These results suggest the central cell column fibers are not nociceptive, consistent with the hypothesis they play a role in low-threshold mechanoreception (i.e.: non-noxious touch) (Lawson and Waddell, 1991; Sann et al., 1995).

DiI and Eimer's Organ Innervation

To investigate how the components of Eimer's organ are differentially innervated we randomly labeled small sets of afferents by applying a few crystals of DiI to the exposed nerve in fixed tissue. The results showed that different parts of the central cell column were innervated by different afferents. For example, the central fiber in the middle of the column was often labeled independently. In addition, groups of satellite terminals supplied by single fibers were often separately labeled.

This innervation pattern is similar to what has been reported for the pushrod skin receptors of monotremes (Andres and von During, 1984). Both the push-rod and Eimer's organ include a similar arrangement of intraepidermal free nerve endings (vesicle chain receptors in push-rods) showing the bead-on-a-string appearance (Andres and von During, 1984; Andres et al., 1991; Manger and Pettigrew, 1996). In both organs the fiber terminals form swellings below an epithelial dome at the surface of the skin, and in both organs the terminal nerve swellings are anchored by a basket-like complex of tonofibrils that may play a role in sensory transduction (Andres and von During, 1984; Catania, 1996). Each organ also has Merkel cell-neurite complexes in the base of the epidermal

compartment and lamellated corpuscles in the dermis below. The peripheral ring of fibers outside of the cell column has not been identified in the monotremes, but this has been variably reported in moles and may be similarly hard to discern in monotremes. Thus both monotremes and moles appear to have convergently evolved a similar sensory complex.

It has been suggested that the radial arrangement of free nerve endings within pushrods provides the organs with directional sensitivity to mechanical displacement (Andres and von During, 1984; Andres et al., 1991). This has also been suggested for Eimer's organ (Catania, 2000). We hypothesize that an array of Eimer's organs provides moles with textural information about minute surface features on objects of interest through the differential stimulation of the terminal nerve swellings within the central cell column (see Catania (2000) for more details). The present results are consistent with this hypothesis, however the specific responses of the free nerve endings within the central column remain to be investigated.

References

Alagramam KN, Stahl JS, Jones SM, Pawlowski KS, Wright CG. 2005. Characterization of vestibular dysfunction in the mouse model for Usher syndrome 1F. J Assoc Res Otolaryngol 6:106-118.

Andres KH, von Düring M. 1984. The platypus bill. A structural and functional model of a pattern-like arrangement of cutaneous sensory receptors. In: Iggo A, editor. Sensory Receptor Mechanisms. Singapore: World Scientific Publishing Company. p. 81-89.

Andres KH, von During M, Iggo A, Proske U. 1991. The anatomy and fine structure of the echidna Tachyglossus aculeatus snout with respect to its different trigeminal sensory receptors including the electroreceptors. Anat Embryol (Berl) 184:371-93.

Balak KJ, Corwin JT, Jones JE. 1990. Regenerated hair cells can originate from supporting cell progeny: evidence from phototoxicity and laser ablation experiments in the lateral line system. J Neurosci 10:2502-2512.

Catania KC. 1995. Structure and innervation of the sensory organs on the snout of the star-nosed mole. J Comp Neurol 351:536-548.

Catania KC. 1996. Ultrastructure of the Eimer's organ of the star-nosed mole. J Comp Neurol 365:343-354.

Catania KC, Kaas JH. 1997. Somatosensory fovea in the star-nosed mole: behavioral use of the star in relation to innervation patterns and cortical representation. J Comp Neurol. 387:215-33.

Catania KC. 2000. Epidermal sensory organs of moles, shrew moles, and desmans: a study of the family talpidae with comments on the function and evolution of Eimer's organ. Brain Behav Evol 56:146-174.

Catania KC, Kaas JH. 1995. Organization of the somatosensory cortex of the star-nosed mole. J Comp Neurol 351:549-567.

Catania KC, Remple FE. 2005. Asymptotic prey profitability drives star-nosed moles to the foraging speed limit. Nature 433:519-522.

Cheatham MA, Huynh KH, Gao J, Zuo J, Dallos P. 2004. Cochlear function in Prestin knockout mice. J Physiol 560:821-830.

Collazo A, Fraser SE, Mabee PM. 1994. A dual embryonic origin for vertebrate mechanoreceptors. Science. 264:426-430.

Eimer T. 1871. Die Schnauze des Malwurfes als Tastwerkzeug. Arch Mikr Anat 7:181-191.

Fukuda J, Ishimine H, Masaki Y. 2003. Long-term staining of live Merkel cells with FM dyes. Cell Tissue Res 311:325-332.

Gale JE, Marcotti W, Kennedy HJ, Kros CJ, Richardson GP. 2001. FM1-43 dye behaves as a permeant blocker of the hair-cell mechanotransducer channel. J Neurosci 21:7013-7025.

Giacometti L, Machida H. 1965. The skin of the mole (Scapanus townsendii). Anat Rec 153:31-39.

Halata Z. 1972. Innervation of hairless skin of the nose of mole. I. Intraepidermal nerve endings. Z Zellforsch Mikrosk Anat 125:108-120.

Kuraishi Y, Hirota N, Sato Y, Hino Y, Satoh M, Takagi H. 1985. Evidence that substance P and somatostatin transmit separate information related to pain in the spinal dorsal horn. Brain Res 325:294-298.

Lawson SN, Crepps BA, Perl ER. 1997. Relationship of substance P to afferent characteristics of dorsal root ganglion neurones in guinea-pig. J Physiol 505:177-191.

Lawson SN, Waddell PJ. 1991. Soma neurofilament immunoreactivity is related to cell size and fibre conduction velocity in rat primary sensory neurons. J Physiol 435:41-63.

Manger PR, Pettigrew JD. 1996. Ultrastructure, number, distribution and innervation of electroreceptors and mechanoreceptors in the bill skin of the platypus, Ornithorhynchus anatinus. Brain Behav Evol 48:27-54.

Meyers JR, MacDonald RB, Duggan A, Lenzi D, Standaert DG, Corwin JT, Corey DP. 2003. Lighting up the senses: FM1-43 loading of sensory cells through nonselective ion channels. J Neurosci 23:4054-4065.

Nunzi MG, Pisarek A, Mugnaini E. 2004. Merkel cells, corpuscular nerve endings and free nerve endings in the mouse palatine mucosa express three subtypes of vesicular glutamate transporters. J Neurocytol 33:359-376.

Nurse CA, Farraway L. 1989. Characterization of Merkel cells and mechanosensory axons of the rat by styryl pyridinium dyes. Cell Tissue Res 255:125-128.

Quilliam TA. 1966a. The mole’s sensory apparatus. J Zool 149:76-88.

Ranvier L. 1880. On the termination of nerves in the epidermis. Quart J micr Sci 20:456-458.

Renger JJ, Egles C, Liu G. 2001. A developmental switch in neurotransmitter flux enhances synaptic efficacy by affecting AMPA receptor activation. Neuron 29:469-484.

Sachdev RN, Catania KC. 2002a. Effects of stimulus duration on neuronal response properties in the somatosensory cortex of the star-nosed mole. Somatosens Mot Res 19:272-278.

Sachdev RN, Catania KC. 2002b. Receptive fields and response properties of neurons in the star-nosed mole's somatosensory fovea. J Neurophysiol 87:2602-2611.

Sann H, McCarthy PW, Jancso G, Pierau FK. 1995. RT97: a marker for capsaicin-insensitive sensory endings in the rat skin. Cell Tissue Res 282:155-161.

CHAPTER III

THE FINE STRUCTURE OF EIMER'S ORGAN IN THE COAST MOLE

Introduction

The coast mole is a small burrowing insectivore that lives in moist soil on the northwestern coast of the United States and Canada. These animals use their sense of touch to navigate and forage for food in dark underground tunnels. They typically tap their nose to the substrate and objects of interest while exploring their environment. A close look at the nose reveals a series of small bumps, or papillae, covering the surface of the glabrous rhinarium (Fig. 8a). Each papilla is an Eimer's organ (after Eimer, 1871) and nearly every species of the talpid mole is endowed with these structures (Catania, 2000). Microelectrode recordings from somatosensory cortex indicate that Eimer's organ is acutely sensitive to mechanosensory stimuli and have small receptive fields (Catania and Kaas, 1995; Sachdev and Catania, 2002 a,b). Analysis of foraging behavior with high speed video shows that Eimer's organs are used to make rapid sensory discriminations as moles explore their environment (Catania and Kaas, 1997; Catania and Remple, 2004,2005).

Each Eimer's organ is a complex receptor unit composed of specialized epidermal cells and sensory receptors (Fig. 8b,c). A conspicuous feature of Eimer's organ is the

Fig. 8. Eimer's organ of the coast mole (*Scapanus orarius*). **A:** Scanning electron micrograph of the glabrous rhinarium of the coast mole. Each of the small bumps evident on the surface of the skin represent the tip of an Eimer's organ. **B:** Vertical fluorescent confocal micrograph of an Eimer's organ in an animal treated with the neural tracer AM1-43. The terminal swellings of the central column intraepidermal free nerve endings that course through the center of the organ to the surface of the skin are visible. The Merkel cell-neurite complexes and lamellated corpuscle at the base of the organ are also visible. **C:** A schematic representation of Eimer's organ showing the general organization of the central free nerve ending (**C-FNE**), satellite free nerve endings (**S-FNE**), peripheral free nerve endings (**Per-FNE**), Merkel cell-neurite complexes (**MC**), and lamellated corpuscle (**LC**) with respect to the epidermis, dermis and the stratum corneum (**SC**). Scale bars = 20 μm.

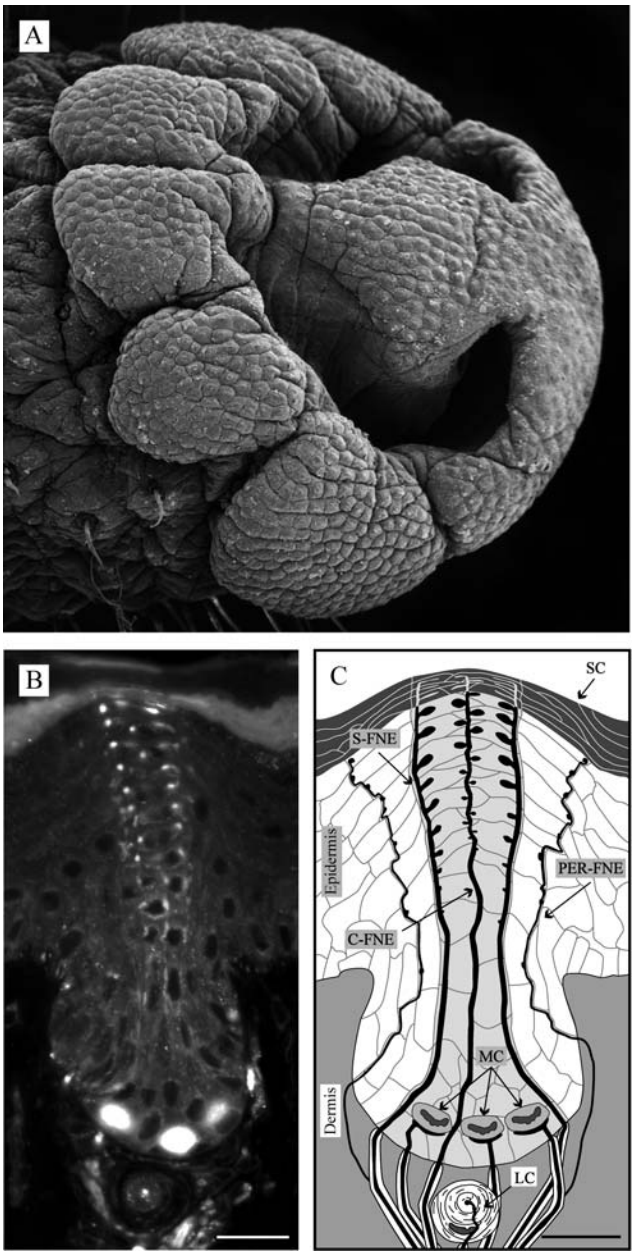
A
B
C
SC
S-FNE
Epidermis
PER-FNE
C-FNE
MC
Dermis
LC

central column (CC) of epidermal cells extending from the dermis to the skin surface. This column is invested with 9-27 intraepidermal free nerve endings (CC-FNEs) that enter the base of the organ and extend in a circular arrangement directly to the skin surface. Recent immunocytochemical analysis support the hypothesis that these nerve endings play an important role in the tactile acuity of the organ (Marasco et al., 2006). A palisade of smaller diameter peripheral intraepidermal free nerve endings (Per-FNEs) is arrayed around perimeter of each organ. These outer terminals are positive for substance P, suggesting they play the major role in nociception. There are generally 7-15 Merkel cell-neurite complexes (MC) at the base of the organ and 1 to 2 lamellated corpuscles (LC) in the dermis below the central cell column.

Eimer's organ is one of the more complex sensory structures to be found in mammalian skin. Our goal in this study was to investigate it's fine structure to provide more detailed information about several newly revealed features and to better understand how its morphology might be related to mechanisms of sensory transduction. In particular, we were interested in the differential morphology of the CC-FNE receptor terminals as they approached and entered the stratum corneum, as a previous investigation (Marasco et al., 2006) suggested they could extend functional terminals into the stratum corneum. We also sought to examine the relationship of the FNEs to the epithelial cells and the state of myelination of the newly characterized Per-FNEs. More generally, we examined the structural details of each receptor class found in Eimer’s organ in the coast mole for comparison with other species.

Materials and Methods

All procedures were approved by the Vanderbilt University Institutional Animal Care and Use Committee and followed the NIH guidelines for the care and use of laboratory animals. Five coast moles (*Scapanus orarius*), provided to us by Dr. Kevin L. Campbell of the University of Manitoba (Winnipeg, Canada) were used. The animals were euthanized with a 150 mg/kg intraperitoneal (i.p.) injection of sodium pentobarbital (Euthasol) and perfused through the heart with 0.1M Na Cacodylate buffer followed by 2.5% Glutaraldehyde in 0.1M Na Cacodylate buffer. Nose tissue containing Eimer's organs was removed and post-fixed overnight in 2.5% Glutaraldehyde in 0.1M Na Cacodylate buffer. The tissue was placed in osmium tetroxide fixative (1%) for 2 hrs on ice then dehydrated in a graded ethanol series and finally transferred to propylene oxide. The tissue was embedded in Spurr's Resin (EM Sciences, Hatfield PA) and thin sections were cut at 90-100 nm with a diamond knife on a Leica Ultracut UCT ultramicrotome. The sections were mounted on grids and stained with uranyl acetate (3-3.5%) and lead citrate (2.5%). The sections were viewed on a Phillips CM-12 transmission electron microscope at 80 kV.

Animals used for immunocytochemistry were euthanized and the tissue was processed as previously reported (Marasco et al., 2006). Briefly, the moles were perfused and the tissue was post-fixed in 4% paraformaldehyde, cryoprotected, sectioned and mounted on slides. Sections were first blocked and then incubated overnight with goat anti-myelin basic protein (MBP) antiserum (Santa Cruz Biotechnology, Santa Cruz, CA) diluted 1:200 and either guinea pig anti-substance P (sP) antiserum diluted 1:20,000

(kindly provided by Dr. John Maggio) or mouse anti-neurofilament 200 (NF-200) (Sigma-Aldrich, St Louis, MO) diluted 1:800. Following washes the sections were incubated with an AlexaFluor 488-coupled rabbit anti-goat antibody (Molecular Probes/Invitrogen, Carlsbad, CA) and either a Texas Red-coupled donkey anti-guinea pig antibody diluted 1:200 (Jackson ImmunoResearch, West Grove, PA) or AlexaFluor 594-coupled donkey anti-mouse antiserum diluted 1:1000 (Molecular Probes/Invitrogen, Carlsbad, CA). After washing the sections were cover-slipped and imaged on a Zeiss Axioskop microscope running MetaMorph (Molecular Devices, Downingtown, PA

The animals used for AM1-43 experiments were treated as previously reported (Marasco et al., 2006). In brief they were injected with AM1-43 (Biotium, Hayward, CA) and then returned to their cages overnight. The dye remained in these animals for an average of 29.5 hours before sacrifice. Following euthanasia and perfusion the nose tissue was cryoprotected and sectioned. Images were gathered using a Zeiss Upright LSM510 confocal microscope (Zeiss, Thornwood, NY). All images were processed for brightness and contrast with Photoshop CS2 9.0 (Adobe Systems Inc., San Jose, CA).

Results

Intraepidermal free nerve endings and associated epithelium. Each individual Eimer's organ on the surface of the mole's nose is formed from an organized group of epithelial cells. The most distinct epidermal specialization evident in these organs is the circular column of epithelial cells that run directly through the center of the organ from the basal layer of the stratum spinosum to the skin surface. The central column (CC) in

Fig. 9. Two horizontal TEM micrographs of the central column in wide view showing the difference in tonofibril concentration between the CC keratinocytes and the surrounding keratinocytes. **A:** A view near the base of the organ. The circular arrangement of cells denoted by the **arrow** is the CC. The cytoplasm of these cells have a more electron-dense appearance than the surrounding epithelium. The **arrowheads** point to the edge of the epidermal papilla at the base of the organ. (Micrograph digitally sharpened.) **B:** Higher magnification view showing the CC keratinocytes with a more dense network of cytoplasmic tonofibrils (**TF**) than the surrounding epithelial cells. The dotted line traces the perimeter of the CC. Three S-FNE nerve fibers (**arrowheads**) and one S-FNE terminal swelling (**double arrowhead**) can be seen in this section.

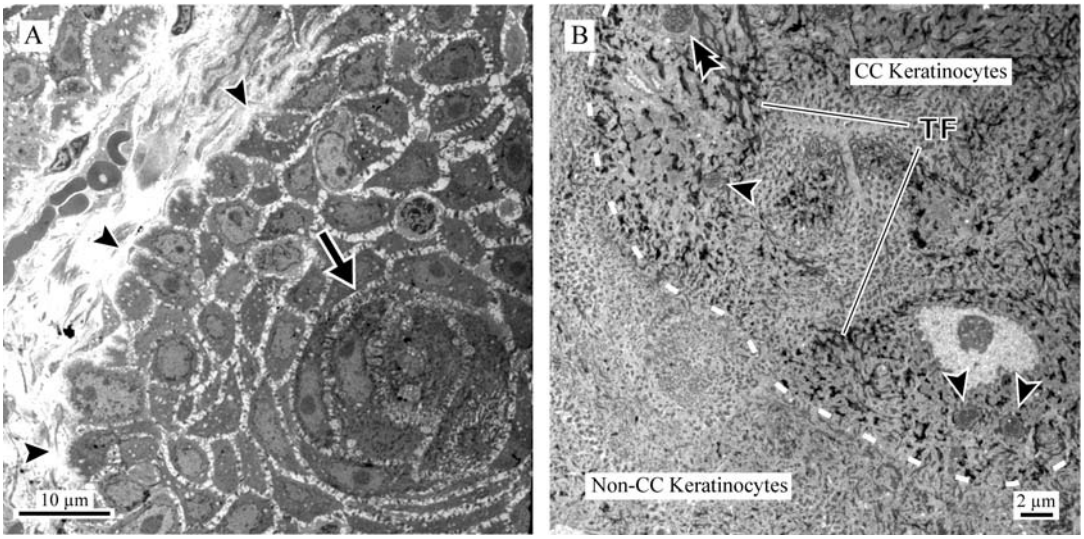
A
10 µm
B
CC Keratinocytes
TF
Non-CC Keratinocytes
2 µm

the coast mole was generally 2-3 cell diameters wide and these keratinocytes were positioned one above the other in a configuration akin to a stack of coins. When viewed from above, the distinct circular shape of the central column was apparent, surrounded by roughly cuboidal epithelial cells (Fig. 9a&10a). The keratinocytes of the central cell column were more electron dense than the surrounding cells (Fig. 9a). Higher magnification images revealed networks of tonofibrils within their cytoplasm that were more densely packed than those of the surrounding epithelial cells (Fig. 9b).

As described in previous investigations, the central column of each Eimer's organ was invested for its entire length with intraepidermal free nerve endings. Satellite FNEs (S-FNEs) resided along the outside edge of the CC and between 1 and 2 central FNEs (C-FNEs) ran directly through the center of the CC (Fig. 10a). The S-FNEs resided within deep invaginations of the CC keratinocyte plasma membranes. The keratinocytes enveloped the S-FNE, surrounding the fibers such that a junction was often formed between two parts of the same keratinocyte (Fig 10b). The junction was held tight with interdigitations and desmosomes in the same manner that attachments were made with adjacent keratinocytes (Fig. 10b). In contrast, the C-FNEs at or near the center of the column did not sit within a deep cleft in the keratinocyte. Instead they were generally at the junction in between the two or three epithelial cells that made up the CC (Fig. 10c).

As the CC-FNEs passed through the epidermis they formed multiple swellings along their course, see Figure 8b&c. This gave the neurites a bead-on-a-string morphology. The nerve fiber that spanned the distance between each terminal was from 0.5-1 μm in diameter. The terminal swellings projected towards the center of the column and in thin section they appeared as spheres (Fig. 10d). The cytoplasm of the CC-FNE

Fig. 10. Multiple views of the central column intraepidermal free nerve ending terminals. **A:** Light micrograph of a toluidine blue stained section taken parallel to the surface of the skin (horizontal section). The arrowheads denote the positions of 8 satellite fibers arranged in a circle around the perimeter of the CC. The **arrow** points to a single central fiber running through the center of the epidermal cell column. **B:** Horizontal TEM micrograph of a single S-FNE showing the terminal (**arrow**) enclosed by a CC keratinocyte. The **arrowheads** point to the junction between the CC keratinocyte and an adjacent epithelial cell. The **double arrowhead** shows where the plasma membrane of the CC keratinocyte doubles back on itself to enclose the S-FNE terminal. **C:** Horizontal TEM micrograph of a single C-FNE. The C-FNE is nested within the junction between two CC keratinocytes (**arrow**). The nuclei of the two cells are in direct apposition to the C-FNE terminal (**NUC**). **D:** Horizontal TEM micrograph of a CC-FNE terminal swelling. Note the dense accumulation of mitochondria (**M**) and small zone filled with microvesicles (**arrowhead**). A group of tonofibrils is clearly evident at the bottom of the picture (**TF**). **E:** Horizontal TEM micrograph of a CC-FNE terminal swelling. This section passed directly through the neck region (**arrow**) that attaches the terminal swelling (**double arrowhead**) to the neurite (**arrowhead**). The neck region appears to be devoid of mitochondria and the plasma membrane has a convoluted appearance. **F:** Vertical TEM micrograph of a CC-FNE terminal swelling. The terminals sit within a base of tonofibrils (**arrowheads**).

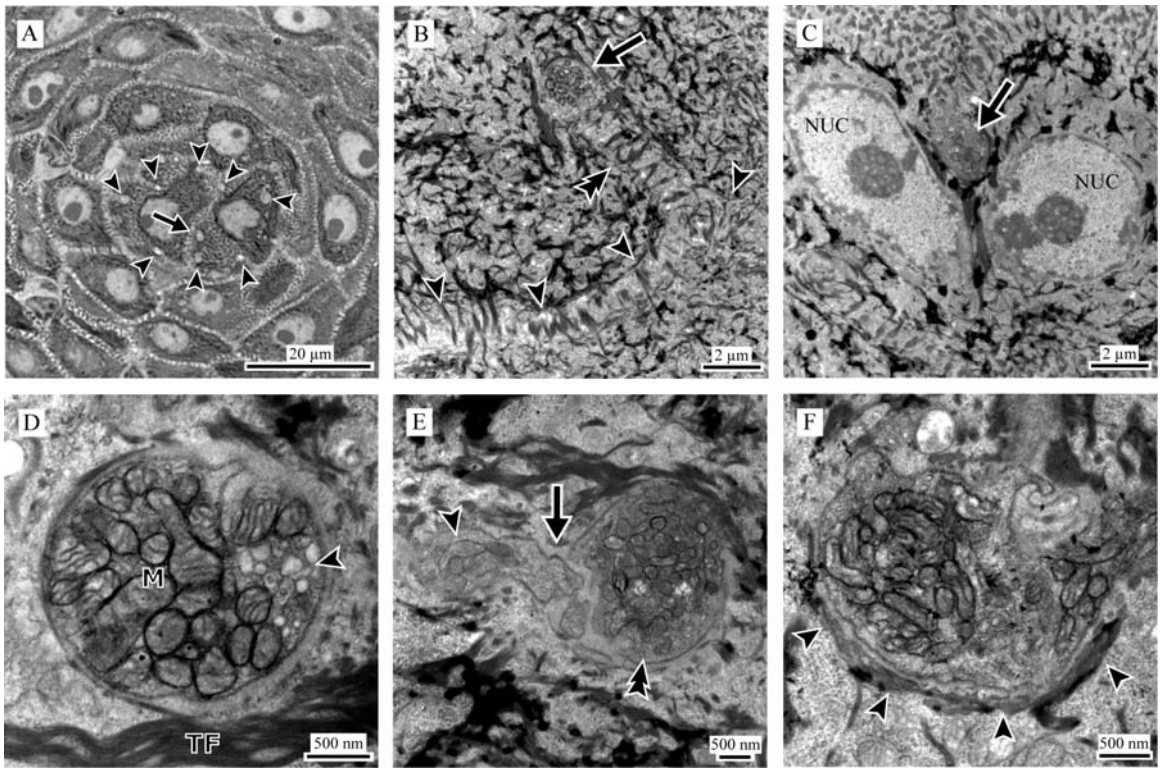
A
20 µm
B
2 µm
C
NUC
NUC
2 µm
D
M
TF
500 nm
E
500 nm
F
500 nm

terminals was densely packed with mitochondria and contained numerous microvesicles that were 75-200 nm in diameter (Fig. 10d). The terminals were approximately 3 µm in diameter and they were connected to the nerve fiber by a convoluted neck region that contained many microvesicles but was generally devoid of mitochondria adjacent to the terminal swelling (Fig. 10e). In favorable sections a thin network of supporting tonofibrils was apparent at the base of the terminal swelling (Fig. 10f).

The structure of the CC-FNE terminals within the stratum spinosum appeared as described above (Fig. 11-b4). As the CC-FNE terminals approached the stratum granulosum (SG) they began to degrade at a distance approximately 15 µm below the base of the stratum corneum (SC). At this level, the mitochondria appeared vacuous and the cytoplasm of the terminals became more homogenous (Fig. 11-b3). This is also at the region where neurofilament 200 labeling became less distinct (Fig. 11c). As the neurite terminals entered the SC their cytoplasm took on an indistinct, nearly homogeneous appearance and the outlines of the numerous mitochondria became obscure (Fig. 11-b2). At more superficial levels in the stratum corneum, just below the outer skin surface, the terminals had degraded further and there were large voids in their cytoplasm and gaps between the terminal and the surrounding keratinized epidermal cells (Fig. 11-b1).

A second ring of small diameter intraepidermal free nerve endings formed a palisade around the CC-FNEs. The peripheral intraepidermal free nerve endings (Per-FNEs) followed a convoluted course to the surface of the organ 1-2 cell diameters removed from the CC (Fig. 12a). In contrast to the circle of CC-FNE's at the margins of the cell column, the Per-FNE's resided within the interstitial space between adjacent epithelial cells. The Per-FNEs also showed swellings intermittently along their course

Fig. 11. The condition of the CC-FNE terminals as they progress through the epidermis. **A:** Vertical fluorescent confocal micrographs of the apical portions of 4 different Eimer's organs in animals treated 29 hrs previously with AM1-43 (scale bars = 10 μm). The stratum corneum (**SC**) can be seen as a bright horizontal band of autofluorescence. AM1-43 labeled CC-FNE terminals can be seen within this band (**arrowheads**). **B:** A schematic rendering of the tip of an Eimer's organ showing the regions (**dotted boxes**) where the representative examples of CC-FNE terminals at various stages of progression through the epidermis were found (B1-B4, TEM micrographs). **B1:** A CC-FNE terminal at the surface of the skin just before being sloughed off. Note the void within the cytoplasm of the terminal and its disengagement from the surrounding keratinocytes. **B2:** A CC-FNE terminal just after entering the SC. The mitochondria appear ghostlike and the cytoplasm has a homogeneous appearance. **B3:** A CC-FNE terminal in the initial stages of degradation nearing the stratum granulosum. The cytoplasm has a heterogeneous appearance and contains numerous microvesicles. However the mitochondria are degrading and appear vacuous. **B4:** A CC-FNE terminal within the stratum spinosum. The mitochondria appear intact and the cytoplasm is heterogeneous with many microvesicles. **C:** Vertical fluorescent light micrograph of an Eimer's organ immunolabeled for NF-200. The dotted white line represents the location of the base of the stratum corneum. The NF-200 immunoreactivity begins to diminish considerably 15-20 μm below the base of the SC.

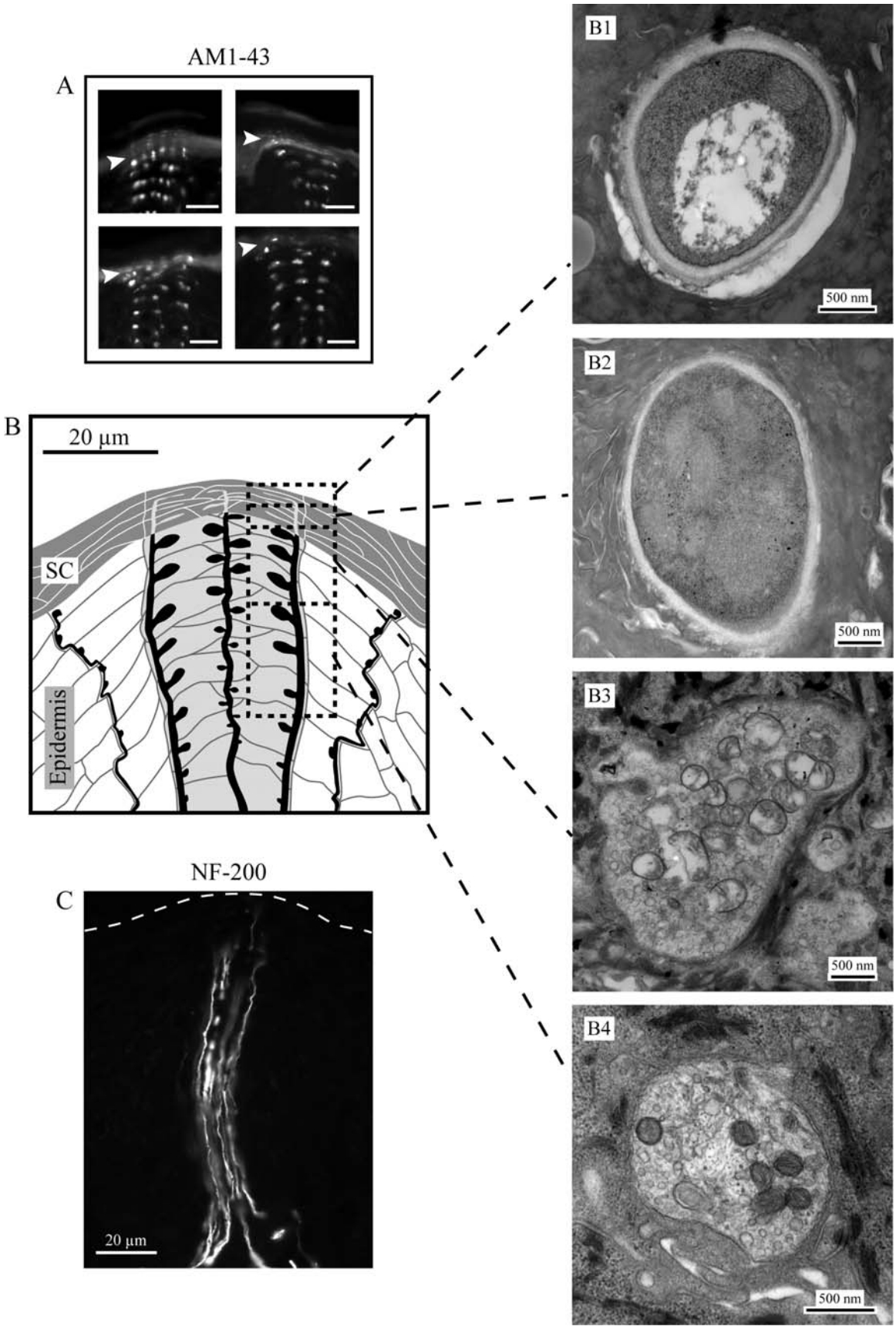
AM1-43
A
B
20 µm
SC
Epidermis
NF-200
C
20 µm
B1
500 nm
B2
500 nm
B3
500 nm
B4
500 nm

Fig. 12. The peripheral intraepidermal free nerve endings. **A:** A schematic representing a horizontal view through the CC showing the concentric relationship of the peripheral free nerve endings (**Per-FNE**) to the satellite free nerve endings (**S-FNE**) and the central free nerve ending (**C-FNE**). The Per-FNEs form a palisade around the CC (filled in grey) and CC-FNEs at a distance of 1-2 cell diameters from the outside edge of the CC. **B:** Horizontal TEM micrograph of a Per-FNE. The terminal can be seen nested within the junction (**arrowheads**) between two different keratinocytes. The cytoplasm of these terminals is relatively sparse in mitochondria and microvesicles. The double arrowhead points to a desmosomal attachment between the adjacent epithelial cells. **C:** This horizontal TEM micrograph within the dermal compartment illustrates the considerable size difference between the Per-FNEs (**arrow**) and the CC-FNEs (**double arrowhead**). There are two Per-FNE fibers within the bundle marked by the **arrow**.

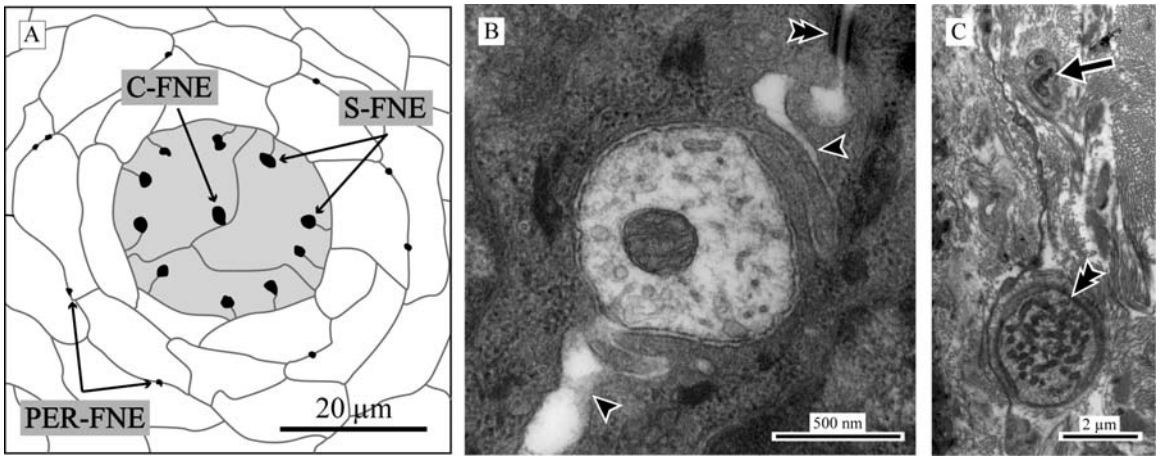
A
C-FNE
S-FNE
PER-FNE
20 µm
B
500 nm
C
2 µm

but no part of the neurites generally exceeded 1 μm in diameter. Much of the cytoplasm of the Per-FNEs was sparsely filled with mitochondria and microvesicles (Fig. 12b). However, occasionally Per-FNEs were densely packed with mitochondria. Figure 12c illustrates the distinct size disparity between the Per-FNEs and the CC-FNEs at the level of the dermis.

As the Per-FNEs exited the epidermis and entered the dermis they immediately converged into small bundles (Fig. 13a). Further down in the dermis, the smaller Per-FNE bundles converged into larger bundles (Fig. 13b). These larger bundles then joined with the large peripheral nerve fascicles that serve each Eimer's organ. At this point the mechanosensory afferents that serve the organs were fully myelinated. However, the Per-FNE bundles within the larger nerves appeared to be un-myelinated (Fig. 13c). Staining of the deep nerve fiber bundles that serve the organs with anti-substance P (sP) and anti-Myelin basic protein (MBP) showed that the sP-positive fibers resided outside and in-between the small rings of MBP immunoreactivity (Fig. 13d-g). MBP is a marker for the peripheral myelin sheath (Mendell and Whitaker, 1978; Kimura et al., 1989). When the nerve fibers are labeled for MBP and NF-200 a different pattern emerged. The labeling for NF-200 was confined within the circles of MBP immunoreactivity (Fig. 13h-j).

Merkel cell-neurite complexes. There was a collection of MCs lying in a flat circular arrangement roughly parallel to the skin surface in the stratum germinativum at the base of each Eimer's organ (Fig. 14a). Each Merkel cell was slightly elliptical with the long axis in parallel to the skin surface and was approximately 10-12 μm at its widest. The deep portion of the cell resided within a cup formed by the closely associated

Fig. 13. An examination of the cellular sheath of the Per-FNEs compared to the cellular sheaths of the mechanosensitive elements of Eimer's organ. **A:** A horizontal TEM micrograph of a small fiber bundle of Per-FNEs within the dermis at the level where the individual neurites have just left the epidermis. The bundle is enclosed within the processes of a single Schwann cell. The **arrowheads** point to the edges of the enveloping Schwann cell. **B:** A horizontal TEM micrograph of a representative Per-FNE bundle deeper in the dermis where multiple fibers have converged to form a larger nerve. **C:** A TEM micrograph of a representative nerve fascicle serving an Eimer's organ in cross section. The large myelinated afferents can be seen as electron-dense rings and the locations of 4 Per-FNE bundles are marked by **arrowheads**. The nucleus of the perineural cell ensheathing the fascicle can be seen clearly (**double arrowhead**). Panels D-J are fluorescent light micrographs of nerve fascicles serving the Eimer's organ array, that are immunoreactive for myelin basic protein (**MBP**), substance P (**sP**), and neurofilament 200 (**NF-200**). Scale bars = 20 μm. **D:** In cross section the immunoreactivity for MBP shows as distinct rings within the nerve fascicle. These MBP+ rings represent the myelin sheaths of the afferent neurons. **E:** Substance P, the marker for the Per-FNEs is seen as small puncta within the nerve fascicle. **F:** The overlay illustrates that the sP+ nerve fibers are unmyelinated because they reside outside of the rings of MBP labeling in positions equating to those seen in panel C of this figure. **G:** A longitudinal overlay view of 2 sP+ fibers within a nerve fascicle. **H:** The MBP again shows as rings equating to the myelin sheaths of the afferent neurons. **I:** In this panel the NF-200, which labels the mechanosensory elements of Eimer's organs, is seen distributed throughout the nerve fascicle. **J:** In the overlay, NF-200 is present in the center of each MBP+ ring as would be expected for these receptors.

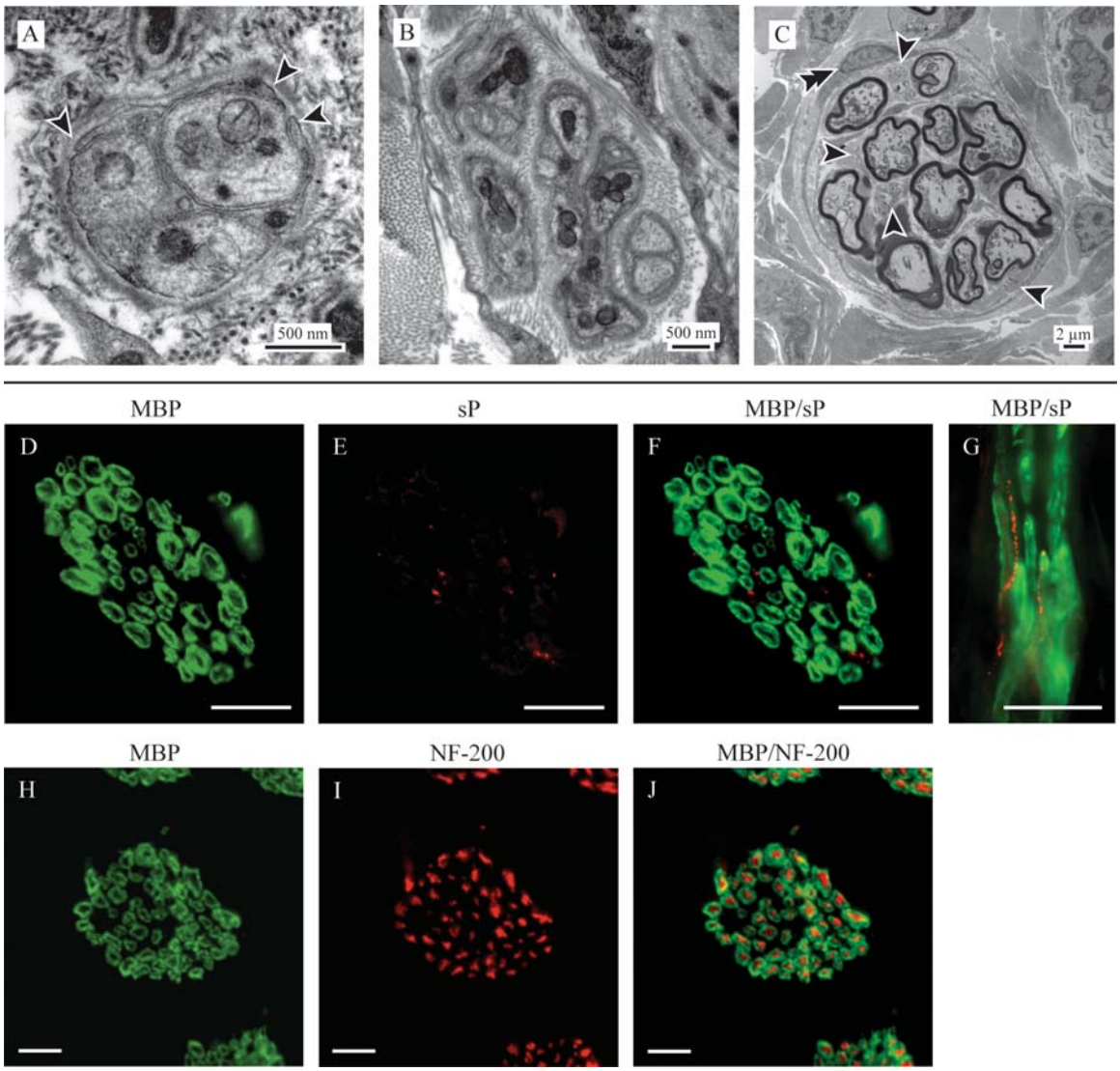
A
500 nm
B
500 nm
C
2 µm
MBP
D
sP
E
MBP/sP
F
MBP/sP
G
MBP
H
NF-200
I
MBP/NF-200
J

Fig. 14. Merkel cell-neurite complexes. **A:** A horizontal TEM micrograph of the base of an Eimer's organ. The edges of the epidermal papilla projecting into the dermis are marked by **double arrowheads**. There are 6 MCs arrayed in a circle visible within a single plane (**arrowheads**). **B:** A vertical TEM micrograph of a single Merkel cell-neurite complex showing the characteristic lobulated nucleus (**N**) of the Merkel cell and the adjoining dish shaped terminal neurite disk (**arrow**). The rod like extensions of the Merkel cell can be seen extending into adjacent keratinocytes (**arrowheads**). There are a number of dense cored vesicles within the region between the nucleus and neurite disk (**double arrowheads**). **C:** A close view of the region between the terminal neurite disk (**TN**) and the nucleus (**N**). The dense core vesicles can be seen as dark inclusions. The inset shows a close-up view of a single vesicle. There is a circular electron-dense (**double arrowhead**) region surrounded by a membranous envelope (**arrowhead**).

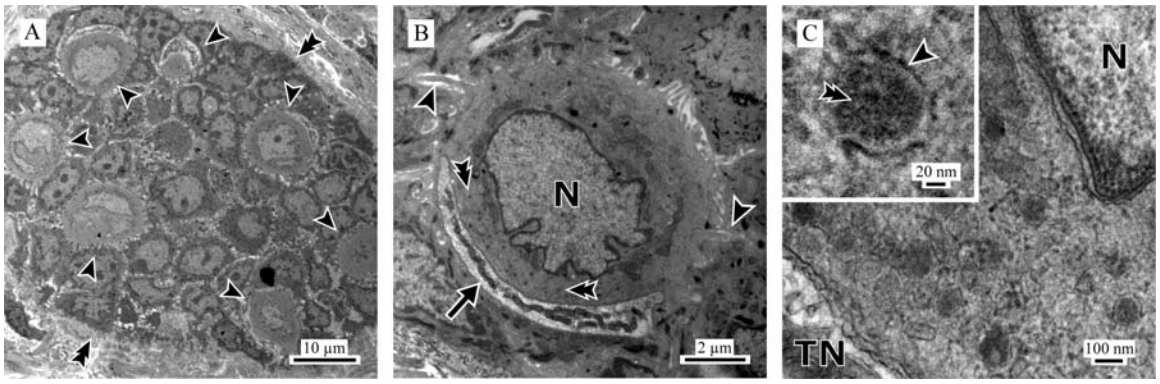
A
10 µm
B
N
2 µm
C
20 nm
N
TN
100 nm

terminal neurite disk. The terminal neurite itself was filled with mitochondria and numerous small clear vesicles. The interface between the Merkel cell and surrounding epithelial cells was characterized by many small interdigitations and desmosomal connections. The junctions at the lateral aspects of the cell tended to be larger than those found on the superficial portion. In addition, there were multiple rod-like extensions of the Merkel cell cytoplasm that penetrated deep into cytoplasmic invaginations in the adjoining epithelial cells. The processes themselves were devoid of desmosomes, however desmosomes were present at the base of each extension. The nucleus of the Merkel cell was multilobulated and occupied a considerable portion of the center of the cell. Golgi complexes were positioned in the cytoplasm superficial to the nucleus. There were numerous mitochondria in the cytoplasm and they tended to be mostly concentrated around the nucleus outside of the region between the nucleus and the neurite disk (Fig. 14b). The cytoplasm between the nucleus and terminal neurite contained multiple membranous dense cored granules (Fig. 14c).

Lamellated corpuscles. There were between 1 and 2 lamellated corpuscles (LC) located in the dermis directly beneath the epidermal central column cells of each Eimer's organ. These corpuscles were approximately 17.5 µm in diameter and 45 µm long. Each LC was innervated by a single terminal neurite aligned parallel to the surface of the skin. The terminal neurite was elliptical in cross-section, approximately 3.5 µm across the widest axis, and contained multiple mitochondria and small vesicles. Two distinct concentric zones of lamellations surrounded the neurite. There was a 4 µm thick, layered, electron-lucent zone that surrounded the terminal neurite and a 3-4 µm thick zone of

Fig. 15. Lamellated corpuscles. **A:** A TEM micrograph of a single lamellated corpuscle in cross section. The terminal neurite (**TN**) is enclosed within the hemilamellations of the internal core (**arrowhead**), followed by the circular lamellations of the outer core (**double arrowhead**). The TN, inner core, and outer core are enclosed by the outer capsule (**arrow**) which appears as a collection of large circularly lamellated cells with electron dense cytoplasms. **B:** A TEM micrograph of a lamellated corpuscle in cross section cut at a slightly different angle than A. The inner core (**arrowhead**), outer core (**double arrowhead**) and outer capsule (**arrow**) are evident however the entire capsule surrounding the terminal neurite appears as 2 ellipsoid caps. This configuration is similar to the configuration of the lamellated corpuscles in the mole as reported by Andres and von During (1973). A filopodial structure extending into the cleft between the hemilamellations is also evident (**F**). **C:** A close-up TEM micrograph of the terminal neurite in B. The terminal neurite is densely packed with mitochondria and microvesicles (**double arrowhead**). The filopodial structure (**arrow**) extends into the cleft of the hemilamellations and is devoid of mitochondria.

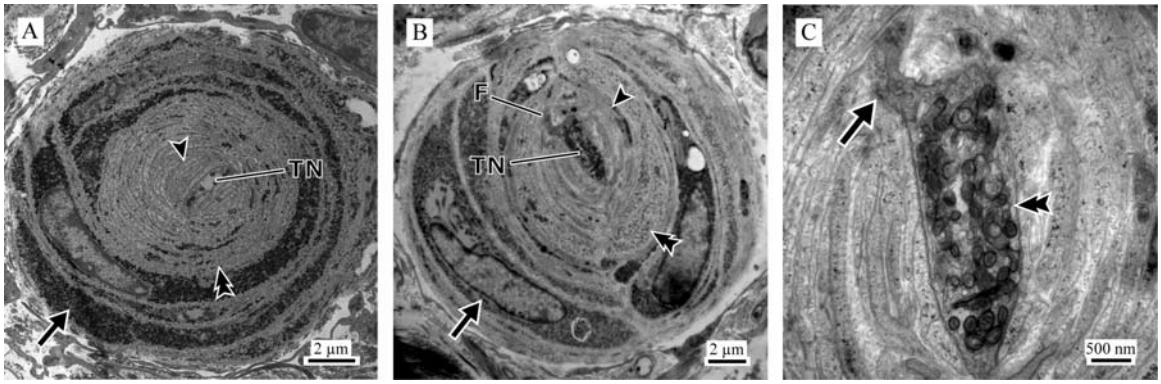
A
TN
2 µm
B
F
TN
2 µm
C
500 nm

circularly layered cells that had a grainy, electron-dense, cytoplasm surrounding the internal region (Fig 15a). Within the lighter inner region multiple layers of bilaterally symmetrical hemilamellae were seen in close apposition to the neurite. These hemilamellae extended approximately 2 µm out from the terminal neurite. Occasionally an extension of the terminal neurite extended perpendicularly from the central axis into the cleft between the hemilamellae (Fig. 15b&c). This structure was similar to the filopodia described by Bolanowski et al. (1994) and Kruger et al. (2003b). In addition, there was a 2 µm thick band of more concentrically organized lamellations surrounding the hemilamellae. These two structures within the lighter zone appeared to correlate to the inner and outer cores that are generally seen in larger Pacinian corpuscles (Pease and Quilliam, 1957; Bolanowski et al., 1994). Three concentric layers of cells with electron-dense cytoplasm formed the outer region. These lamellations were much less tightly wrapped than those within the inner portion of the corpuscle and the nuclei of the cells were clearly visible. This outer region appears similar to the outer perineural capsule of the Pacinian corpuscle (Andres and von During, 1973; Molinovsky et al., 1990, Andres et al., 1991).

Discussion

Eimer's organ of the mole is an interesting mechanosensory complex that is formed from both epidermal and neural specializations. Most other mole species share this particular adaptation, and it appears to play a major role tactile acuity (Catania, 2000). A structure in the monotreme called a push rod also has similar configuration of epithelial cells and sensory receptors (Andres and von During, 1984; Andres et al., 1991;

Manger and Hughes,1992; Iggo et al., 1996; Manger and Pettigrew, 1996). The mole, platypus and echidna all rely on touch to an important extent as they often forage for small prey in environments where there is little visual information. Moles and monotremes appear to have developed a convergent structure, using common components of mammalian skin, to maximize tactile sensitivity.

Tonofibrils and the central column. The most conspicuous feature of Eimer's organ is the circular arrangement of receptor terminals arrayed around the perimeter and at the base of a central column of epithelial cells (Fig. 8). Upon close examination it is evident that the CC epithelial cells have a cytoplasm with a much more dense concentration of tonofibril bundles than the surrounding non-CC epithelial cells (Fig. 9). Tonofibrils serve as a structural support network that imparts rigidity to the cell and provides resilience to mechanical stresses (Janmey et al., 1991; Goldman et al., 1996; Yoon et al., 2001). A similar arrangement of tonofibrils is seen in the push rod and it has been suggested that the CC cells function as a rigid rod (hence the name) that is supported by more flexible cells that can be bent from tangentially applied stimuli or moved up and down with compressive stimuli (Andres and von During, 1984; Manger and Pettigrew, 1996). It is interesting to note that the 19th century anatomist who first described the push rod likened it to the "push" (push-button) of a doorbell and suggested that it served to transmit surface pressure to the terminals at the base of the organs (Poulton, 1885).

It has been proposed that Eimer's organ of the mole may function to bend and conform to objects possibly relating fine textural details (Catania, 2000). The position of

the CC at the center of the organ and extending to the surface of the epithelial dome may provide a means for the entire structure to respond to very slight indentations thus allowing for a high degree of tactile acuity. The CC-FNEs in particular, located in a circular arrangement along the outside edge of the CC, are in an ideal position to register the mechanical stresses within the CC and to register the deflection of the column in different directions (Catania, 2000). This directional sensitivity has also been suggested for the vesicle chain receptors of the push rod (Andres and von During, 1984; Andres et al., 1991). In addition, the more rigid structure of the CC within the surrounding flexible epithelial cells may help to focus mechanosensory stimuli down through the column of sensory terminals from the FNEs at the tip of the organ to the lamellated corpuscles in the dermis below. The punctate nature of the organs and cell column presumably restricts mechanical deflections from being transmitted to wide regions of the skin surface and may play an important role in restricting receptive field size, and conversely increasing tactile acuity (Manger and Pettigrew, 1996; Marasco et al., 2006).

The condition of the central column free nerve endings within the stratum corneum. Studies by Gale et al. (2001) and Meyers et al. (2003) provide evidence that the sensory neural tracer AM1-43, a styryl pyridinium dye, enters mechanosensory cells in an activity dependant manner. Recently this dye was used to label the elements of Eimer's organ in the Coast mole (Marasco et al., 2006). As would be predicted from their proposed mechanosensory function, the terminal swellings of neurites in the central column were heavily labeled after approximately 30 hours. However, it was of great interest to see dye apparent in nerve terminals within the outer layer of stratum corneum.

This result suggested exceptionally superficial nerve terminals might be transducing sensory information in Eimer's organ. This would be surprising, as we are unaware of active sensory terminals in this skin layer in other species, and because ultrastuctural evidence from the star-nosed mole indicates that the CC-FNE terminals are degraded and non-functional in the SC (Catania, 1996). In this study we focused considerable attention on the state of the CC-FNE terminals within the SC of the coast mole to determine if they might be functional from a morphological perspective.

We found that the CC-FNE terminals of the coast mole began the process of degradation in the living epidermis approximately 15 μm from the SC (Fig. 11-b3). As the terminals enter the SG the mitochondria become vacuous and the cytoplasm developed a homogeneous appearance. Once the terminals transitioned into the SC there were only light outlines of the once prominent mitochondria evident and the cytoplasm was entirely uniform in appearance (Fig. 11-b2). Prior to being sloughed off with the enclosing keratinocyte, the terminals developed large internal voids and appear to disengage from the surrounding keratinocytes. It is also interesting to note that immunoreactivity for NF-200 drops off considerably as the terminals approach the SC (Fig. 11c). This zone where the reduction in NF-200 immunoreactivity occurs appears to coincide with the region where the CC-FNE terminals begin to undergo ultrastructural degradation. Together these findings suggest the terminals are not functional as they progress into the SC and appear to degrade at a position even deeper in the epidermis than those of the star-nosed mole. This raises the question of why the terminals should be labeled by AM-143?

The SC directly over the CC in the coast mole is approximately 8 cell layers thick. In mouse the SC of the footpad is 31 cell layers thick and is entirely turned over within 198 hrs (Kvidera and Mackenzie, 1994). Since the mole uses its nose to probe relatively abrasive soil it would be reasonable to assume the rate of turnover for the cells in the nose SC is similar, if not faster, considering the high metabolic rate of insectivores. Using the turnover rate for the mouse footpad SC as a guide, the hypothetical turnover rate for the mole's nose SC could easily be approximately 50 hrs. After 30 hours cells entering the SC would progress over halfway through. This equates well to what is seen in Figure 11a where AM1-43 is found progressing through the SC after being in the system for 29 hrs. It appears that the presence of AM1-43 in the terminals within the SC is most likely due to the retention of label in terminals that were active in the non-keratinized epidermis and were subsequently transported to the SC in the normal progression of epidermal cell layers. Given the morphology of the nerve terminals within the SC (Fig. 11) it seems very unlikely the presence of AM-143 is a reflection of receptor activity at this level in the skin.

Structure of the peripheral free nerve endings and the nature of their cellular sheath. Early anatomists initially described smaller fiber terminals residing outside of the CC in the European mole (Eimer, 1871; Ranvier, 1880) but they were seldom identified in subsequent studies. Their significance and consistency across species remained obscure until a recent a recent investigation with an immunocytochemical marker directed towards substance P (Marasco et al., 2006). This study routinely revealed a

palisade of small free nerve endings surrounding the CC-FNEs that was positive for substance P (Marasco et al., 2006).

In an effort to learn more about the Per-FNEs we examined their general morphology, their relationship to the keratinocytes, and their course within the dermis. The Per-FNEs reside 1-2 cell diameters to the outside of the CC. In our initial confocal study the fibers appeared to follow a convoluted course between the keratinocytes (Marasco et al., 2006). Under EM the fibers were found within the interstitial space between adjoining keratinocytes confirming the suggestion from earlier confocal work. In contrast to the CC-FNEs the Per-FNEs do not reside within a cleft inside the keratinocytes (Fig. 12b). However, as with the CC-FNEs the keratinocytes appear to have a very close relationship with the Per-FNEs though there is no evidence of a direct structural connection. The Per-FNEs are much smaller than their CC-FNE counterparts and tend to have smaller swellings along their length. In addition the Per-FNEs contain far fewer mitochondria and microvesicles than the CC-FNEs (Fig. 12b&c). It should be noted that the morphological qualities of both the CC-FNEs and Per-FNEs correspond well to those reported for the varicose (beaded) and fine (plain) free nerve endings respectively in human digital skin (Cauna, 1980). However, the Per-FNEs in this system appear to lack a distinct axonal reticulum and dense aggregations of microvesicles and appear to differ somewhat from the canine and rodent testicular free nerve endings described by Kruger et al. (2003a), though without serial sectioning the length of the terminals the presence of these structures cannot be ruled out.

In an effort to gain an understanding of the nature of the cellular sheath surrounding the Per-FNEs we used semi-serial sectioning (4 thin sections every 1 μm) to

follow the courses of these fibers deep into the dermal compartment. As the Per-FNEs left the epidermis they immediately coalesced into small bundles with 2-3 separate fibers (Fig. 13a). The bundles were wrapped with a single Schwann cell and as they coursed deeper into the dermis and more small fibers joined together to form larger bundles with no evidence for a myelin sheath (Fig. 13b). Deep within the dermis the Per-FNE bundles converge with the large peripheral nerves that serve the individual Eimer's organs. The large afferents within the peripheral nerves were myelinated, however the Per-FNE bundles, composed of between 3 and 8 fibers, remained unmyelinated and resided in the spaces between the myelinated afferents (Fig. 13c). In previous examinations with immunocytochemical markers the Per-FNEs were found to be immunoreactive for sP and the CC-FNEs, LCs and MCs were immunoreactive for NF-200 (Marasco et al., 2006). We used this distinction to verify the location and state of myelination of the Per-FNEs within the peripheral nerve fascicles that serve the organs. Immunolabeling for sP and NF-200 was compared to immunolabeling for MBP. Within the peripheral nerves NF-200 immunoreactivity was restricted within the circles of MBP (Fig. 13h-j). Conversely, sP immunoreactivity was only apparent outside of the rings of MBP labeling (Fig. 13d-g). The position of the sP labeling in relationship to the MBP and NF-200 labeling correlates well to the position of the Per-Bundles seen with EM. These results suggest that the sP positive components of the peripheral terminal ring are derived from small diameter unmyelinated high-threshold nociceptors.

The structure of the Merkel cell-neurite complexes. The structure of the MCs in the coast mole appears very similar to that typically reported for MC's in many different

species (Munger, 1965; Iggo and Muir, 1969; Andres and von During, 1973; Gottschaldt and Vahle-Hinz, 1981; Munger and Ide, 1988). In particular, the MCs in the coast mole have prominent rod-like cytoplasmic extensions into surrounding keratinocytes and deeply lobulated nuclei. In addition, the MCs also have numerous dense cored vesicles concentrated between the nucleus and the adjacent terminal neurite disk (Fig. 14b&c). Given this, it is reasonable to suggest that the MCs provide a slowly adapting SA-1 signaling component to the Eimer's organ receptor complex (Iggo and Muir, 1969; Gottschaldt and Vahle-Hinz, 1981). The circular arrangement of these receptors around the base of the CC, in conjunction with the presumably more rigid cells of the central column, may also provide these receptors with the ability to code for directional input as provided by differential pressure transmitted through the CC (Quilliam, 1966).

The structure of the lamellated corpuscles. The Pacinian corpuscle in the mesentery of the cat measures 1000 µm by 670 µm (Quilliam and Sato; 1955). The lamellated corpuscles in the coast mole measure approximately 45 µm by 17 µm. Aside from the substantial difference in size between the typical Pacinian corpuscle in the cat and the LC in the coast-mole these two receptor end organs appear to share a number of similarities. In one section in particular, a set of 8 bilaterally symmetrical hemilamellations was evident surrounding the elliptical terminal neurite (Fig. 15a). This 2 µm thick inner core was surrounded by a 1.9 µm thick ring of 10 circular lamellations, most likely representative of the outer core (Pease and Quilliam, 1957; Bolanowski et al., 1994). The inner and outer cores were surrounded by a large 3 µm thick outer capsule consisting of 4 circular lamellations. However, this outer capsule was somewhat different

than the typical Pacinian capsule as it is quite electron dense and is composed of more lamellations than is generally reported (Andres and von During, 1973; Molinovsky et al., 1990, Andres et al., 1991). In addition there was evidence of filopodial structures extending from the terminal neurite into the cleft between the hemilamellations (Bolanowski et al., 1994; Kruger et al., 2003b). Thus despite being smaller than the typical Pacinian corpuscle, the LC of the coast mole has many of the structural components in place that suggest it is a rapidly adapting FA-2 sensory receptor (Loewenstein, 1958, 1961; Sato, 1961).

References

Andres KH, and von During M. 1973. Morphology of cutaneous sensory receptors. In A. Iggo (ed): Handbook of Sensory Physiology. New York: Springer, pp. 3-28.

Andres KH, von Düring M. 1984. The platypus bill. A structural and functional model of a pattern-like arrangement of cutaneous sensory receptors. In: Iggo A, editor. Sensory Receptor Mechanisms. Singapore: World Scientific Publishing Company. p. 81-89.

Andres KH, von During M, Iggo A, Proske U. 1991. The anatomy and fine structure of the echidna Tachyglossus aculeatus snout with respect to its different trigeminal sensory receptors including the electroreceptors. Anat Embryol (Berl) 184:371-93.

Bolanowski SJ, Schyuler JE, Slepecky NB. 1994. Semi-serial electron-micrographic reconstruction of putative transducer sites in Pacinian corpuscles. Somatosens Mot Res. 11:205-18.

Catania KC. 1996. Ultrastructure of the Eimer's organ of the star-nosed mole. J Comp Neurol. 365:343-54.

Catania KC. 2000. Epidermal sensory organs of moles, shrew moles, and desmans: a study of the family talpidae with comments on the function and evolution of Eimer's organ. Brain Behav Evol. 56:146-74.

Catania KC, Kaas JH. 1995. Organization of the somatosensory cortex of the star-nosed mole. J Comp Neurol. 351:549-67.

Catania KC, Kaas JH. 1997. Somatosensory fovea in the star-nosed mole: behavioral use of the star in relation to innervation patterns and cortical representation. J Comp Neurol. 387:215-33.

Catania KC, Remple FE. 2004. Tactile foveation in the star-nosed mole. Brain Behav Evol. 63:1-12.

Catania KC, Remple FE. 2005. Asymptotic prey profitability drives star-nosed moles to the foraging speed limit. Nature. 433:519-22.

Cauna N. 1980. Fine morphological characteristics and microtopography of the free nerve endings of the human digital skin. Anat Rec. 198:643-56.

Eimer T. 1871. Die Schnauze des Malwurfes als Tastwerkzeug. Arch Mikr Anat 7:181-191.

Gale JE, Marcotti W, Kennedy HJ, Kros CJ, Richardson GP. 2001. FM1-43 dye behaves as a permeant blocker of the hair-cell mechanotransducer channel. J Neurosci

21:7013-7025.

Gottschaldt KM, Vahle-Hinz C. 1981. Merkel cell receptors: structure and transducer function. Science. 214:183-6.

Goldman RD, Khuon S, Chou YH, Opal P, Steinert PM. 1996. The function of intermediate filaments in cell shape and cytoskeletal integrity. J Cell Biol. 134:971-83.

Iggo A, Gregory JE, Proske U. 1996. Studies of mechanoreceptors in skin of the snout of the echidna Tachyglossus aculeatus. Somatosens Mot Res. 13:129-38.

Iggo A, Muir AR. 1969. The structure and function of a slowly adapting touch corpuscle in hairy skin. J Physiol. 200:763-96.

Janmey PA, Euteneuer U, Traub P, Schliwa M. 1991. Viscoelastic properties of vimentin compared with other filamentous biopolymer networks. J Cell Biol. 113:155-60.

Kimura M, Sato M, Akatsuka A, Nozawa-Kimura S, Takahashi R, Yokoyama M, Nomura T, Katsuki M. 1989. Restoration of myelin formation by a single type of myelin basic protein in transgenic shiverer mice. Proc Natl Acad Sci U S A. 86:5661-5.

Kruger L, Kavookjian AM, Kumazawa T, Light AR, Mizumura K. 2003a. Nociceptor structural specialization in canine and rodent testicular "free" nerve endings. J Comp Neurol.463:197-211.

Kruger L, Light AR, Schweizer FE. 2003b. Axonal terminals of sensory neurons and their morphological diversity. J Neurocytol. 32:205-16.

Kvidera A, Mackenzie IC. 1994. Rates of clearance of the epithelial surfaces of mouse oral mucosa and skin. Epithelial Cell Biol. 3:175-80.

Loewenstein WR. 1961. On the 'specificity' of a sensory receptor. J Neurophysiol. 24:150-8.

Loewenstein WR. 1958. Generator processes of repetitive activity in a pacinian corpuscle. J Gen Physiol. 41:825-45.

Manger PR, Hughes RL. 1992. Ultrastructure and distribution of epidermal sensory receptors in the beak of the echidna, Tachyglossus aculeatus. Brain Behav Evol. 40:287-96.

Manger PR, Pettigrew JD. 1996. Ultrastructure, number, distribution and innervation of electroreceptors and mechanoreceptors in the bill skin of the platypus, Ornithorhynchus anatinus. Brain Behav Evol. 48:27-54.

Marasco PD, Tsuruda PR, Bautista DM, Julius D, Catania KC. 2006. Neuroanatomical evidence for segregation of nerve fibers conveying light touch and pain sensation in Eimer's organ of the mole. Proc Natl Acad Sci U S A. 103:9339-44.

Mendell JR, Whitaker JN. 1978. Immunocytochemical localization studies of myelin basic protein. J Cell Biol. 76:502-11.

Meyers JR, MacDonald RB, Duggan A, Lenzi D, Standaert DG, Corwin JT, Corey DP. 2003. Lighting up the senses: FM1-43 loading of sensory cells through nonselective ion channels. J Neurosci 23:4054-4065.

Malinovsky L, Pac L, Vega-Alvarez JA, Bozilow W. 1990. The capsule structure of Pacinian corpuscles from the cat mesentery. Z Mikrosk Anat Forsch. 104:193-201.

Munger BL. 1965. The intraepidermal innervation of the snout skin of the opossum. A light and electron microscope study, with observations on the nature of Merkel's Tastzellen. J Cell Biol. 26:79-97.

Munger BL, Ide C. 1988. The structure and function of cutaneous sensory receptors. Arch Histol Cytol. 51:1-34.

Pease DC, Qulliam TA. 1957. Electron microscopy of the pacinian corpuscle. J Biophys Biochem Cytol. 3:331-42.

Poulton E.B. 1885. On the tactile terminal organs and other structures in the bill of *Ornithorhynchus*. J. Physiol. 5:15-16.

Quilliam TA. 1966. The mole’s sensory apparatus. J Zool 149:76-88.

Quilliam TA, Sato M. 1955. The distribution of myelin on nerve fibres from Pacinian corpuscles. J Physiol. 129:167-76.

Ranvier L. 1880. On the termination of nerves in the epidermis. Quart J micr Sci 20:456-458.

Sachdev RN, Catania KC. 2002a. Effects of stimulus duration on neuronal response properties in the somatosensory cortex of the star-nosed mole. Somatosens Mot Res. 19:272-8.

Sachdev RN, Catania KC. 2002b. Receptive fields and response properties of neurons in the star-nosed mole's somatosensory fovea. J Neurophysiol. 87:2602-11.

Sato M. 1961. Response of Pacinian corpuscles to sinusoidal vibration. J Physiol. 159:391-409.

Yoon KH, Yoon M, Moir RD, Khuon S, Flitney FW, Goldman RD. 2001. Insights into the dynamic properties of keratin intermediate filaments in living epithelial cells. J Cell Biol. 153:503-16.

CHAPTER IV

RESPONSE PROPERTIES OF PRIMARY AFFERENTS SUPPLYING EIMER'S ORGAN

Introduction

Moles are experts at finding prey and navigating dark underground tunnels using the tip of their snout to make sensory discriminations. A close examination of the nasal skin of talpid moles reveals a dense array of small (60 μm) raised bumps. These bumps are specializations of the epidermis called Eimer's organs (after Eimer, 1871). Each organ contains Merkel cell-neurite complexes (MCs) lamellated corpuscles (LCs) and a collection of geometrically arranged free nerve endings (FNEs) within a central cell column (Fig 16). Arrays of Eimer's organs are the most densely innervated areas of skin to be found among mammals (Catania and Kaas, 1997) and the predictable arrangement of associated sensory receptors has made them a convenient model system for examining nerve endings. Pioneers of nervous system anatomy, such as Ranvier (1880, 1889) Merkel (1875, 1880) and others (Retzius, 1892; Bielschowsky, 1907; Dogiel, 1903; Botezat, 1903; Kandanoff, 1928; Boeke, 1907, 1932, 1940; Gronweg, 1923) made frequent use of Eimer's organ to examine mammalian sensory receptors.

Eimer's organ has also been of more recent interest (Cauna and Alberti, 1961; Quilliam, 1966 a,b; Andres and von During, 1973; Gorman and Stone, 1990; Catania, 1995a, 1996; Marasco et al., 2006) because the conspicuous and stereotypic structure of associated nerve endings suggests they are performing unique functions that underlie the

Fig. 16. Schematic representations of the structure of the Eimer's organ in the coast mole (*Scapanus orarius*) as viewed from the side (**A**) and from above (**B**). A distinct feature of the Eimer's organ is the central column of epithelial cells that are intimately associated with a number of mechanoreceptive intraepidermal free nerve endings arranged in a ring (C-FNE & S-FNE) that extend from the dermis through the epidermis up to the stratum corneum (SC). A second set of smaller peripheral nociceptive free nerve endings surrounds the central column (PER-FNE). There are a number of Merkel cell-neurite complexes that are arrayed at the base of the Eimer's organ slightly above the dermis (MC) and 1 to 2 lamellated corpuscles (LC) sit within the dermis just below the Merkel cell-neurite complexes. Scale bars = 20μm.

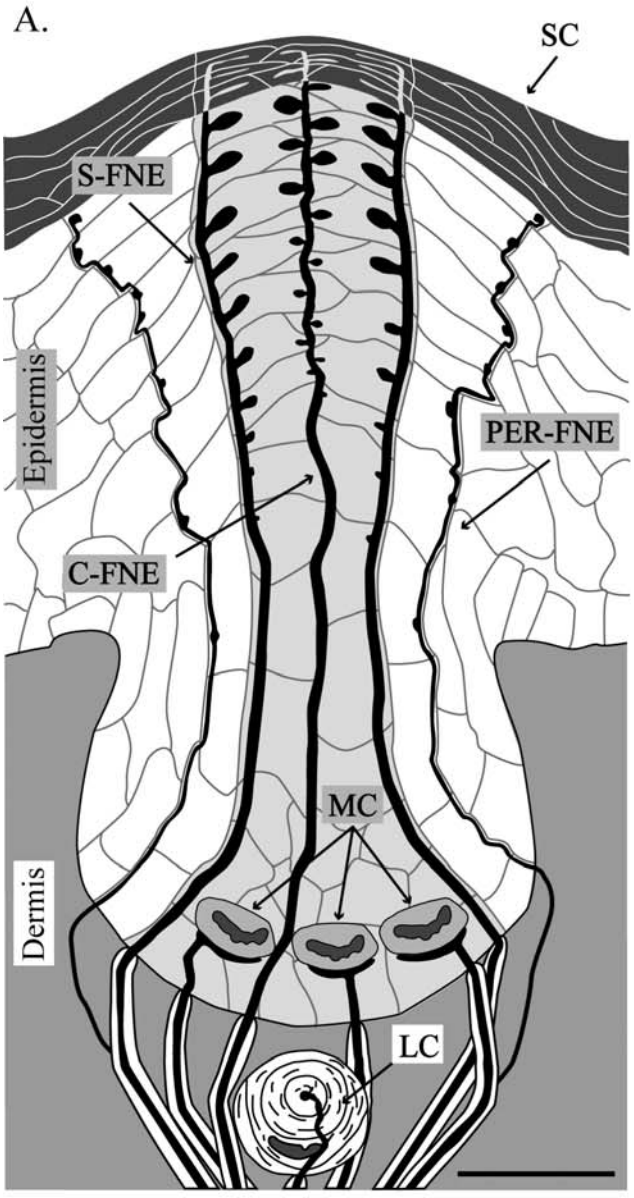
A.
SC
S-FNE
Epidermis
PER-FNE
C-FNE
MC
Dermis
LC
B.
C-FNE
S-FNE
PER-FNE

ability of moles to make rapid sensory discriminations (e.g. Catania and Remple, 2005). It has been suggested from anatomical studies that Eimer's organ could function to detect minute surface textures through the differential deflection of the central cell column and subsequent selective activation of parts of the circular arrangement of associated nerve terminals (Catania, 2000). The circular arrangement of nerve terminals is found in Eimer's organ of nearly every mole species (Catania, 2000) and a similar structure, the push rod, is found in monotremes (Andres and von During 1984; Andres et al., 1991; Manger and Hughes, 1992; Iggo et al., 1996; Manger and Pettigrew, 1996). Comparative evidence indicates that push rods and Eimer's organs are analogous structures and that monotremes and moles independently arrived at the same structural solution for increasing tactile acuity of the skin.

Despite a longstanding interest in the structure and function of Eimer's organ, nothing is known about response properties of the primary afferent neurons that serve the organ and transmit information to the CNS. This is likely because insectivores have been historically difficult to anesthetize for electrophysiological investigations (e.g. Allison and Van Twyver, 1970) and the anatomy of their trigeminal system differs significantly from that found in more common laboratory animals. However advances in the ability to anesthetize small mammals have allowed neural recordings to be made even from small-brained shrews (e.g. Catania et al.,1999) and moles (Catania and Kaas, 1995) and it is now possible to apply these techniques to investigating subcortical components of the CNS as well.

In this study single unit electrophysiological recordings were made from primary afferents at the level of the trigeminal ganglion of star-nosed moles and coast moles to

examine the response properties of receptors within Eimer's organ. A range of different stimuli were used to help distinguish different receptor subclasses and to examine threshold sensitivity to different amplitudes of step displacements and indentation velocities. We also used directionally applied stimuli to assess the ability of the receptors to code for differential displacements of Eimer's organ. Although some of the longer analyses were only possible from a limited number of cells, the results provide important new insights and support the hypothesis that Eimer's organ transduces textural information from objects in the environment.

Materials and Methods

For this study two star-nosed moles (*Condylura cristata*) were collected in Potter County under permit COL00087 and eleven coast moles (*Scapanus orarius*) were provided by Dr Kevin L. Campbell of the University of Manitoba (Winnipeg, Canada). All procedures were approved by the Vanderbilt University Institutional Animal Care and Use Committee and followed the NIH guidelines for the care and use of laboratory animals.

Animals were anesthetized with an intraperitoneal dose of 1.0 g/kg urethane supplemented with 20 mg/kg ketamine hydrochloride and 0.5 mg/kg xylazine as needed. The head was immobilized and the trigeminal ganglion was exposed. Large diameter (0.010"), 12^{o} taper, epoxy insulated tungsten microelectrodes (5 MΩ at 1kHz; A-M Systems Inc. Carlsborg, WA) were used to record responses in the trigeminal ganglion. Data was collected using a Cambridge Electronic Designs (CED) Power 1401 computer

interface and Spike 2 software (Cambridge Electronic Designs; Cambridge, England). After recordings the animals were euthanized with a 150 mg/kg intraperitoneal injection of sodium pentobarbital and perfused with 1x phosphate buffered saline pH 7.3 (PBS) followed by 4% paraformaldehyde (PFA) in PBS and tissue was used in anatomical studies.

Using a Zeiss OPMI Pico surgical stereomicroscope (Zeiss. Thornwood, NY) the receptive field (RF) for each response was determined by hand using a blunted insect pin and drawn on a schematic representation of the mole snout. After determination of the RF a Chubbuck mechanosensory stimulator (Chubbuck, 1966) and a piezo bending element stimulator (Piezo Systems Inc. Cambridge, MA) were applied to the RF to supply compressive and sweeping stimuli respectively.

The Chubbuck stimulator and piezo stimulator were mounted to micromanipulators and were controlled by output voltage from the CED data collection unit. Compressive stimulus was applied with the Chubbuck stimulator through an acrylic tip tapered to a terminal diameter of 0.5mm. The position of the Chubbuck stimulator probe tip was monitored by recording the pickoff circuit output signal in Spike 2. This voltage output was calibrated against the displacement by direct measurement of the tip movement using a projection microscope. The axial direction of the piezo stimulator probe tip sweep was determined by splitting the Power 1401 output voltage prior to linear amplification and recording the change from +5V to -5V in Spike 2. Changes in voltage and polarity equated well to visual examination of the probe tip motion. During data

collection the probe tips, at resting position, were brought into contact with the surface of the nose under close visual examination by stereomicroscope.

Responses to sinusoidal stimuli were measured subjecting each cell to 5 banks of 100 cycles at frequencies of 10, 50, 100, 150, 200, 250, and 300 Hz. Each 5-bank frequency run was repeated at displacement amplitudes of 1, 5, 10, 20, and 28 μm. Following the convention of Gibson and Welker (1983), responses that fired within 98 and 102 times for each set of 100 cycles were considered to be following the stimulus at 1:1 (one impulse per cycle). Any number of responses elicited by the sinusoidal stimuli that occurred less than 98 per 100 cycles were considered to be intermittent. If no responses were elicited at any of these frequencies and displacements then the receptor was subjected to large-displacement sinusoidal stimuli. In these cases the input signal to the Chubbuck was first attenuated to 0 volts for 0 microns displacement then slowly raised to the maximum voltage/displacement possible for each frequency and then brought slowly back down to 0. The displacement ranges for each frequency were as follows: 0-600 μm at 5 Hz, 0-600 μm at 10 Hz, 0-580 μm at 25 Hz, 0-535 μm at 50 Hz, 0-235 μm at 100 Hz, 0-180 μm at 150, Hz and 0-50 μm at 200 Hz. This paradigm allowed us to determine the range of displacements to which cells responded for each frequency of stimulation and could be broken down into 1:1 response ranges, intermittent response ranges, and no-response ranges.

Depression threshold responses were measured in response to step indentations applied in displacement increments of 1, 5, 10, 25, 50, 75, 100, 125, and 150 μm. Each indentation consisted of a square wave that lasted for 500 ms with an 84.5 mm/sec onset and retraction velocity. Five individual banks of 10 indentations were applied at each

displacement increment. The resulting collective responses were considered to be firing at 1:1 only if all 50 indentations elicited a response and any responses that occurred less than 50 times were considered to be intermittent.

Velocity dependant responses were measured with ramp indentations applied with onset velocities of 3.0, 10.0, 25.0, 46.2, and 84.5 mm/sec. Each ramp had a 500 μm displacement and five individual banks of 10 indentations were applied at each onset velocity. Responses elicited across all trials for each velocity were considered to be firing at 1:1 only if all 50 indentations elicited a response and all responses that occurred less than 50 times were considered to be firing intermittently. As part of this analysis, a behaviorally relevant onset velocity of 46.2 mm/sec (see above) was chosen as a test velocity by determining the actual velocity of the nose during touches to objects while the mole foraged. This was calculated by taking high-speed video (125 frames/sec) of the moles in a clear filming chamber (Redlake MASD, Inc., San Diego, CA). The resulting video clips were downloaded to I-Movie (Macintosh Computers. Cupertino, CA) and advanced frame by frame while a landmark on the nose was tracked.

Directional sensitivity was tested with a sweeping stimulus applied parallel to the surface of the skin by a sweeping stimulator made from a 2 mm diameter wooden probe fixed to a bending element (Fig. 17A). The tip of the probe was tapered to 1 mm and rounded. In instances when the directional sensitivity of a cell could be determined by stimulation with a hand-held probe the sweep axis of the bending element was aligned with the direction of maximal sensitivity. The stimulator was swept back and forth across the center of the receptive field in 5 banks of 100 cycles at 2 Hz. The piezo stimulator

Fig. 17. A representation of the directional stimulus (not to scale). **A:** The probe tip was affixed to a piezo electric bending element. Application of a 2 Hz sinusoidal voltage change from +127 to – 127 Volts across the element caused it to sweep back and forth. The stimulator was placed so that it brushed across the Eimer's organs (represented here as raised bumps containing the intraepidermal free nerve endings). **B:** When possible the initial (0^o) sweep of the stimulator was aligned with the apparent preferred direction of the receptor. From that starting axis the stimulator was rotated clockwise in 60^o increments for 2 more successive trials. For receptors that were clearly directional, in that there was little signal generated in directions other than the preferred direction, the stimulator was rotated an additional 60^o to 180^o to verify that the afferent was still active. In this picture the sweep directions have been superimposed over a schematic of an Eimer's organ to illustrate how the movement of the probe tip may serve to apply directional stimulus across an organ in 6 different directions. **C:** This picture illustrates how the stimulator may function to cause the Eimer's organs to signal directional displacements. We hypothesize that the Eimer's organs function as small spring-like columns that are able to conform to small surface features and code positional information related to the direction of maximal displacement (see Fig. 30). We suppose that the stimulator probe is sliding across the surface of the skin and pushing the Eimer's organs over to one side and then the other. When the probe displaces the Eimer's organ to one side the receptor in line with that compression fires an impulse. When the stimulator swings back and displaces the organ in the opposite direction that same receptor is now extended and does not fire.

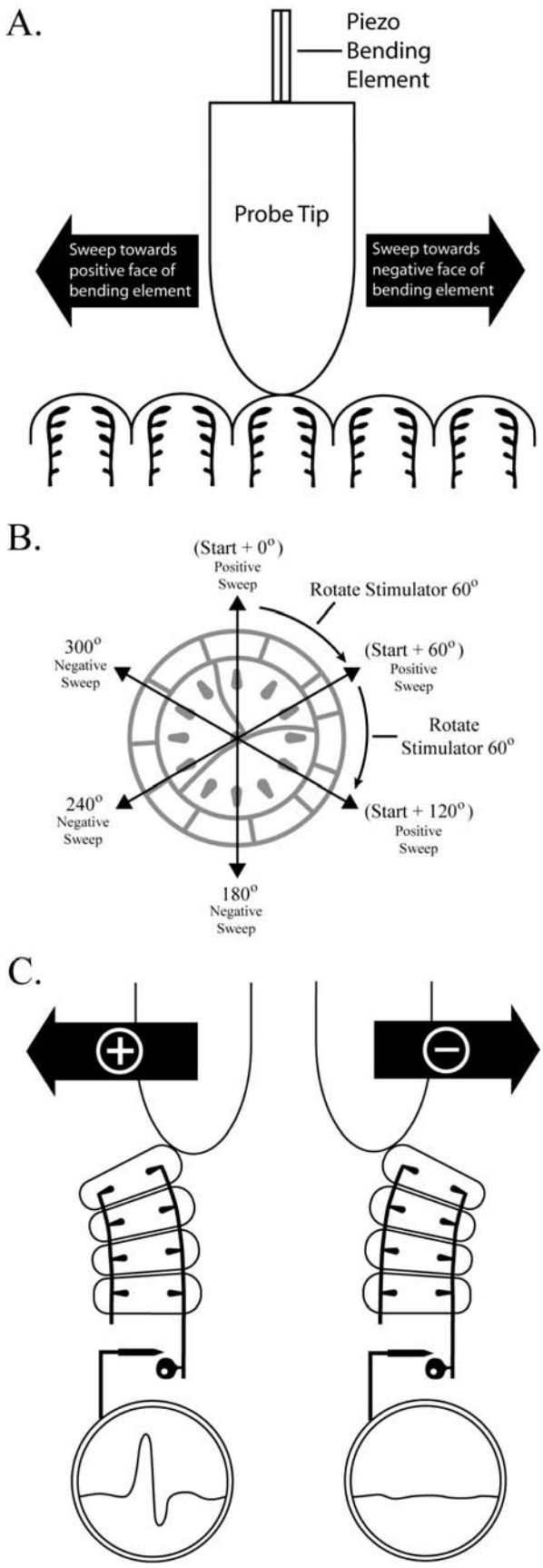
A.
Piezo
Bending
Element
Probe Tip
Sweep towards
positive face of
bending element
Sweep towards
negative face of
bending element
B.
(Start + 0°)
Positive
Sweep
Rotate Stimulator 60°
300°
Negative
Sweep
(Start + 60°)
Positive
Sweep
Rotate
Stimulator 60°
240°
Negative
Sweep
(Start + 120°)
Positive
Sweep
180°
Negative
Sweep
C.

was then rotated clockwise 60^{o} and the 500 cycles were repeated. Following this, the stimulator was rotated another 60^{o} and the 500 cycles were repeated (Fig. 17B). In two cases where there was little activity in directions other than the initial 0^{o} sweep the stimulator was rotated another 60^{o} clockwise to 180^{o} as a control to ensure that the cell was still responding. When no specific directionality could be established with the hand probe the sweep axis was initially aligned in a random direction and then rotated clockwise from that initial axis. For all trials the placement of the stimulator was monitored with the stereomicroscope to make sure that the probe tip remained in direct contact with the RF on both the positive and negative sweeps in all directions at all times. This stimulation paradigm was designed to mirror the hand applied sweeping stimulus that robustly activated directionally sensitive receptors and it was hypothesized that this type of stimulus was pushing the Eimer's organs from side to side causing the receptors to fire differentially depending on displacement direction (Fig. 17C).

The total number of impulses generated in relation to the positive and negative sweeps for each deflection angle were sorted into 60^{o} bins. To facilitate comparisons across all cases the histograms were rotated so that the maximally responsive direction for each case was aligned to 0^{o} and the responses at all of the other directions in each histogram were normalized as a percentage of the maximally responsive direction. After normalization, three different methods of analysis were used to evaluate directional sensitivity of each receptor. The Rayleigh test was used as a liberal measure of directionality (Batschelet, 1981; Fisher, 1993; Zar, 1999). The Rayleigh Z value (Rz) and p values were calculated using Oriana (Kovach Computing Services. Wales, UK) and were considered significant at $p<0.05$.

The tuning ratio (TR) and tuning index (TI) were used as measures of directional sensitivity previously established in the literature (Minnery and Simons, 2003). The TR is the ratio of the average response across all directions to the maximal response and provides a measure of how much greater the maximal response is in relationship to the average response for all the directions. The TR was established for each unit by taking the proportion of responses for each direction compared to the number of responses elicited at the maximally active direction (taken as 100%). The resulting proportions were averaged and divided by 100 to yield the TR. If a TR value is less than 0.5 it means that the maximum response is twice the magnitude of the average response. If all of the responses occurred in a single direction and all 5 of the other directions had no response the TR would equal 0.16, conversely, if all angles had an equal response the TR would be 1. The TI is a measure of the degree of directional tuning for each unit and was derived by determining the number of directions with response proportions that were significantly smaller than the response proportion at the maximum direction. Comparisons between the mean values of the response magnitudes were made at the $p<0.05$ level using the Student-Newman-Kreuls method for pair-wise multiple comparisons. Calculations were performed using SigmaStat (Systat Software, Inc. Point Richmond, CA). For example, a TI of 5 means that all of the directions had a response that was significantly smaller in magnitude than the maximally responsive direction and that this unit is highly directionally responsive. Conversely, a TI of 0 means that all of the directions are not significantly different in magnitude than the maximum and the cell has no preference for any direction.

Fig. 18. Single unit receptive field diagrams for three coast moles that were examined during the qualitative phase of this study. Neurons that were found to be slowly adapting are labeled SA. Neurons that were rapidly adapting are labeled RA. If a receptor clearly responded to directionally applied stimuli it was considered directionally sensitive and labeled DS. Lat.=lateral view, Ant.=anterior view, Vent.=ventral view.

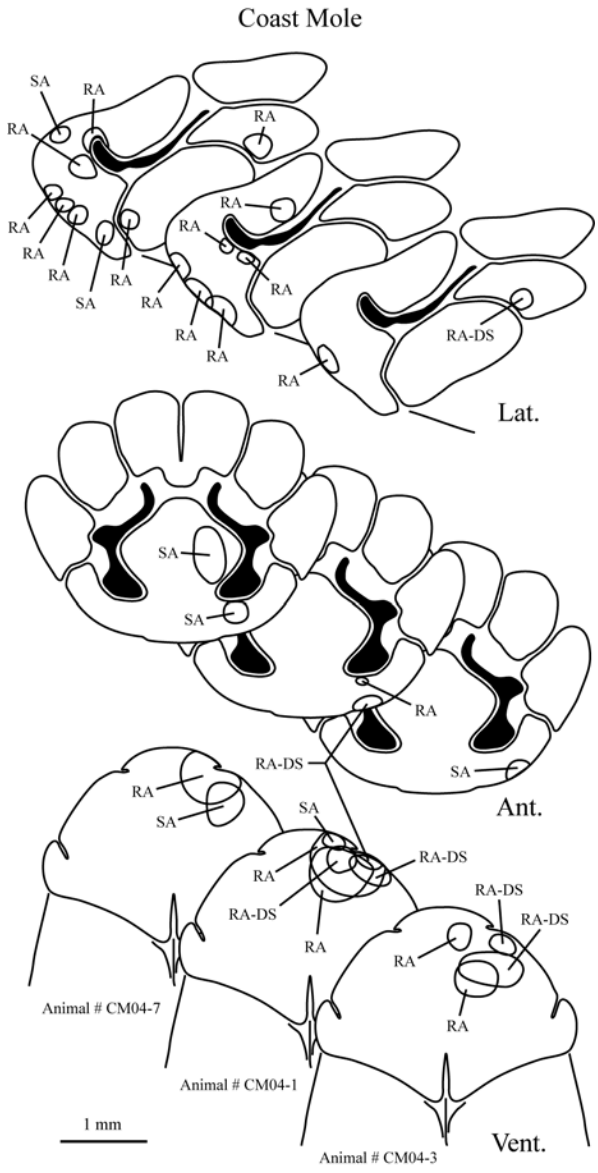
Coast Mole
SA
RA
RA
RA
RA
RA
RA
RA
RA
SA
RA
RA
RA
RA
RA
RA
RA
RA-DS
Lat.
SA
SA
RA
RA-DS
SA
Ant.
RA
SA
SA
RA-DS
RA
RA-DS
RA-DS
RA-DS
RA
RA
RA
Animal # CM04-7
Animal # CM04-1
1 mm
Animal # CM04-3
Vent.

To determine degree of phase locking cycle histograms (CH) were generated from the responses to sinusoidal stimulation for each cell. One hundred impulses collected at the frequency of peak activation were used to construct the CH for each cell so that comparisons of phase locking could be made across all recordings. The location in degrees of each response was calculated with respect to a set starting point for each cycle and bin widths for each histogram were calculated to represent a window of 0.1 ms so that the temporal resolution for each histogram would be equal regardless of frequency. The length of the mean vector [*resultant* (R)] was calculated for each distribution. The *resultant* is used as a measure of the concentration of a circular distribution and has been historically used to indicate the degree of phase locking to sinusoidal stimuli in a number of somatosensory and auditory investigations (Lavine, 1971; Bledsoe et al., 1982; Vickery et al., 1992; Coleman et al., 2001; Mahns et al., 2003). For a CH with a sample size of 100 or more impulses an R value <0.17 indicates no phase locking. Conversely, R values >0.3 are indicative of a very high degree of phase locking (Durand and Greenwood, 1958; Bledsoe et al., 1982; Coleman et al., 2001; Mahns et al., 2003).

Results

Recordings were made from a total of 55 primary afferent mechanosensory neurons serving the glabrous rhinarium of the coast mole. The recording sessions were conducted in two phases, a qualitative mapping phase and a quantitative examination phase.

In the first phase, the activity from 33 neurons was examined. The general mapping experiments in these three animals were undertaken to explore the layout of the

trigeminal ganglion. It was determined that the rostral/medial portion of the ganglion provided the best chances to record from receptors located in the rhinarium (this is consistent with previous investigations in rats - see Gregg and Dixon, 1973). The RF and general response properties were qualitatively documented for each receptor (Fig. 18). The receptors were placed into two broad classes depending on their response to sustained compression of the skin. If the surface of the nose was pushed for a prolonged period with a hand probe and the cell responded only to the onset of the stimulus we considered that neuron to be rapidly adapting (RA). If a neuron responded continuously to the stimulus as it was held against the nose the receptor was classified as slowly adapting (SA). In addition a number of the cells examined also showed an obvious preference to having the probe brushed across the RF in a particular direction. When this type of response was encountered the cell was considered to be directionally sensitive (DS). Of the 33 cells examined in the qualitative phase 26 (78.8%) were RA and 7 (21.2%) were SA. Within the population of RA responses 6 (18% of all of the neurons, 23.1% of the RAs only) responded in a directionally selective manner to stimuli that was applied with the hand-held probe in a brushing motion parallel to the surface of the skin.

In the second phase of the experiments the response properties from 22 cells in 8 animals were quantitatively analyzed with respect to sinusoidal tuning properties, skin indentation thresholds, static displacements, stimulus onset velocity, and directional sensitivity. These neurons were broadly classified as RA or SA by response to a 500 μm static indentation lasting for 500 ms. Within the scope of the quantitative phase 21 (95.5%) of the cells were classified as RA because they responded only to the dynamic

Fig. 19. Peristimulus time histograms showing the representative examples of the 3 primary response profiles found during the quantitative phase of experiments in the coast mole. **A:** A slowly adapting type response with a high dynamic sensitivity and a random sustained discharge. This activity closely resembles the Merkel cell-neurite (SA-I) response profile. **B:** A rapidly adapting type of response showing sensitivity to the changes in the dynamic phase of the indentation with no response to the static portion of the indentation. This activity closely resembles the Pacinian corpuscle (FA-II) response profile. **C:** A rapidly adapting type response that fires a single impulse during the compressive phase of the indentation. These receptors are silent through the static phase and they occasionally fire an impulse during the retraction phase but only when the compression lasts for 500 ms or less. This response profile most likely represents the activity of the mechanosensory intraepidermal free nerve endings.

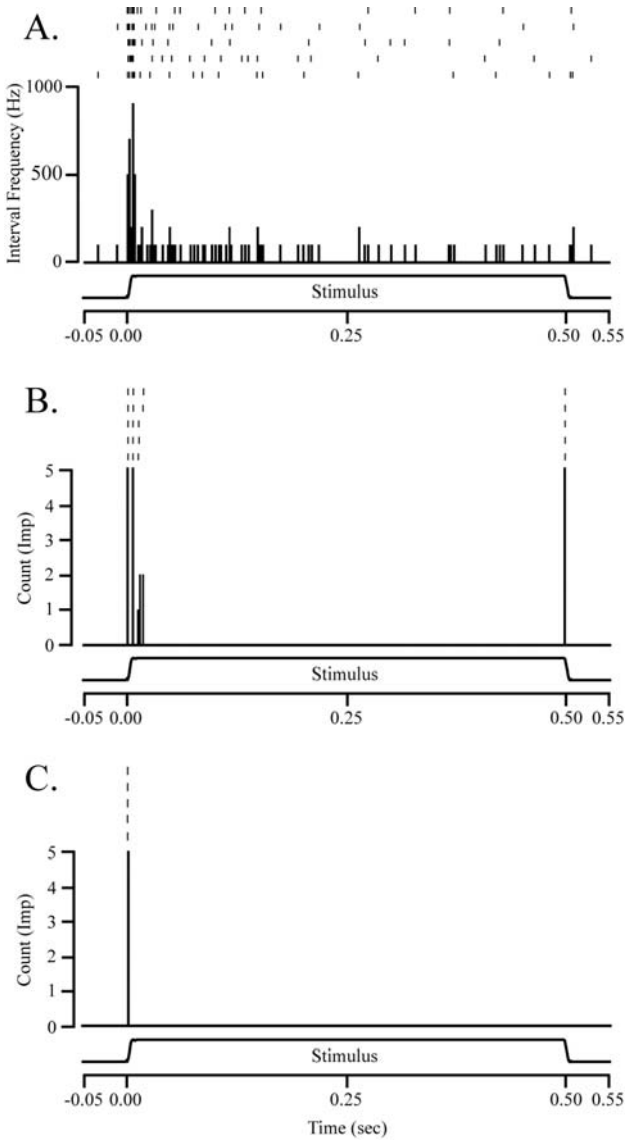
A.
Interval Frequency (Hz)
1000
500
0
Stimulus
-0.05 0.00
0.25
0.50 0.55
B.
Count (Imp)
5
4
3
2
1
0
Stimulus
-0.05 0.00
0.25
0.50 0.55
C.
Count (Imp)
5
4
3
2
1
0
Stimulus
-0.05 0.00
0.25
0.50 0.55
Time (sec)

portions of the stimulus. One cell (4.5%) responded to both the dynamic and static portion of the stimulus and was classified as SA.

Receptor Classes Three distinct sub-types of responses were evident across the broad RA and SA classifications. The SA response showed a typically SA-1 Merkel cell-like response to a static displacement (Fig. 19A). This was seen as the characteristic robust response to the initial dynamic phase of the compression followed by an irregular discharge during the sustained portion of the indentation (Iggo and Muir, 1969). Within the RA category two

distinct patterns of discharge relating to static indentation became evident. The first followed a characteristic Pacinian corpuscle-like response profile, showing a response to the changes in the dynamic portions of the indentation with no response during the static phase (Loewenstein, 1958; Talbot et al., 1968). The second group of response profiles showed a single impulse at the onset of the stimulus and no activity during the static phase. Receptors exhibiting this response profile occasionally fired one impulse upon retraction of the stimulator but generally no responses to the retraction were seen on compressions longer than 500 ms in duration.

Recording experiments in the star-nosed mole appeared to show a similar division of receptor response profiles into three distinct subtypes. Figure 20 shows the traces in 7 single units that correspond well with the responses seen in the coast mole. Of the 7 cells recorded from this animal, 3 receptors (Fig. 20D-F) showed typical SA-I Merkel cell-neurite complex response profiles to static compression, 2 cells (Fig. 20C&G) showed FA-II Pacinian corpuscle-like responses, however neither cell fired at the retraction of the

Fig. 20. Peristimulus time histograms and single electrophysiological traces showing representative examples of the response profiles found during preliminary experiments in the star-nosed mole. **A:** The RF for each cell is presented on a schematic of the mole's nose (anterior view). It is interesting to note that the 3 distinct receptor classes seen in the coast mole are also evident in the star-nosed mole (**B-H**). **D-F:** These receptors display the typical SA-I response with an initial robust reaction to the onset of the stimulus and an irregular pattern of impulses occurring through the static phase. **C&G:** These receptors display a possible FA-II response profile. Both receptors signal the changes in the dynamic phase and do not respond during the static phase. Interestingly, neither receptor signals the retraction of the stimulator. **B:** This receptor shows an RA response that signals the onset of the compression with a single impulse. This response profile correlated well to similar profiles seen in the coast mole. This receptor was also directional. An arrow on the RF diagram shows the preferred direction of the receptor. **H:** No static displacement data was collected for this cell and as such this receptor was not assigned to a class.

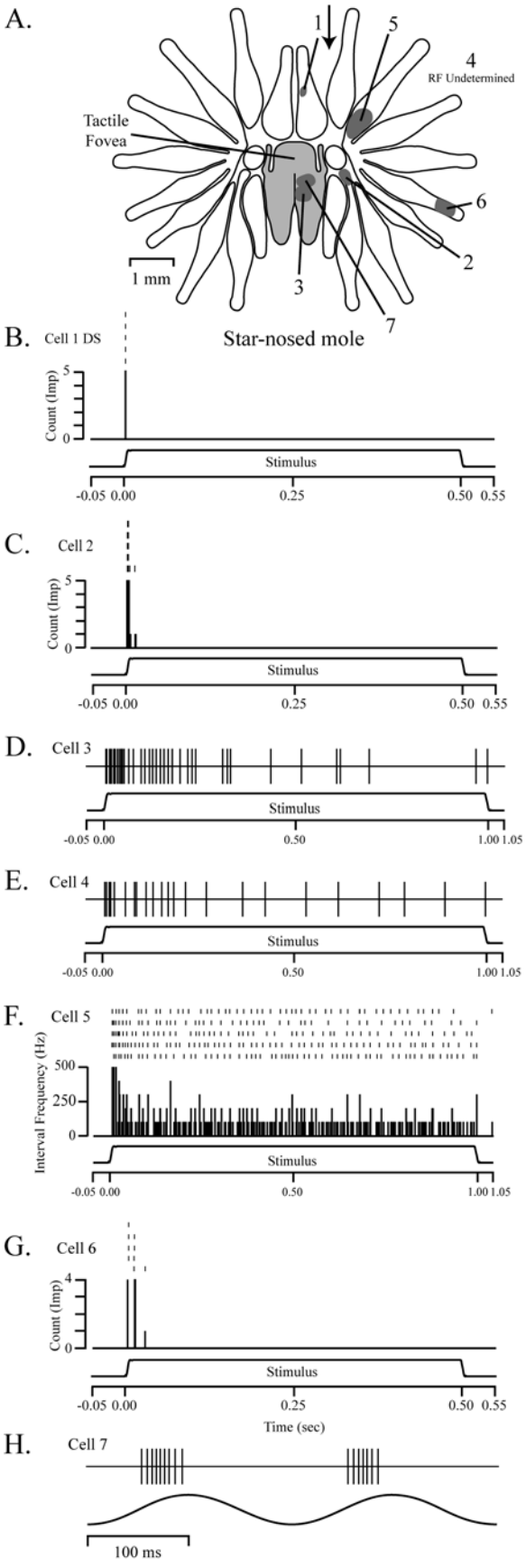
A.
1
5
4
RF Undetermined
Tactile
Fovea
6
2
1 mm
3
7
Star-nosed mole
B.
Cell 1 DS
Count (Imp)
5
0
Stimulus
-0.05 0.00
0.25
0.50 0.55
C.
Cell 2
Count (Imp)
5
0
Stimulus
-0.05 0.00
0.25
0.50 0.55
D.
Cell 3
Stimulus
-0.05 0.00
0.50
1.00 1.05
E.
Cell 4
Stimulus
-0.05 0.00
0.50
1.00 1.05
F.
Cell 5
Interval Frequency (Hz)
500
250
0
Stimulus
-0.05 0.00
0.50
1.00 1.05
G.
Cell 6
Count (Imp)
4
0
Stimulus
-0.05 0.00
0.25
0.50 0.55
Time (sec)
H.
Cell 7
100 ms

stimulus. One RA cell (Fig. 20B) responded with a single impulse at the onset of the compression and also responded in a directionally selective manner. The seventh cell (Fig. 20H) responded to a 5 Hz sinusoidal stimulus with multiple impulses per cycle (average instantaneous frequency of 239 Hz). However, no static indentation data was collected for this receptor, and it was not classified.

Peak Activation Frequency An interesting pattern in the RA response to compressive stimuli emerged during the recording sessions. There seemed to be RA receptors that were relatively unresponsive to compressive stimuli of any type but were acutely responsive to any kind of stimulus that brushed or slid across the surface of the nose. These receptors were generally activated by compressive stimuli applied with large displacements and high velocity. In contrast there were a great number of RA receptors that responded robustly to small magnitude compressions of any kind but were not as clearly responsive to the sweeping stimuli.

When sinusoidal compressive stimuli were applied to the RA receptors a quantitative distinction between these two qualitative measures also became evident. The receptors that were very sensitive to sweeping stimuli and difficult to activate with compressive stimuli were maximally activated across a broad range of frequencies, running from 5-150 Hz, at large displacements, ranging from 85-485 μm. Conversely, the receptors that were more responsive to compressive stimuli showed a narrow peak of maximal activity at 250-300 Hz with displacements that were an order of magnitude smaller, extending from 10-28 μm. Figure 21 plots the frequency at which these cells were maximally sensitive (the smallest displacements that activated them robustly) for

Fig. 21. Plot of the frequency maximum sensitivity for all RA cells. Two distinct populations of receptor are evident on this graph. There is a cluster of units that were most responsive to sinusoidals at 250-300 Hz that had displacement amplitudes at 20 and 28 μm. There was a more diffuse cluster of units at the lower right that were most responsive to sinusoidals ranging from 5-100 Hz at displacement amplitudes from 100-485 μm. Based on the different responses to sinusoidals the population at the upper left was classified as PC-like whereas the group at the lower right was classified as RA-Unknown (RA-X). There were two receptors that appeared to bridge the gap between these two groups. Both of these units showed peak activation at 150 Hz but one (cell 8-1) was responding to a 10 μm displacement amplitude and the other (cell 14-2) was responding at an 85 μm amplitude. Inset 1 shows the response of 8-1 to a static displacement and this receptor displayed a classic Pacinian dynamic response and was classed with the PC-like receptors. Inset 2 shows that cell 14-2 was unresponsive to sinusoidals at 200 Hz and as such was not considered part of the PC-like group and was classed as RA-X.

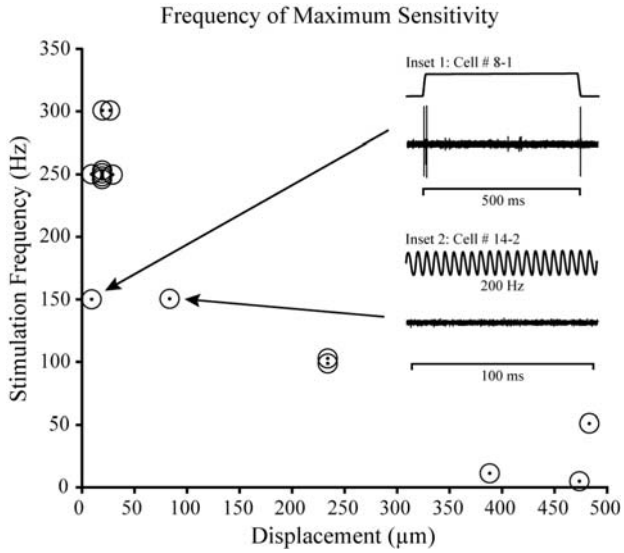
Frequency of Maximum Sensitivity
Stimulation Frequency (Hz)
Displacement (μm)
Inset 1: Cell # 8-1
500 ms
Inset 2: Cell # 14-2
200 Hz
100 ms

each of the cells that were held long enough to record the full course of sinusoidal data. There were two clusters of response properties evident, one in the upper left of the graph (high frequency and small displacements) and one at the lower right (low frequency and large displacements). On the basis of the tight clustering of RA receptors maximally tuned to frequencies of 250-300 Hz at relatively small displacements, these neurons were classified putatively as Pacinian-like (PC-like) in nature. This follows from the general diagnostic features of Pacinian activity with maximal activation at 200-300 Hz (Sato, 1961; Janig et al., 1968; Talbot et al., 1968; Johansson et al., 1982; Bolanowski and Zwislocki, 1984; Mahns et al., 2003). The receptors that were more diffusely clustered in the low frequency, large displacement range were classified putatively as Rapidly Adapting-Unknown (RA-X) cells.

Two cells that were maximally active at 150 Hz appeared to fall in intermediate categories. However, a more detailed examination of their response profiles allowed them to be tentatively assigned to specific classes. For example, inset 1 in Figure 21 shows the response of cell 8-1 to a static indentation. The cell responded to the changes in the dynamic portions of the compression stimulus in a characteristically Pacinian fashion, and as such was included within the PC-like population. Inset 2 in Figure 21 shows that cell 14-2 was entirely unresponsive to sinusoidal compression at 200 Hz, as would be expected for a Pacinian corpuscle. As a result it was considered to be separate from the PC-like group and included with the RA-X group.

Fig. 22. Composite drawing of the coast mole nose showing all of the RFs from the quantitative phase of the experiments. Each RF is labeled with its respective cell number and receptor sub-classification. All RFs are to scale. Lat.=lateral view, Ant.=anterior view, Vent.=ventral view.

Coast Mole Quantitative RF and Response Composite

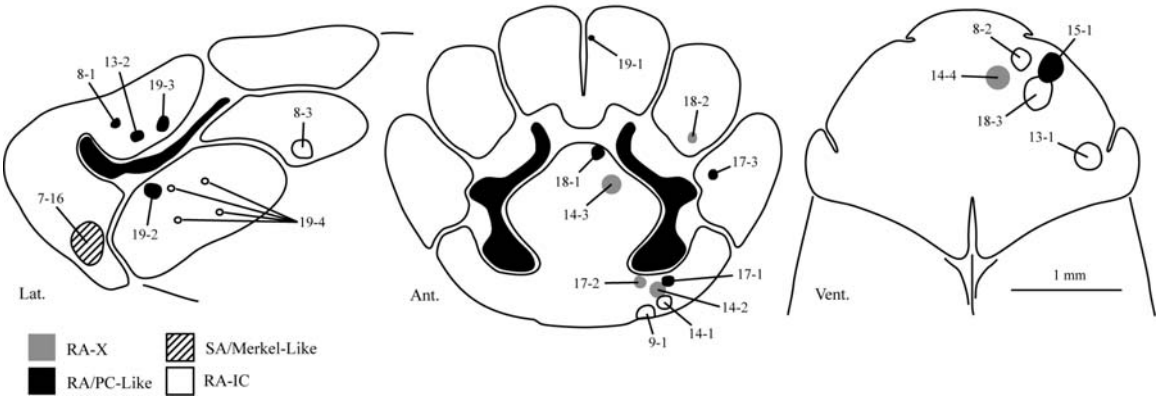

Quantitative Receptive Fields The RFs were found to be extremely small: averaging 119 μm in diameter, measured across the longest axis, ranging from 50 to 210 μm. The RFs were represented on the composite schematic according to the following classes: SA-I/Merkel-like, FA-II/PC-like, RA-X, and RA-Incomplete Classification (RA-IC) (Fig. 22). The cells labeled RA-IC were qualitatively determined to be RA but were not held long enough during recording to allow for a definitive characterization. There did not appear to be a drastic difference in the diameter of the RFs between the PC-like (Ave. = 94.4 μm), RA-X (Ave. = 119.2 μm) and RA-IC (Ave. = 128.3 μm) receptors, however the RF for the single SA-1 response (275 μm) was somewhat larger in diameter.

Indentation Velocity When we stimulated the skin surface containing Eimer's organ with handheld probes, some receptors responded most robustly to taps. These responses seemed consistent with mole behavior, as moles repeatedly tap and probe the ground with their nose while foraging. The velocity at which the nose contacts the substrate was determined from high-speed video to be an average of 46.2 mm/second. To examine afferent responses to different velocities of indentation, a 500 μm displacement ramp stimulus was applied at 3.0, 10.0, 25.0, 46.2 and 84.5 mm/second (84.5 was the maximum indentation velocity attainable).

The effects of indentation velocity were examined across 13 RA receptors (Fig. 23A). Our goal was to determine the lowest indentation velocities at which the receptors responded, as this is another measure of sensitivity to mechanical stimuli. We found that for a number of cells (5 or 39%) the minimal velocity at which they responded (at 1:1)

Fig. 23. Receptor responses to indentation velocity related to the average speed at which the mole taps its nose to the ground when foraging (46.2 mm/sec) for 13 RA receptors. **A:** Lowest indentation velocity required to elicit a 1:1 response representing the activity of all of the RA units combined (left graph). There were a peak number of cells that were most highly activated near the behaviorally relevant speed. The same graph divided by sub-class (right graph). This graph shows that the PC-like units tended to be more sensitive to the lower velocities and the RA-X group tended to be more sensitive to the higher indentation velocities. **B:** Lowest velocity required to elicit any response for all cells combined (left graph). Most cells responded at less than 1:1 to the lower velocities. The same graph divided by sub-class (right graph). The PC-like units tended to be minimally responsive at the lowest velocity and as such appeared to be more sensitive than the RA-X group. It is interesting to note that the minimal response for the RA-X group still tended to cluster at the higher velocities suggesting that they showed little sub-1:1 activity. **C:** Stimulus response relations for two cells that appeared to code indentation velocity (left panel). For both of these units as indentation velocity increased the average interval frequency increased. It is interesting to note that both cells appeared to be tuned near the behaviorally relevant velocity. Representative traces for each cell showing the multiple spikes elicited during the ramp indentation (right panel).

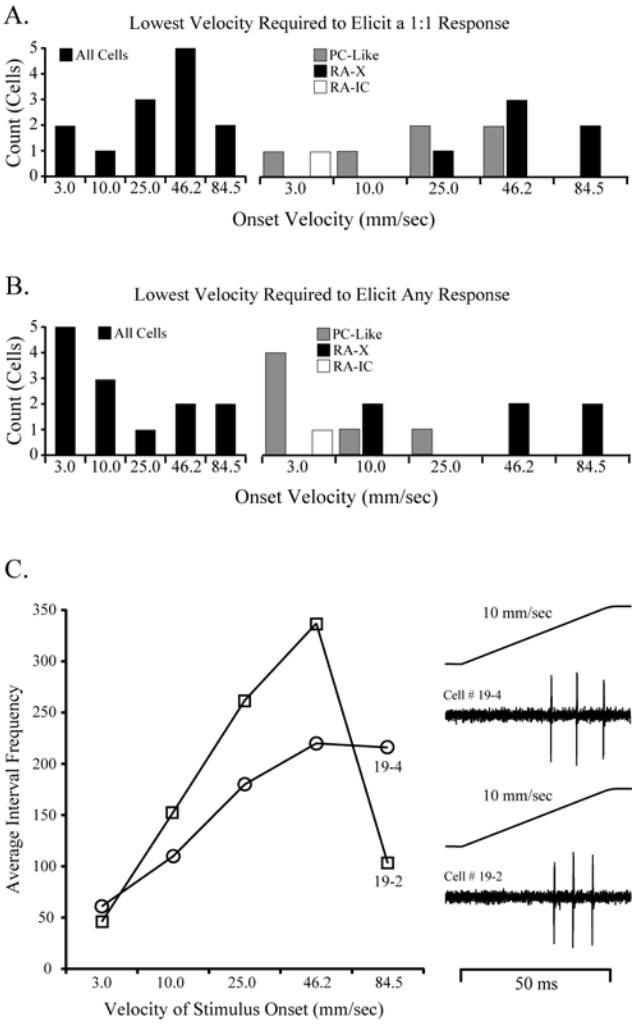
A.
Lowest Velocity Required to Elicit a 1:1 Response
All Cells
PC-Like
RA-X
RA-IC
Count (Cells)
0
1
2
3
4
5
3.0
10.0
25.0
46.2
84.5
Onset Velocity (mm/sec)
B.
Lowest Velocity Required to Elicit Any Response
All Cells
PC-Like
RA-X
RA-IC
Count (Cells)
Onset Velocity (mm/sec)
C.
Average Interval Frequency
0
50
100
150
200
250
300
350
19-4
19-2
Velocity of Stimulus Onset (mm/sec)
10 mm/sec
Cell # 19-4
10 mm/sec
Cell # 19-2
50 ms

was 46.2 mm/second, corresponding to the approximate speed of the nose during foraging behavior. In addition, for two cells (15%) the minimal velocity for 1:1 responding was 84.5 mm/sec, for 3 cells it was 25 mm/sec (23%), for 1 cell (8%) it was 10 mm/sec and for 2 cells (15%) is was 3 mm/sec. When examined by subclass, the PC-like units tended to be active at 1:1 threshold for a broad range starting at 3 mm/sec and ending at 46.2 mm/sec. Conversely, the RA-X units tended to respond at 1:1 across a slightly smaller range beginning at the higher indentation velocities (25 – 84.5 mm/sec). The RA-IC unit responded at 1:1 through the entire range of indentation velocities.

The cells were also examined in terms of the lowest indentation velocity required to elicit a response of any kind (i.e. absolute threshold-Mahns et al., 2003) (Fig. 23B). The graph for all neurons together shows an overall trend toward absolute threshold activation at the lower velocities. Five units (39%) responded at absolute threshold beginning at 3 mm/sec, 3 cells (23%) were active beginning at 10 mm/sec, 1 (8%) at 25 mm/sec, 2 (15%) at 46.2 mm/sec and 2 (15%) at 84.5 mm/second. When examined according to class, the PC-like units responded at generally lower velocities of indentation (Fig. 23A). Conversely, the RA-X units tended to respond at higher indentation velocities - 67% at 46.2 mm/sec and above.

Two RA cells had a velocity dependant response to the ramp stimuli (Fig. 23C). These units generally fired multiple pulses upon indentation and both cells were active at 1:1 threshold in response to all velocities. In each case, from velocities of 3 mm/sec up to 46.2 mm/sec, the instantaneous average frequency of the inter-spike intervals increased

as the velocity of the indentation increased. Interestingly, the average interval frequency in both units appeared to be tuned near the behaviorally relevant velocity (46.2 mm/sec). Cell 19-4 plateaued in average interval frequency above 46.2 mm/sec and cell 19-2 decreased in the average interval frequency above 46.2 mm/second. Cell 19-2 was classified as PC-like and cell 19-4 was categorized as RA-IC because we were unable to apply sinusoidal stimuli to provide subclass assignment.

Depression Thresholds The static indentation threshold levels of 13 RA receptors were evaluated by applying 50 ms duration step indentations at a range of displacements running from 1 to 150 μm (Fig. 24). Of the 13 units, 5 did not respond at any level to indentations ≤ 150 μm. Out of all the units that responded none fired at 1:1 thresholds for displacements smaller than 125 μm. Three cells fired at 1:1 starting at 150 μm and one unit did not respond 1:1 at any displacement. All of the units responded at absolute threshold levels to displacements smaller than those at which they responded 1:1.

While the 1:1 responses of the PC-like and RA-X classes were very similar the two groups responded differently at absolute threshold levels. The PC-like group appeared to be considerably more sensitive to small displacements than the RA-X group. In particular, one PC-like unit responded to static displacements as small as 5 μm. The other 3 units in the PC-like class responded at absolute levels to displacements at 50, 75 and 125 μm. The RA-X had no responses to displacements smaller than 125 μm.

Fig. 24. Graphs of receptor response to multiple static displacement amplitudes for 13 RA receptors divided by subclass. In all, most receptors had responses beginning at 125-150 μm displacement amplitudes, if they responded at all. However, the PC-like group tended to be more sensitive to smaller displacements at absolute levels. The RA-X group was not responsive at any level to displacements smaller than 125 μm.

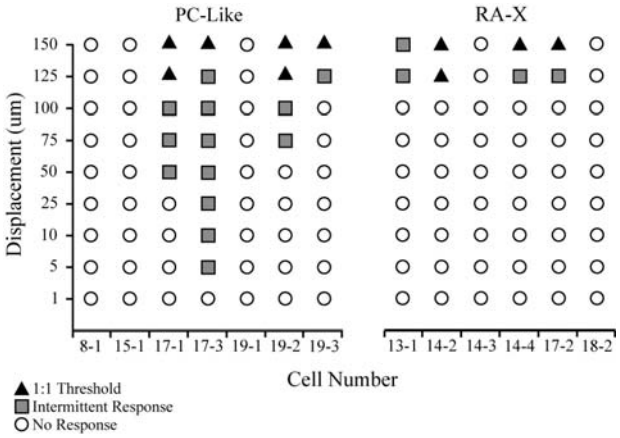
PC-Like
RA-X
Displacement (um)
150
125
100
75
50
25
10
5
1
8-1
15-1
17-1
17-3
19-1
19-2
19-3
13-1
14-2
14-3
14-4
17-2
18-2
Cell Number
1:1 Threshold
Intermittent Response
No Response

Fig. 25. Receptive fields of directional receptors isolated during the qualitative phase. The arrows represent the direction that was determined to be the most active when brushed with the hand-held stimulator. Two cells appeared to be directional but were lost before a specific direction of highest activity could be established. A=anterior view, L=lateral view, V=ventral view.

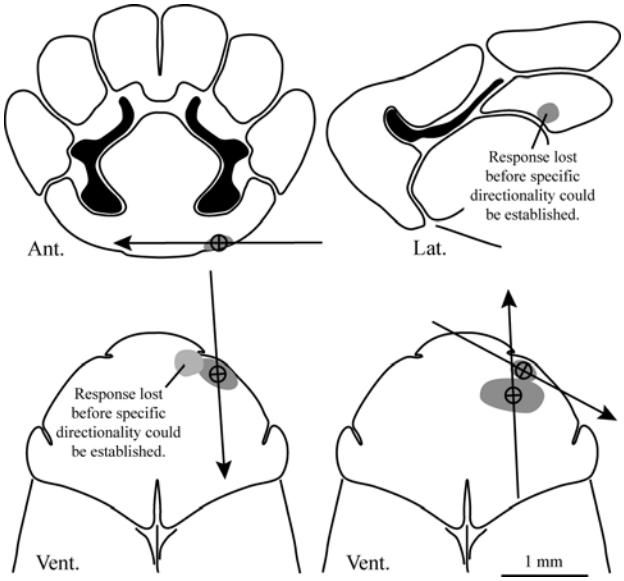
Ant.
Lat.
Response lost
before specific
directionality could
be established.
Response lost
before specific
directionality could
be established.
Vent.
Vent.
1 mm

Directional Sensitivity During qualitative mapping experiments in both the coast mole and the star-nosed mole there were receptors that were preferentially activated by directionally applied stimuli (see Figs. 20&25). Figure 25 shows the composite receptive fields, in the coast mole, for these receptors. The overlying arrows denote the preferred direction of stimulation. We hypothesized that the individual Eimer's organs were being deflected in line with the sweep of the probe as it was brushed back and forth across the surface of the nose.

Directional data was gathered from a total of 17 units. Figure 26(A-C) shows the directional histograms and receptive fields of representative units from each subclass, closely matching the average values for the three directional measures (Rayleigh test, TR and TI) across each individual group. When all units were examined all, but two receptors scored as significantly directional by the Rayleigh test (Table 1). Six (35%) of the units had TR values less than 0.5 and 4 (24%) more units had TR values less than 0.6. The average TR value for all the units was 0.53 ranging from 0.19 to 0.73 (Table 1). Eight units (47%) had TIs of 5 and one (6%) cell had a TI of 4. This indicates that 53% of the neurons examined were highly directionally tuned. The average TI for all receptors was 3.5 and ranged from 0 to5 (Table 1).

Table 1. Summary of values for all measures of directional tuning.

Cell #	Group	Rayleigh Z value	Rayleigh p value	Tuning Ratio	Tuning Index
8-1	PC-Like	36.09	0.00	0.59	1
15-1	PC-Like	7.18	7.63E-04	0.59	3
17-1	PC-Like	11.45	1.07E-05	0.63	2
17-3	PC-Like	10.55	4.30E-05	0.48	5
18-1	PC-Like	0.88	0.41	0.67	0
19-1	PC-Like	6.47	0.0020	0.69	2
19-2	PC-Like	34.81	0.00	0.56	5
19-3	PC-Like	3.32	0.036	0.73	3
13-1	RA-X	46.98	0.00	0.27	5
14-2	RA-X	62.29	0.00	0.61	3
14-3	RA-X	1.81	0.16	0.63	4
14-4	RA-X	20.10	1.86E-09	0.55	5
18-2	RA-X	94.31	0.00	0.19	5
7-16	Merkel-Like	55.46	0.00	0.41	5
8-3	RA-IC	39.48	0.00	0.42	5
9-1	RA-IC	51.08	0.00	0.66	2
14-1	RA-IC	61.01	0.00	0.37	5

Fig. 26. Representative normalized and rotated circular histograms of directional activity for all three sub-classes of receptor (**A, B, & C**). The RF and stimulus directions, including the direction of maximum activity (**MAX**), for each receptor are depicted to the right of each graph (**a1-d1**). **A:** Receptor number 17-1 was most closely representative of the average values for all three measures of directionality for the PC-like population. This receptor was moderately directionally tuned by the Rayleigh statistic but showed low scores for the TR and TI (see table 1). **B:** Receptor number 7-16 was the only slowly adapting response isolated in the quantitative phase. This receptor was strongly directionally tuned. **C:** Receptor 13-1 was most closely representative of the average values for all three measures of directionality for the RA-X population. This receptor was strongly directionally tuned and when the stimulator was rotated to 180^{o} the responses occurred as strongly as in the 0 direction (**c2**). **D:** This is the directionality graph and RF diagram for the most highly directionally tuned receptor found in the course of this study. Receptor 18-1 can be seen to be almost entirely insensitive to any direction other than the preferred direction. This receptor scored very highly on all measures of directionality and when the stimulator was rotated to 180^{o} the responses occurred as strongly as in the 0 direction (**d2**). Scale bars = 1 mm.

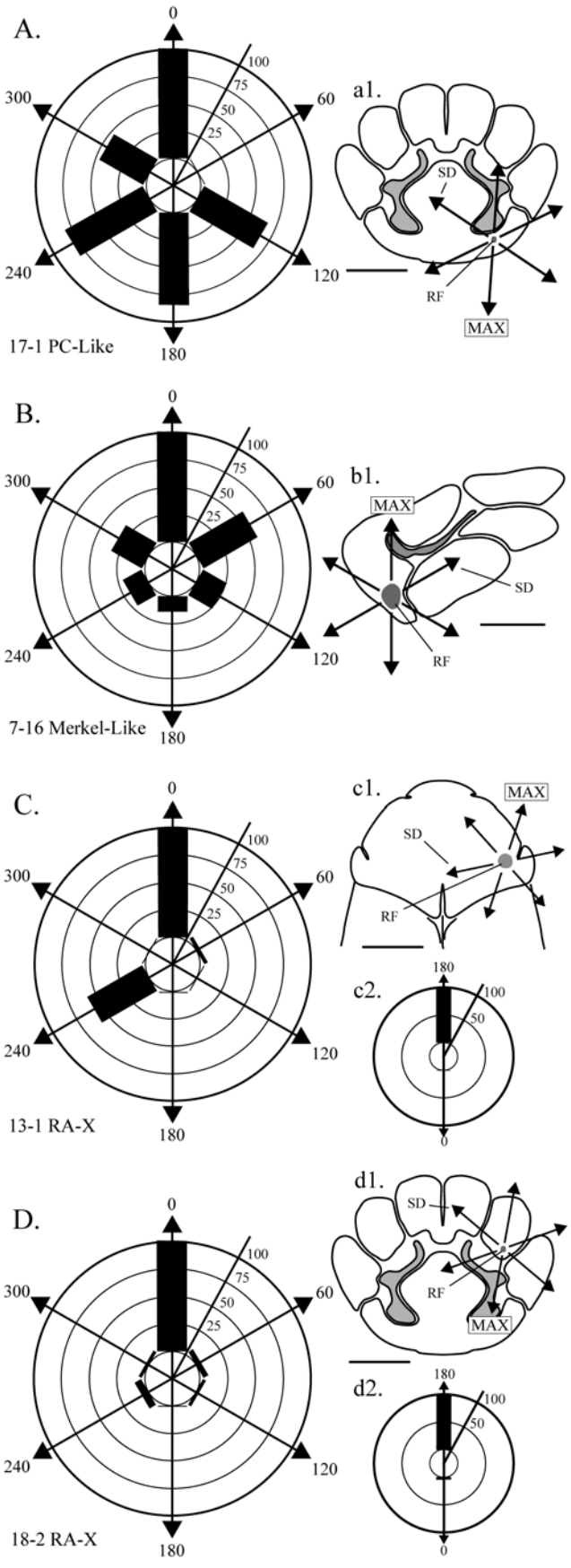
A.
0
60
120
180
240
300
100
75
50
25
17-1 PC-Like
a1.
SD
RF
MAX
B.
0
60
120
180
240
300
100
75
50
25
7-16 Merkel-Like
b1.
MAX
SD
RF
C.
0
60
120
180
240
300
100
75
50
25
13-1 RA-X
c1.
MAX
SD
RF
c2.
180
100
50
0
D.
0
60
120
180
240
300
100
75
50
25
18-2 RA-X
d1.
SD
RF
MAX
d2.
180
100
50
0

Two receptors, cases 18-2 and 13-1, stand out as being almost entirely silent in directions other than the preferred direction (Fig. 26 C, D). Receptor 13-1 had an Rz of 46.98 with a p value of 0, a TR of 0.27 and a TI of 5. Receptor 18-2 had an Rz of 94.31 with a p value of 0, a TR of 0.19 and a TI of 5 (Table 1). Cell 18-2 was nearly completely directionally tuned by all measures. These two most profoundly directional units were part of the RA-X population.

Directional tuning within the PC-like class appeared to be less distinct when compared to the RA-X class and the single Merkel-like receptor. The average Rz for the PC-like units was 13.84 compared to 45.08 and 55.46 for the RA-X group and the Merkel-like response respectively. The average TR for the PC-like class was 0.62 whereas the RA-X average was 0.45 and the Merkel-like response was 0.41. In addition, the average TI for the PC-like group was at 2.6 the TI for the RA-X class was 4.4 and the Merkel-like response had a TI of 5. Normalized response magnitudes for each direction were averaged for the RA-X and PC-like populations so that a graphical comparison could be made between the two. Figure 27 shows that while both populations are directionally tuned the RA-X class is more narrowly tuned than the PC-like class.

Temporal Patterning All of the units analyzed showed a considerable capacity for phase locking. The average R value for all of the cells together was 0.953 as measured with bins equaling 0.1 ms for all peak frequencies ranging from 10 to 300 Hz. Nine receptors (69%) had R values greater than 0.95. There were no R values less than 0.847 and the highest R value

Fig. 27. A graphical comparison of directional tuning between the normalized and rotated average response magnitudes for the PC-like and RA-X populations. The RA-X population was strongly directionally tuned. The PC-like population was more broadly tuned than the RA-X population, yet still considerably directional.

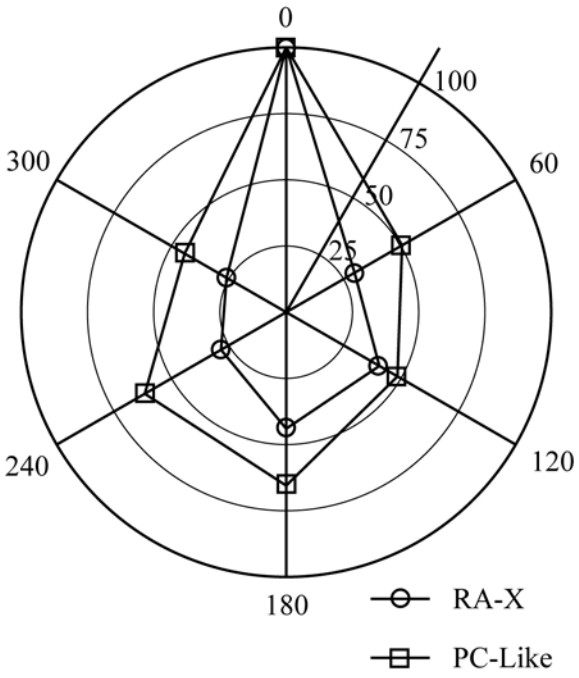
0
100
75
60
50
300
25
240
120
180
RA-X
PC-Like

Fig. 28. Cycle histograms relating the precision of temporal patterning with respect to vibrotactile stimuli at peak frequency of activation. **A:** Representative cycle histograms from each of the three receptor classes present in the nose (n=100). The R value for each unit shown was similar to the average R value for the population it represents. Note: there was only one Merkel cell-neurite receptor. **B:** Three units with the highest degree of phase locking (n=100). If all 100 impulses were to fall in one 0.1 ms bin the variance would be equal 0. **C:** There was adequate data present to calculate cycle histograms across each stimulus frequency for unit number 14-4. If all 50 impulses were to fall in one 0.1 ms bin the variance would be equal 0. As frequency increased the receptor became less phase locked, however all impulses still fell within a 1 ms time frame.

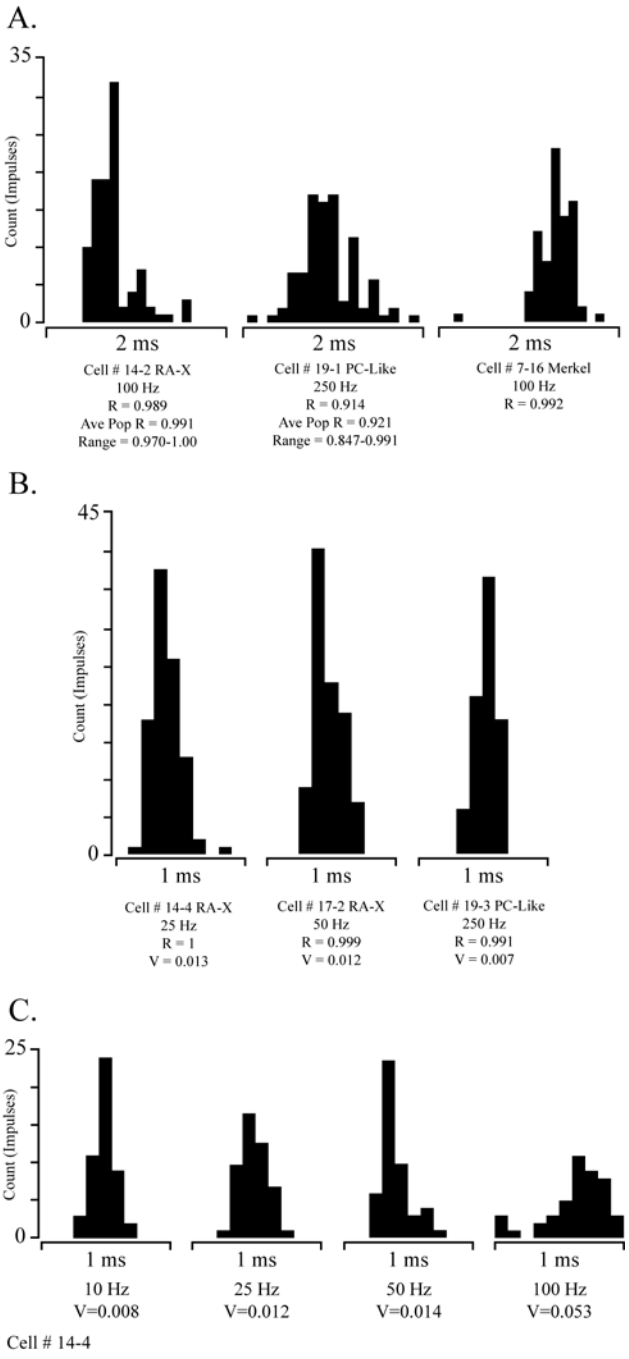
A.
35
Count (Impulses)
0
2 ms
2 ms
2 ms
Cell # 14-2 RA-X
100 Hz
R = 0.989
Ave Pop R = 0.991
Range = 0.970-1.00
Cell # 19-1 PC-Like
250 Hz
R = 0.914
Ave Pop R = 0.921
Range = 0.847-0.991
Cell # 7-16 Merkel
100 Hz
R = 0.992
B.
45
Count (Impulses)
0
1 ms
1 ms
1 ms
Cell # 14-4 RA-X
25 Hz
R = 1
V = 0.013
Cell # 17-2 RA-X
50 Hz
R = 0.999
V = 0.012
Cell # 19-3 PC-Like
250 Hz
R = 0.991
V = 0.007
C.
25
Count (Impulses)
0
1 ms
1 ms
1 ms
1 ms
10 Hz
V=0.008
25 Hz
V=0.012
50 Hz
V=0.014
100 Hz
V=0.053
Cell # 14-4

was 1. Figure 28A shows representative CHs for all three receptor types. Note that the time frame that these responses fall within does not exceed 2 ms in duration. The average R values for the PC-like population, RA-X group and Merkel-like response was 0.92, 0.99, and 0.99 respectively.

Because these responses were so highly phase locked it was necessary to quantify the slight differences in the distribution about the mean for 0.1 ms bins across the different peak frequencies with the linear variance. The variance provides a measure of the distribution of the spike timing around the endpoint of the latency between the stimulus onset and response. This is irrespective of the fractional clustering of the responses within the stimulus cycle as calculated by the length of the mean vector. At n=100 the variance for a CH with all counts falling within one 0.1 ms bin would be 0. Conversely, a CH with all 100 counts distributed to 100 0.1 ms bins would have a variance of 8.42. Figure 28B shows the CHs for 3 receptors with an increased propensity for phase locking. In the least phase locked of these 3 the distribution around the mean falls within a 0.8 ms time frame and the most phase locked has a distribution within a 0.4 ms time frame. The variance for each of these CHs is 0.013, 0.012, and 0.007 for 14-4, 17-2 and 19-3 respectively. In each of these cases the variance is more representative of the distribution of the responses in time when comparing different sinusoidal periods. In case 14-4 the data were available to examine the temporal coding properties for a single receptor across a range of sinusoidal frequencies (Fig. 28C). In this instance 50 responses were analyzed at each frequency to account for the lower number of responses elicited at non-peak frequencies. The variance for all 50 counts in one 0.1 ms bin would be 0 and each response falling within 50 different 0.1 ms bins would be 2.13. This

Fig. 29. Receptive field diagrams and representative electrophysiological traces for units that were positively attributed to individual Eimer's organs. Units represented in **A** and **B** were from the coast mole (RF size ≈ 50 μm). The unit represented in **C** was from the star-nosed mole (RF size ≈ 40 μm).

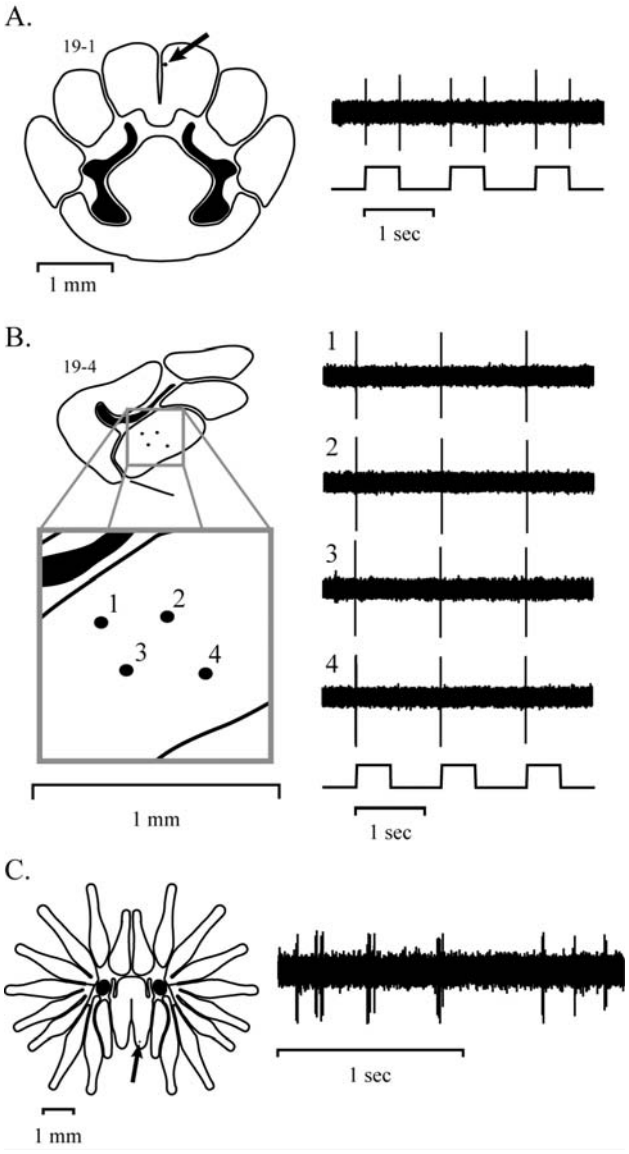
A.
19-1
1 mm
1 sec
B.
19-4
1
2
3
4
1 mm
1
2
3
4
1 sec
C.
1 mm
1 sec

receptor shows the highest degree of temporal fidelity at 10 Hz and it degrades slightly at each increase in frequency. However, even at the least clustered frequency all of the responses fall within a 1 ms time frame.

Manipulation of Individual Eimer's Organs Within the scope of this study mechanoreceptive function was positively assigned to 6 individual Eimer's organs. In each case single unit activity was recorded while the receptive field for that neuron was reduced to a single Eimer's organ under direct stereomicroscopic observation (Fig. 29). The receptive fields for these neurons in the coast mole and the star-nosed mole were extremely small. An Eimer's organ in the coast mole is approximately 70 μm in diameter and a star-nosed mole Eimer's organ is approximately 40 μm in diameter (Catania, 1996; Marasco et al., 2006).

In case 19-1 the neuron responded to stimulation of a single Eimer's organ. Stimulating each of the Eimer's organs immediately adjacent to this single organ did not elicit a response from the recorded neuron (Fig. 29A). No other Eimer's organs appeared to activate this cell. In contrast, the receptive field for neuron 19-4 was activated by 4 separate fairly distant Eimer's organs (Fig. 29B). Eimer's organ number 1 and organ number 4 were separated by 0.7 mm. Organs number 2 and 3 were separated by 0.4 mm. Displacing the Eimer's organs in the region between and around the four active organs did not elicit a response.

During preliminary experiments in the star-nosed mole the receptive field for one neuron was narrowed down to a single Eimer's organ. This organ was located on the tip of ray 11. Under microscopic control, the single organ was manipulated by hand using a

slightly blunted insect pin. Figure 29C shows the response over 2 seconds to repeated slight movements of the probe tip. Displacing adjacent Eimer's organs did not elicit a response.

Discussion

The primary goal of this study was to begin to develop an understanding of how Eimer's organs may function to transduce tactile signals. To this end our investigation provides evidence that Eimer's organs respond to directional input, transducing tactile signals with a high level of spatial and temporal resolution, and some receptors may have tuning properties that filter behaviorally irrelevant mechanosensory input. Although a mechanoreceptive function has been proposed for these structures based on their anatomy and the behavior of moles, the results of the present investigation provide definitive evidence and new details about response properties. In addition, some of the responses are consistent with the hypothesis that differential deflection of the ring of nerve terminals in the cell column provides information about surface features on object that have been contacted. Receptive fields were exceptionally small, and this is consistent with the high tactile acuity of moles and the correspondingly high innervation density of the Eimer's organ arrays. These different aspects of Eimer's organ response to mechanosensory stimuli are discussed further below.

Receptive Fields Previous recordings from the neocortex indicate that arrays of Eimer's organs are sensitive to mechanosensory stimuli (Catania and Kaas, 1995; Sachdev and Catania, 2002a,b) In addition, recent investigation of immunoreactivity of

different components of Eimer's organ suggest the three main sensory components of the organ associated with the cell column (Merkel cells, lamellated corpuscles, and intraepidermal free nerve endings) are mechanoreceptive (Marasco et al., 2006). In further support of these findings, the results of the present study provide evidence that individual Eimer's organs are responsive to mechanosensory stimulation. This is significant because it is often difficult to isolate individual, small epidermal receptors when recording from afferents (e.g. Iggo et al., 1996) and so the present results regarding small Eimer's organ receptive fields provide new data confirming a mechanosensory function.

The RFs in the coast mole were an average of 119 μm across with the smallest RFs for individual Eimer's organs being 70 μm across. In the star-nosed mole the RF for a single receptor was a single 40 μm diameter Eimer's organ. These RFs are much smaller than those reported for glabrous skin in a number of different model systems and likely represent the smallest RFs recorded for a skin surface (Jänig et al., 1968; Talbot et al., 1968; Johansson and Vallbo, 1980; Leem et al., 1993; DiCarlo et al., 1998; Xerri et al., 1998; Vega-Bermudez and Johnson, 1999).

Interestingly, we did not find an obvious difference in the size of RFs for the different receptors classes. This is somewhat surprising, because relative RF size is often used to differentiate between RA receptor classes. For instance, Pacinian responses can be differentiated from other RA responses by their large RFs with indistinct borders (Talbot et al., 1968; Knibestol and Vallbo, 1970; for review see Vallbo and Johansson, 1984). However in Eimer's organ, the lamellated "paciniform" corpuscles are much smaller (45 μm, Marasco and Catania, 2006) than typical Pacinian receptors (1 mm,

Quilliam and Sato, 1955). In addition, it is possible that the structure of Eimer's organ isolates each receptor complex within the surrounding skin by focusing the tactile input along the cell column (Manger and Pettigrew, 1996; see also: Cauna, 1954). This would also be consistent with the 1:1 ration of lamellated corpuscles to Eimer's organs - a configuration that would seem redundant if receptive fields were very large.

Receptor Classes In the coast mole three main classes of receptor were evident that differed in their response to static indentation. These included one slowly adapting type and two rapidly adapting types. Recordings from the star-nosed mole also suggested this separation into three classes. This division of afferents serving glabrous skin into three classes is well established for a considerable number of different animal model systems and humans (Lindblom, 1965; Janig et al., 1968; Talbot et al., 1968; Iggo and Ogawa, 1977; Janig, 1971; Pubols et al., 1971; Pubols and Pubols, 1973; Johnson, 1974; Dykes and Terzis, 1979; Johansson and Vallbo, 1979; Ferrington and Rowe, 1980; Vallbo and Johansson, 1984; Gregory et al., 1988; Leem et al., 1993; Iggo et al., 1996; Coleman et al., 2001; Mahns et al., 2003;).

Previous histological studies in the mole routinely reveal a preponderance of three main types of receptor end-organ in the glabrous rhinarium in these animals (Fig. 16). Eimer's organs are associated with Merkel cell-neurite complexes, Paciniform corpuscles, and intraepidermal free nerve endings. (Halata, 1972; Andres and von During, 1973; Catania, 1995a,b, 1996; Marasco et al., 2006). Based on the average number of receptor subtypes present within each Eimer's organ we would expect 58% of the receptors to be RA and 42% to be SA. The recordings made during the qualitative

phase of the experiments revealed a different division of responses - 78.8% RA and 21.2% SA responses. Recordings made during the quantitative phase revealed an even greater bias towards the RA units as 95 % of these responses were RA and 4.5% were SA. This difference in actual percentages of the responses may reflect differential innervation rations for the different receptors classes, and could also reflect the organization of receptors classes within the trigeminal ganglion. The rostral-most portion of the ganglion was located within the infraorbital foramen leaving the front of the ganglion inaccessible. In addition, most of the quantitative recording data were obtained from the rostral-medial portion of the exposed ganglion, where the nose representation was most prominent. In contrast the larger survey of qualitative receptive fields was obtained from a more evenly distributed sampling of penetrations as there were fewer time constraints during the experiments allowing more of the ganglion to be explored.

All of the SA responses recorded from the nose in both species of mole compared well to the response profile of typical SA-I Merkel cell-neurite complexes (Iggo and Muir, 1969). This electrophysiological characterization is not surprising given the large number of Merkel cell-neurite complexes present in Eimer's organ. This is also true for the PC-like responses, as lamellated corpuscles are found at the base of each Eimer's organ. The characterization of these receptors as PC-like is also suggested by the activity elicited during sinusoidal stimulation between 200 and 300 Hz - another typically Pacinian trait (Sato, 1961). Although the main criteria for distinguishing between the PC-like and RA-X responses was their respective responses to sinusoidal mechanosensory stimulation, there were other differences in response profiles that seemed to distinguish these two receptors. For example the PC-like units tended to be more responsive to lower

indentation velocities than the RA-X units (Fig. 23). The PC-like receptors were more sensitive to small amplitude static displacements than the RA-X afferents (Fig. 24). Finally, as a whole the PC-like units were less directionally sensitive than the RA-X units.

In addition to Merkel cells and lamellated corpuscles, the intraepidermal free nerve endings are the third major sensory component of Eimer's organ evident from anatomical studies. Our finding of three different potential types of mechanoreceptive afferents suggests each major sensory receptor class was represented in our recording data. Interestingly the responses of RA-X receptors reported here were similar to those reported by Lynn (1969) in the cat. In cats these receptors had very high minimum thresholds for activation and were generally isolated to superficial positions in the epidermis. In addition, they had peak activation through a broad range of lower frequencies and were typically difficult to drive at frequencies greater than 150-200 Hz.

These units were also similar to receptors found by Iggo et al. (1996) in the snout skin of the echidna. The push rod sensory end-organ of the monotremes is similar to the Eimer's organ in cellular structure and innervation patterns (Andres and von During, 1984; Andres et al., 1991; Manger and Hughes, 1992; Manger and Pettigrew, 1996). Iggo et al. (1996) reported RA receptors with high thresholds to stimulation and some that were most responsive to sliding motions of the stimulus probe. These two features parallel the properties of the putative RA-X receptors reported here and may represent analogous receptors in push-rods and Eimer's organs.

Given the preponderance of three major sensory receptors associated with Eimer's organs, and three presumptive response classes from associated afferents, it seemed

reasonable to hypothesized which receptors were represented in the recording data. The PC-like and RA-1 responses presumably correspond to lamellated corpuscles and Merkel-cells respectively. This suggests that the putative RA-X response profile represents the activity of the mechanoreceptive intraepidermal free nerve endings.

Mole Behavior and Eimer's organ Stimulation As the moles forage and move about their tunnels they repeatedly touch the nose to the ground for durations of 30-35 ms. Given this is the fundamental unit of mole foraging behavior, the kinematics of these movements seemed important to consider. We used high-speed videography to calculate the velocity of the mole's nose during a series of exploratory contacts. The average velocity was 46.2 mm/s during a contact. We subsequently included this velocity in our stimulation paradigm, along with a series of other stimulation velocities. A number of afferents responded to this stimulation velocity in preference to lower velocities (Fig.24). This was particularly true of the RA-X units. In contrast, the PC-like units were, in general, more sensitive to the lower velocities, although this distinction was not characteristic of every unit.

Two of the units examined occasionally responded with multiple spikes to the ramp stimulus. When the average instantaneous interval frequency for these responses was calculated for each velocity it appeared that these units were coding the velocity of indentation. As the velocity increased the interval frequency increased. Interestingly, both units appeared to be tuned near the behavioral velocity of 46.2 mm/s. The interval frequency for both increased with increasing velocity up to 46.2 mm/sec. At 84.5 mm/sec the interval frequency for cell 19-4 reached a plateau and the interval frequency for cell

19-2 dropped precipitously. Higher velocities could not be explored because of the mechanical limits of the stimulator.

The results from this stimulation paradigm are consistent with behavioral observations suggesting at least some units are particularly responsive to indentation velocities of 46.2 mm/sec. This could filter some of the tactile stimulation that inevitably occurs when moles are not actively exploring their environments. Further evidence for this possibility comes from the motor component of exploratory behaviors. Both star-nosed moles and Coast moles have a series of tendons that serve to move the modules of Eimer's organs at increased velocities during contact.

Temporal Precision All of the receptors examined from the coast mole nose responded to sinusoidal stimuli with a high level of temporal precision. When examined collectively the average R value for all of the receptors was 0.953 and the least phase locked response corresponded to an R value of 0.847. Considering that a receptor with an R value greater than 0.3 has a significant capacity for phase locking (Durand and Greenwood, 1958; Bledsoe et al., 1982; Coleman et al., 2001; Mahns et al., 2003), the fidelity with which the receptors in the mole are able to track a vibratory stimulus is remarkable for the somatosensory system (Mountcastle et al., 1969; Greenstein et al., 1987; Vickery et al., 1992; Coleman et al., 2001; Mahns et al., 2003). The temporal acuity of responses, as measured by the time span of the entire distribution of impulses around the mean for the three most phase locked cells, was within an order of magnitude of similar distributions reported for primary afferents in electric fish (*Eigenmannia*) and magnocellular neurons in barn owls (Sullivan and Konishi, 1984; Rose and Heiligenberg,

1985; Carr et al., 1986; Carr and Konishi; 1990). The two receptor types that had the greatest capacity for phase locking, the Merkel cell-neurite complex and the RA-X group, were also the most directionally tuned (see next section).

Directional Sensitivity and the Function of Eimer's Organ The conspicuous circular organization of nerve endings (Fig. 16) and its innervation pattern in Eimer's organs (Marasco et al. 2006) and push-rods (Andres and von During, 1984) has led to speculation that both organs may transduce directional information (Quilliam, 1966; Andres and von During, 1984; Catania, 1996, 2000; Marasco et al., 2006). In support of this possibility, we noticed that some responses in the present study were elicited by stimuli applied in a specific direction when using a hand-held probe (Fig. 25). These receptors could be brushed in one direction to elicit a strong response but when brushed in other directions were silent. To provide more consistent and controlled directional stimulation, we built a piezo-electric sweeping stimulator to provide directional displacements to the Eimer's organs (Fig. 17C). The stimulator was designed to rotate in its holder so that axial displacements could be applied in any direction over the top of a given receptor (Fig. 17B).

The recordings resulting from these trials revealed that nearly all of the receptors examined had a preference for particular directions of applied stimuli with respect to multiple measures of directionality (Table 1). Two cells in particular, 13-1 and 18-2, were almost exclusively unidirectional (Fig. 26C, D). These 2 units were also classified as RA-X receptors, which possibly represent the free nerve endings. In all, most of the RA-X units were well tuned to directional input. The Merkel cell-neurite complex also showed a

strong directional response suggesting the structure of the Eimer's organ allows for transduction of directional displacements to the deep layers of the epidermis (Manger and Pettigrew, 1996; see also: Cauna, 1954). In general, the PC-like units were also directionally tuned, however this group was less robustly directional than the RA-X group (Fig. 27).

Together these data support the hypothesis that one of the functions of Eimer's organ is to transduce directional displacements of the central cell column. However it is important to point out that our directional stimulation paradigm does not mimic natural stimuli. Moles make single brief contacts to the substrate or objects while searching their environment, and do not slide or rub the nose over objects. In a behaving mole, the direction stimulation of the cell column that we propose would likely result from the mechanical deflections caused by small surface features as the Eimer's organs are compressed against the surface of an object (Fig 30A). Presumably such direction displacements would reveal patterns representing fine surface details and contours.

If this is indeed a basic component of Eimer's organ function, a simple and powerful model for coding shapes and textures naturally follows when one considers the integration of information from a skin surface containing multiple Eimer's organs. Figure 30 outlines this proposal in schematic form. The main feature of this proposal, is the differential stimulation of terminal neurites in the cell column indicating the direction of deflection for each Eimer's organ. Information from a single Eimer's organ would be of

Fig. 30. The hypothetical function of Eimer's organ. Each Eimer's organ is depicted schematically as a stack of epithelial cells that form a spring-like column with the free nerve endings running up each side. This column is free to conform to the small surface features and contours of objects that the nose makes contact with and the free nerve endings signal the direction of maximal displacement. This structural configuration may allow for a detailed tactile "snapshot" to be instantaneously created each time the nose strikes a surface. Silent free nerve endings are marked with an X and free nerve endings generating an impulse are marked with an arrow. **A:** The Eimer's organs in a resting position with no tactile surface present and no impulses being generated. **B:** A surface with small features is presented to the Eimer's organs. The organs conform to the surface and send positional information from the resulting compression reflecting the surface details at a resolution of approximately 50 μm. **C:** A surface with large contours is presented to the Eimer's organs. The organs conform to the surface and send positional information from the resulting compression reflecting the overall shape of the object. **D:** The free nerve terminals at the surface of an Eimer's organ in the star-nosed mole revealed with DiI. Each satellite terminal is given a number to represent position. **E:** A schematic representation of the numbered terminals color-coded and arranged in a hexagon. **F:** A scanning electron micrograph of the surface of the nose of the star-nosed mole. The Eimer's organs are arranged in a hexagonal array. **G:** The schematic Eimer's organs arranged in a hexagonal array to represent the organization of the organs on the nose. **H:** A sheet of Eimer's organs that has been compressed by a cylinder and a sphere. The color of the deflected hexagon reflects the direction that it was predominantly displaced. **I:** The two objects have been made translucent. The deflected Eimer's organs generate a stereotypic output signaling the shape and contours of the applied objects.

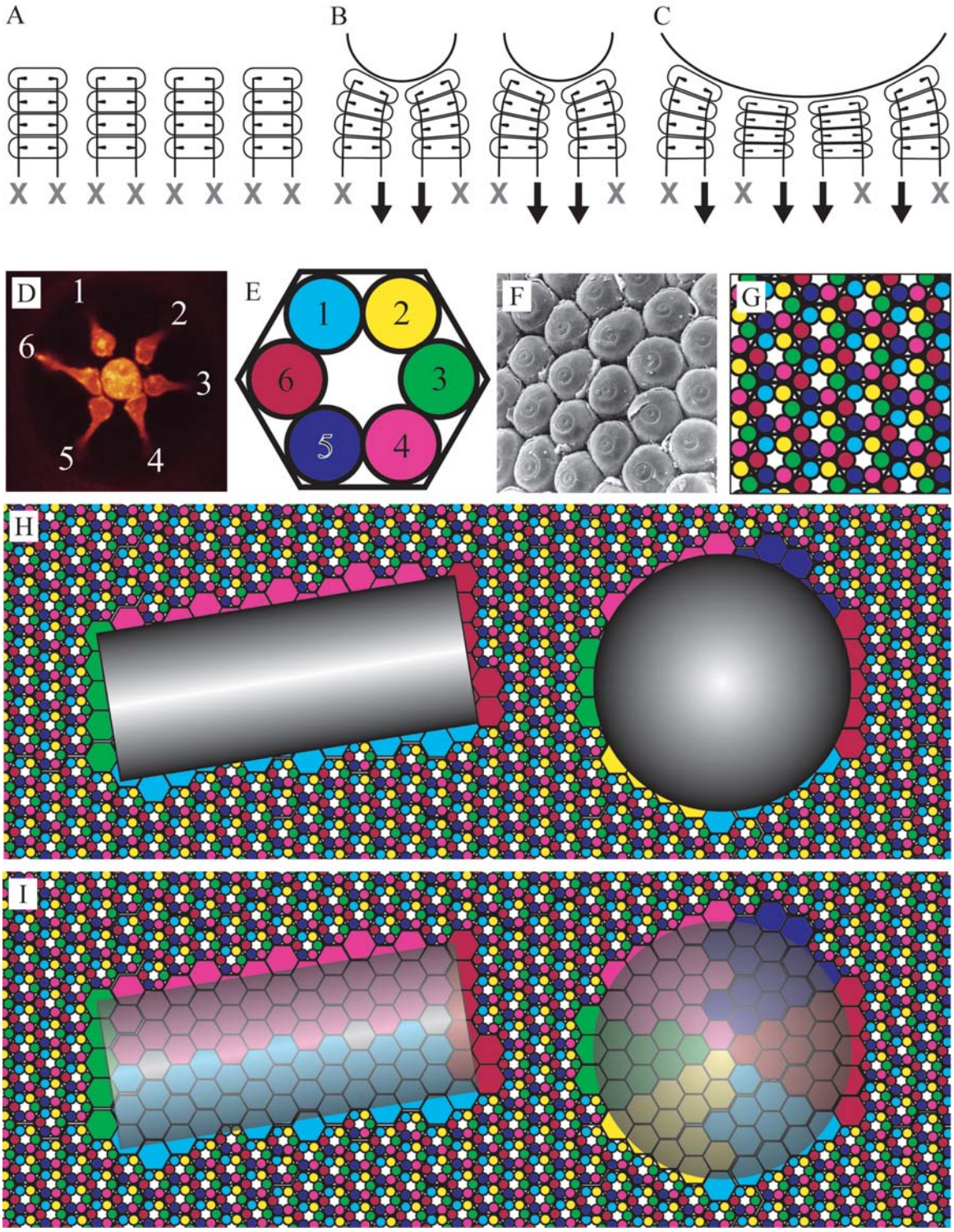
A
B
C
D
1
2
3
4
5
6
E
1
2
3
4
5
6
F
G
H
I

little use, but the deflection of groups of Eimer's organs in unison, or in opposition, could reliably indicate the shape and relative location of curves and edges of objects. This is illustrated for a sphere and a cylinder applied to an array of Eimer's organs in figure 30,plates H and I. Note that a single compression of the skin surface against the objects is sufficient for generating the stereotypic output signaling the different shapes. This would explain a hallmark feature of mole tactile behavior, as single, firm touches to objects are the unit of mechanosensory behavior in these species. Invertebrate prey items exhibit ample textural cues in the appropriate size range - such as repeated ridges, spines, and cuticular segments - that would allow moles to distinguish prey items by this mechanism.

References

Allison T, Van Twyver H. 1970. Sensory representation in the neocortex of the mole, Scalopus aquaticus. Exp Neurol. 27:554-63.

Andres KH, von During M. 1973. Morphology of cutaneous sensory receptors. In A. Iggo (ed): Handbook of Sensory Physiology. New York: Springer. p 3-28.

Andres KH, von Düring M. 1984. The platypus bill. A structural and functional model of a pattern-like arrangement of cutaneous sensory receptors. In: Iggo A, editor. Sensory Receptor Mechanisms. Singapore: World Scientific Publishing Company. p 81-89.

Andres KH, von During M, Iggo A, Proske U. 1991. The anatomy and fine structure of the echidna Tachyglossus aculeatus snout with respect to its different trigeminal sensory receptors including the electroreceptors. Anat Embryol (Berl) 184:371-93.

Batschelet E. 1981. Circular statistics in biology. New York: Academic Press. p 54-58

Bielschowsky M. 1907. Über sensible Nervendigungen in der Haut zwier Insectivoren (Talpa europoea und gentetes ecaudatus). Anat Anz. 31:189.

Bledsoe SC Jr, Rupert AL, Moushegian G. 1982. Response characteristics of cochlear nucleus neurons to 500-Hz tones and noise: findings relating to frequency-following potentials. J Neurophysiol. 47:113-27.

Boeke J. 1932. Nerve endings, motor and sensory. In W. Penfield (ed): Cytology and Cellular Pathology of the Nervous System. New York: Paul B. Hoeber, Inc.

Boeke J. 1940. Problems of nervous anatomy. London: Oxford University Press.

Boeke J, deGroot GJ. 1907. Physiologische Regenerate van neurofibrillaire Eindretten. Koninkl Ned Akad Wentenschap Proc. 16:319.

Bolanowski SJ Jr, Zwislocki JJ. 1984. Intensity and frequency characteristics of pacinian corpuscles. I. Action potentials. J Neurophysiol. 51:793-811.

Botezat E. 1903. Üeber die epidermoidalen Tastapparate in der Schnauze des Maulwurf und andere Säiugetiere mit besonderer Berücksichtigung derselben fur die Phylogenie der Haare. *Arch micr Anat.* 61:730.

Carr CE, Heiligenberg W, Rose GJ. 1986. A time-comparison circuit in the electric fish midbrain. I. Behavior and physiology. J Neurosci. 6:107-19.

Carr CE, Konishi M. 1990. A circuit for detection of interaural time differences in the brain stem of the barn owl. J Neurosci. 10:3227-46.

Catania KC. 1995a. Structure and innervation of the sensory organs on the snout of the star-nosed mole. J Comp Neurol. 351:536-48.

Catania KC. 1995b. A comparison of the Eimer's organs of three North American moles: the hairy-tailed mole (Parascalops breweri), the star-nosed mole (Condylura cristata), and the eastern mole (Scalopus aquaticus). J Comp Neurol. 354:150-60.

Catania KC. 1996. Ultrastructure of the Eimer's organ of the star-nosed mole. J Comp Neurol. 365:343-54.

Catania KC. 2000. Epidermal sensory organs of moles, shrew moles, and desmans: a study of the family talpidae with comments on the function and evolution of Eimer's organ. Brain Behav Evol. 56:146-74.

Catania KC, Kaas JH. 1995. Organization of the somatosensory cortex of the star-nosed mole. J Comp Neurol. 351:549-67.

Catania KC, Kaas JH. 1997. Somatosensory fovea in the star-nosed mole: behavioral use of the star in relation to innervation patterns and cortical representation. J Comp Neurol. 387:215-33.

Catania KC, Remple FE. 2004. Tactile foveation in the star-nosed mole. Brain Behav Evol. 63:1-12.

Catania KC, Remple FE. 2005. Asymptotic prey profitability drives star-nosed moles to the foraging speed limit. Nature. 433:519-22.

Cauna N. 1954. Nature and functions of the papillary ridges of the digital skin. Anat Rec. 119:449-68.

Cauna N, Alberti P. 1961. Nerve supply and distribution of cholinesterase activity in the external nose of the mole. Z Zellforsch Mikrosk Anat. 54:158-66.

Chubbuck JG. 1966. Small motion biological stimulator. Appl. Phys. Lab. Tech. Digest, May-June, 19-23.

Coleman GT, Bahramali H, Zhang HQ, Rowe MJ. 2001. Characterization of tactile afferent fibers in the hand of the marmoset monkey. J Neurophysiol. 85:1793-804.

DiCarlo JJ, Johnson KO, Hsiao SS. 1998. Structure of receptive fields in area 3b of primary somatosensory cortex in the alert monkey. J Neurosci. 18:2626-45.

Dogiel AS. 1903. Über die Nervendapparte in der Haut des Menschen. Z wissensch Zool 65:46

Durand D, Greenwood JA. 1958. Modifications of the Rayleigh test for uniformity in analysis of two-dimensional orientation data. J. Geol 60:229-238.

Dykes RW, Terzis JK. 1979. Reinnervation of glabrous skin in baboons: properties of cutaneous mechanoreceptors subsequent to nerve crush. J Neurophysiol. 42:1461-78.

Eimer T. 1871. Die Schnauze des Malwurfes als Tastwerkzeug. Arch Mikr Anat 7:181-191.

Ferrington DG, Rowe MJ. 1980. Functional capacities of tactile afferent fibres in neonatal kittens. J Physiol. 307:335-53.

Fisher NI. 1993. Statistical analysis of circular data. Cambridge [England]: Cambridge University Press. p 69-71

Gibson JM, Welker WI. 1983. Quantitative studies of stimulus coding in first-order vibrissa afferents of rats. 2. Adaptation and coding of stimulus parameters. Somatosens Res. 1:95-117.

Gorman ML, Stone RD. 1990. The natural history of moles. Ithaca, New York: Cornell University Press. p 47-48

Greenstein J, Kavanagh P, Rowe MJ. 1987. Phase coherence in vibration-induced responses of tactile fibres associated with Pacinian corpuscle receptors in the cat. J Physiol. 386:263-75.

Gregg JM, Dixon AD. 1973. Somatotopic organization of the trigeminal ganglion in the rat. Arch Oral Biol. 18:487-98.

Gregory JE, Iggo A, McIntyre AK, Proske U. 1988. Receptors in the bill of the platypus. J Physiol. 400:349-66.

Gronweg W. 1928. Over de Ontwikkeling van het orgaan van Eimer in den Snuit van den Mol [dissertation]. Utrecht: University of Utrecht.

Halata Z. 1972. [Innervation of hairless skin of the nose of mole. I. Intraepidermal nerve endings]. Z Zellforsch Mikrosk Anat. 125:108-20.

Hämäläinen H, Jarvilehto T, Soininen K. 1985. Vibrotactile atonal interval correlated with activity in peripheral mechanoreceptive units innervating the human hand. Brain Res. 333:311-24.

Iggo A, Gregory JE, Proske U. 1996. Studies of mechanoreceptors in skin of the snout of the echidna Tachyglossus aculeatus. Somatosens Mot Res. 13:129-38.

Iggo A, Muir AR. 1969. The structure and function of a slowly adapting touch corpuscle in hairy skin. J Physiol. 200:763-96.

Iggo A, Ogawa H. 1977. Correlative physiological and morphological studies of rapidly adapting mechanoreceptors in cat's glabrous skin. J Physiol. 266:275-96.

Janig W. 1971. Morphology of rapidly and slowly adapting mechanoreceptors in the hairless skin of the cat's hind foot. Brain Res. 28:217-31.

Janig W, Schmidt RF, Zimmermann M. 1968. Single unit responses and the total afferent outflow from the cat's foot pad upon mechanical stimulation. Exp Brain Res. 6:100-15.

Johansson RS, Landstrom U, Lundstrom R. 1982. Responses of mechanoreceptive afferent units in the glabrous skin of the human hand to sinusoidal skin displacements. Brain Res. 244:17-25.

Johansson RS, Vallbo AB. 1979. Tactile sensibility in the human hand: relative and absolute densities of four types of mechanoreceptive units in glabrous skin. J Physiol. 286:283-300.

Johansson RS, Vallbo AB. 1980. Spatial properties of the population of mechanoreceptive units in the glabrous skin of the human hand. Brain Res. 184:353-66.

Johnson KO. 1974. Reconstruction of population response to a vibratory stimulus in quickly adapting mechanoreceptive afferent fiber population innervating glabrous skin of the monkey. J Neurophysiol. 37:48-72.

Kadanoff D. 1928. Über die intraepithelialen Nerven und ihre Endigungen biem Menschen und bei den Säugetieren. Z Zellforsch u mikr Anat. 7:553.

Knibestol M, Vallbo AB. 1970. Single unit analysis of mechanoreceptor activity from the human glabrous skin. Acta Physiol Scand. 80:178-95.

Lavine RA. 1971. Phase-locking in response of single neurons in cochlear nuclear complex of the cat to low-frequency tonal stimuli. J Neurophysiol. 34:467-83.

Leem JW, Willis WD, Chung JM. 1993. Cutaneous sensory receptors in the rat foot. J Neurophysiol. 69:1684-99.

Lindblom U. 1965. Properties of touch receptors in distal glabrous skin of the monkey. J Neurophysiol. 28:966-85.

Loewenstein WR. 1958. Generator processes of repetitive activity in a pacinian

corpuscle. J Gen Physiol. 41:825-45.

Loewenstein WR. 1961. On the 'specificity' of a sensory receptor. J Neurophysiol. 24:150-8.

Lynn B. 1969. The nature and location of certain phasic mechanoreceptors in the cat's foot. J Physiol. 201:765-73.

Mahns DA, Coleman GT, Ashwell KW, Rowe MJ. 2003. Tactile sensory function in the forearm of the monotreme Tachyglossus aculeatus. J Comp Neurol. 459:173-85.

Manger PR, Hughes RL. 1992. Ultrastructure and distribution of epidermal sensory receptors in the beak of the echidna, Tachyglossus aculeatus. Brain Behav Evol. 40:287-96.

Manger PR, Pettigrew JD. 1996. Ultrastructure, number, distribution and innervation of electroreceptors and mechanoreceptors in the bill skin of the platypus, Ornithorhynchus anatinus. Brain Behav Evol. 48:27-54.

Marasco PD, Tsuruda PR, Bautista DM, Julius D, Catania KC. 2006. Neuroanatomical evidence for segregation of nerve fibers conveying light touch and pain sensation in Eimer's organ of the mole. Proc Natl Acad Sci U S A. 103:9339-44.

Merkel F. 1875. Tastzellen und Tastkörperchen bei den Hausthieren und beim Menschen. Arch Micr Anat. 11:636-652

Merkel F. 1880. Über die Endigungen der sensiblen Nerven in der Haut der Wirbelthiere. Rostock: H. Schmidt.

Minnery BS, Simons DJ. 2003. Response properties of whisker-associated trigeminothalamic neurons in rat nucleus principalis. J Neurophysiol. 89:40-56.

Mountcastle VB, Talbot WH, Sakata H, Hyvarinen J. 1969. Cortical neuronal mechanisms in flutter-vibration studied in unanesthetized monkeys. Neuronal periodicity and frequency discrimination. J Neurophysiol. 32:452-84.

Pubols LM, Pubols BH Jr. 1973. Modality composition and functional characteristics of dorsal column mechanoreceptive afferent fibers innervating the raccoon's forepaw. J Neurophysiol. 36:1023-37.

Pubols LM, Pubols BH Jr, Munger BL. 1971. Functional properties of mechanoreceptors in glabrous skin of the raccoon's forepaw. Exp Neurol. 31:165-82.

Quilliam TA. 1966a. The mole’s sensory apparatus. J Zool 149:76-88.

Quilliam TA. 1966b. Structure of receptor organs: unit design and array patterns in receptor organs. In: DeReuck A, Knight J, editors. Touch heat and pain. Boston: Little Brown and Company. p 86-116.

Quilliam TA, Sato M. 1955. The distribution of myelin on nerve fibres from Pacinian corpuscles. J Physiol. 129:167-76.

Ranvier L. 1880. On the termination of nerves in the epidermis. Quart J micr Sci 20:456-458.

Ranvier L. 1889. Traité technique d'Histologie, 2nd edition. Paris: F. Savy.

Retzius G. 1892. Ueber die sensiblen Nervendigungen in den Epithelien den Wirbeltieren. Biol Untersuch. 4:37-44

Rose G, Heiligenberg W. 1985. Temporal hyperacuity in the electric sense of fish. Nature. 318:178-80.

Sachdev RN, Catania KC. 2002a. Effects of stimulus duration on neuronal response properties in the somatosensory cortex of the star-nosed mole. Somatosens Mot Res. 19:272-8.

Sachdev RN, Catania KC. 2002b. Receptive fields and response properties of neurons in the star-nosed mole's somatosensory fovea. J Neurophysiol. 87:2602-11.

Sato M. 1961. Response of Pacinian corpuscles to sinusoidal vibration. J Physiol. 159:391-409.

Sullivan WE, Konishi M. 1984. Segregation of stimulus phase and intensity coding in the cochlear nucleus of the barn owl. J Neurosci. 4:1787-99.

Talbot WH, Darian-Smith I, Kornhuber HH, Mountcastle VB. 1968. The sense of flutter-vibration: comparison of the human capacity with response patterns of mechanoreceptive afferents from the monkey hand. J Neurophysiol. 31:301-34.

Vallbo AB, Johansson RS. 1984. Properties of cutaneous mechanoreceptors in the human hand related to touch sensation. Hum Neurobiol. 3:3-14.

Vega-Bermudez F, Johnson KO. 1999. SA1 and RA receptive fields, response variability, and population responses mapped with a probe array. J Neurophysiol. 81:2701-10.

Vickery RM, Gynther BD, Rowe MJ. 1992. Vibrotactile sensitivity of slowly adapting type I sensory fibres associated with touch domes in cat hairy skin. J Physiol. 453:609-26.

Xerri C, Merzenich MM, Peterson BE, Jenkins W. 1998. Plasticity of primary somatosensory cortex paralleling sensorimotor skill recovery from stroke in adult monkeys. J Neurophysiol. 79:2119-48.

Zar JH. 1999. Biostatistical analysis (4th ed.). Upper Saddle River, N.J.: Prentice Hall. p 616-621

CHAPTER V

CONCLUSIONS

The results stemming from this dissertation work have served to expand our understanding of the structure and function of Eimer's organ in the mole. The work using the styryl pyridinium dye AM1-43 yielded a number of exciting results. This dye was found to robustly label the Merkel cell-neurite clusters, lamellated corpuscles and large diameter central column intraepidermal free nerve endings. The dye provided very good structural detail and offers good utility as an anatomical tracer. The Merkel cell-neurite complexes and lamellated corpuscles are both known mechanoreceptors (Loewenstein, 1958; Iggo and Muir, 1969). The presence of the dye in these receptors in addition to the large diameter intraepidermal free nerve endings lent credence to the hypothesis that these receptors were also mechanoreceptive. However this was not an exhaustive test for mechanosensation as the dye also labeled non-mechanosensory structures such as taste buds (Meyers et al., 2003). The AM1-43 label also revealed the presence of a previously uncharacterized receptor component of Eimer's organ. These were small diameter intraepidermal free nerve endings that resided in a ring outside of the central ring of large diameter intraepidermal free nerve endings.

In an effort to understand more about the free nerve ending components of Eimer's organs we used the immunocytochemical markers neurofilament 200 (NF-200) and substance P (sP) to label the system. NF-200 and sP are markers for large diameter peripheral mechanoreceptors and high threshold peptidergic nociceptors respectively.

The large diameter central column free nerve endings were reactive for NF-200 and the smaller peripheral nerve terminals were reactive with sP. This differential labeling of the free nerve ending components provides two interesting clues to the function of these organs. First it supported the hypothesis that the large diameter free nerve endings were mechanosensory, and second it provided evidence that mechanosensory and nociceptive function is segregated to two different but closely arrayed groups of intraepidermal free nerve endings. The large central column free nerve ending terminals may transduce tactile signals while the smaller nociceptive peripheral free nerve endings are in an optimal position to quickly signal if any damaging input occurs.

Differential innervation patterns within the central column free nerve endings were revealed with DiI tracing. We found that different portions of the central column were innervated by different receptor terminals. This was a result that was very similar to what had been reported for the innervation patterns of the push rod in monotremes (Andres and von During, 1984). This pattern of innervation may serve as a component of directional signaling. It suggests that different free nerve ending receptor terminals are able to read differential displacements of the central column cells.

Investigations of this system with electron microscopy revealed a number of new insights into the structure of Eimer' organ and also complemented the work done previously. The central column epithelial cells were found to have a more dense internal network of tonofibrils than surrounding epithelial cells. It appears that this configuration makes the central column more rigid than surrounding tissue possibly helping to focus mechanosensory input down through all of the sensory receptor terminals of the complex.

In addition the central column free nerve endings are arrayed in positions that may allow for the registration of stresses within this more rigid column when it is deflected in different directions. The initial AM1-43 study suggested the possibility that the free nerve endings were extending active terminals into a region of skin normally associated with nonfunctional terminals. Our examination provided evidence that the central column free nerve endings degrade before entering the stratum granulosum and the presence of the dye in the stratum corneum was most likely a product of the sloughing off of the nonfunctional nerve terminals with the epidermis.

We found that the structure of the Merkel cell-neurite complexes and lamellated corpuscles of Eimer's organ in the coast mole closely resembled that of their counterparts in many different species. We also were able to examine the newly characterized peripheral free nerve endings. The structure of these receptors was found to closely resemble the morphology of the fine free nerve endings in human digital skin reported by Cauna (1980). In addition we were able to determine that the afferents serving these receptors were most likely unmyelinated. This finding may provide a new model system to learn more about the ultrastructure of nociceptive free nerve endings within the integument.

The direct electrophysiological examination of the receptors within the organs complemented well with the anatomical studies. We were able to directly assign mechanoreceptive function to Eimer's organ because the receptive field for a number of neurons could be isolated to single Eimer's organs. In general the receptive fields were found to be small and discrete. These findings supported our assertion that the structure

of Eimer's organ may serve to focus mechanosensory input down through the receptor complexes within individual organs.

We found evidence for three different classes of mechanosensory responses in the nose of the mole, one slowly adapting and two different rapidly adapting. The slowly adapting responses resembled the typical SA-1 Merkel cell-neurite complex profile and one class of rapidly adapting response equated well to the typical FA-2 Pacinian profile. The evidence from the anatomical suggests that the Merkel cell-neurite complexes and lamellated corpuscles in Eimer's organ most likely provide these two response profiles. The second class of rapidly response showed similarities with the RA receptors described by Lynn (1969) in the cat and the RA receptors reported by Iggo et al. (1996) in the echidna. We suspect that the second class of RA receptors that we found equates to the activity of the mechanosensory central column intraepidermal free nerve endings.

In addition to the anatomical lines of evidence that suggest Eimer's organs are able to code directional input the electrophysiological results support this view as well. We find that nearly all of the receptors recorded from in this study had at least some capacity to signal directional input. Some of the receptors were so highly directionally tuned that they were nearly unresponsive to displacements applied from anywhere other than the preferred direction. The receptors tentatively considered to represent the intraepidermal free nerve endings also tended to be the most directionally tuned overall. In addition, the structure of the rigid central column also seems to transfer directional input to the Merkel cell-neurite complexes at the base of the organs. Because this type of receptor was also strongly directionally sensitive.

We also found that a number of receptors tended to respond best to stimuli that struck the surface of the nose with the same average velocity that the mole strikes its nose to the ground. We inferred from this interesting result that this tuned response might function as a filter to pass only tactile signal that the mole intends to gather when it taps its nose down. Most other stimuli that occurs at velocities different than the nose tapping velocity, such as dirt falling onto the nose or the pressure resulting from pushing dirt with the snout, may not be as readily passed. This study also yielded the interesting result that most of the receptors in Eimer's organ are able to phase lock to a high degree. This ability for precise temporal coding leads to the suggestion that timing information is an important feature of the tactile input. It might be assumed that since the nose of the mole makes only brief contact with the substrate on each touch the information that is needed to make a tactile discrimination must be gathered quickly with a high degree of fidelity.

In summary we suggest that Eimer's organs function to provide the mole with detailed textural information about the small surface variations on objects. It appears that the organs are able to conform to these small variations and code the differential displacements of the central cell column. Tactile acuity is increased by reducing receptive field size and non-critical tactile information that the mole does not intend to gather appears to be filtered out. All of this takes place on a rapid time scale as reflected in the precise temporal coding and the short duration of the nose taps. In addition, the organs have a protective array of nociceptors around the mechanosensory elements to rapidly alert the mole to damaging influences before the delicate mechanosensory elements are harmed.

This investigation has provided clues to the function of this interesting mechanosensory complex in the mole. In addition, studying these sensory specialists has provided information that might help to understand how sensory information is gathered, handled and processed in mammals in general. This study provides insight into the response properties of a previously uncharacterized receptor class. It begins to shed light on the interrelationship between the skin and its receptors and it provide clues to processing of sensory input at the level of the primary afferents.

References

Andres KH, von Düring M. 1984. The platypus bill. A structural and functional model of a pattern-like arrangement of cutaneous sensory receptors. In: Iggo A, editor. Sensory Receptor Mechanisms. Singapore: World Scientific Publishing Company. p. 81-89.

Cauna N. 1980. Fine morphological characteristics and microtopography of the free nerve endings of the human digital skin. Anat Rec. 198:643-56.

Iggo A, Gregory JE, Proske U. 1996. Studies of mechanoreceptors in skin of the snout of the echidna Tachyglossus aculeatus. Somatosens Mot Res. 13:129-38.

Iggo A, Muir AR. 1969. The structure and function of a slowly adapting touch corpuscle in hairy skin. J Physiol. 200:763-96.

Loewenstein WR. 1958. Generator processes of repetitive activity in a pacinian corpuscle. J Gen Physiol. 41:825-45.

Lynn B. 1969. The nature and location of certain phasic mechanoreceptors in the cat's foot. J Physiol. 201:765-73.

Meyers JR, MacDonald RB, Duggan A, Lenzi D, Standaert DG, Corwin JT, Corey DP. 2003. Lighting up the senses: FM1-43 loading of sensory cells through nonselective ion channels. J Neurosci 23:4054-4065.